

PETROGENESIS OF THE MCCLURE MOUNTAIN MAFIC-ULTRAMAFIC AND ALKALIC COMPLEX,  
FREMONT COUNTY, COLORADO

by

NEIL ANTHONY KILBANE

B. S., Cleveland State University, 1976

---

A MASTER'S THESIS

submitted in partial fulfillment of the

requirements of the degree

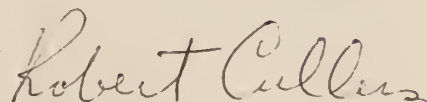
MASTER OF SCIENCE

Department of Geology

KANSAS STATE UNIVERSITY  
Manhattan, Kansas

1978

Approved by:



Major Professor

## CONTENTS

ACKNOWLEDGEMENTS .....	viii
INTRODUCTION .....	1
Statement of the Problem .....	1
Previous Investigations .....	2
GEOLOGY .....	5
General .....	5
Petrology .....	8
Geochronology .....	12
EXPERIMENTAL METHODS .....	13
RESULTS .....	15
Major Elements .....	15
Rb-Sr Isotopic Results .....	28
Trace Elements .....	31
General .....	31
Major Intrusives .....	33
Rare Earth Elements .....	33
Other Trace Elements .....	40
Layered Series .....	47
Rare Earth Elements .....	47
Other Trace Elements .....	49
Nepheline Syenite Dikes and Stocks .....	50
Rare Earth Elements .....	50
Other Trace Elements .....	50
Carbonatite Dike .....	51
DISCUSSION .....	52
Introduction .....	52
Experimental Investigations .....	56
Field Relations .....	58
Major Elements .....	58
Sr Isotopes .....	61
Ages .....	61
Initial Ratios .....	66
Trace Elements .....	68
General .....	68
Derivation of the Model .....	70

## CONTENTS--CONTINUED

Rare Earth Elements .....	72
General .....	72
Primary Melt .....	73
Major Intrusive Biotite Syenite, Feldspathoidal Syenite, and Malignite .....	74
Layered Series .....	81
Dikes and Stocks .....	84
Other Trace Elements .....	89
General .....	89
Primary Melt .....	89
Major Intrusive Biotite Syenite, Feldspathoidal Syenite, and Malignite .....	90
Layered Series .....	94
Dikes and Stocks .....	95
Relation to Gem Park .....	96
SUMMARY .....	99
APPENDIX .....	101
Appendix A: Petrographic Descriptions .....	102
Appendix B: Sample Collection and Preparation .....	115
Appendix C: Atomic Absorption and Emission Spectrophotometry .....	116
Appendix D: Mass Spectrometry .....	124
Appendix E: X-Ray Fluorescence Spectrography .....	128
Appendix F: Instrumental Neutron Activation Analyses .....	130
Appendix G: Gravimetric Determinations .....	146
Appendix H: Distribution Coefficients .....	147
REFERENCES .....	149

## TABLES

1. Major element content and CIPW normative mineral composition of McClure Mountain major rock types .....	16
2. Major element analyses of rock types from selected alkaline complexes .....	19
3. Rb-Sr isotopic data of samples from the McClure Mountain complex .....	29
4. $^{87}\text{Sr}/^{86}\text{Sr}$ initial ratios from select alkaline complexes .....	30
5. Trace element contents of the McClure Mountain rock samples .....	42
6. Summary of trace element data .....	45
7. Trace elements from other alkaline complexes .....	48
8. Flow diagram summarizing the possible relations of the McClure Mountain rock types .....	54
9. Radiometric ages for the McClure Mountain complex .....	62
10. "Model" ages of McClure Mountain biotite separates .....	64
11. Initial ratios of rocks in the McClure Mountain and Gem Park complexes .....	67
12. Trace element contents in peridotites and alkali basalts .....	90
A-1. Modal analyses of McClure Mountain rocks .....	112
C-1. Primary standard solution concentrations .....	118
C-2. Dilution schemes for atomic absorption and emission spectrophotometry .....	119
C-3. Instrument settings for atomic absorption Spectrophotometer .....	122
C-4. Comparison of standard rock W-1 elemental analyses .....	123
E-1. Rb and Sr values determined by X-ray emission .....	129

F-1.	Summary of nuclide properties used in INAA .....	133
F-2.	Analytical results of instrumental activation analyses for reference soil S0-1 .....	142
F-3.	Analytical results of instrumental activation analyses for U.S.G.S. standard G-2 .....	143
F-4.	Multiple analyses of McClure Mountain major rock types .....	144

## FIGURES

1.	Index map of Fremont and Custer counties, Colorado .....	6
2.	Generalized geologic map of the McClure Mountain complex .....	7
3.	Geologic map of the mafic-ultramafic layered intrusion at Iron Mountain, Fremont County, Colorado .....	11
4.	Alkali-lime differentiation index of the McClure Mountain syenite and malignite .....	22
5.	Major element variation diagram for the McClure Mountain complex. Weight percent oxide versus differentiation index .....	24
6.	Major element variation diagram for the McClure Mountain complex. $\text{Fe}_2\text{O}_3/(\text{Fe}_2\text{O}_3 + \text{MgO})$ versus $\text{Al}_2\text{O}_3$ .....	25
7.	Major element variation diagram for the McClure Mountain complex. $\text{CaO}/(\text{CaO} + \text{Na}_2\text{O})$ versus $\text{Al}_2\text{O}_3$ .....	26
8.	Major element variation diagram for the McClure Mountain complex. AFM diagram .....	27
9.	Rb-Sr evolution diagram for the McClure Mountain complex .....	32
10a.	Chondrite-normalized REE plots for the McClure Mountain complex: malignite, biotite syenite, feldspathoidal syenite .....	34
10b.	Chondrite-normalized REE plots for the McClure Mountain complex: gabbro, pyroxenite, anorthosite .....	35
10c.	Chondrite-normalized REE plots for the McClure Mountain complex: carbonatite, nepheline syenite dikes and stocks .....	36
11.	Chondrite-normalized ranges of the REE content in the major McClure Mountain rock types .....	37
12.	Range of trace elements plotted against average differentiation index for the McClure Mountain intrusives .....	38
13.	Chondrite-normalized REE distribution for rocks from select alkaline complexes .....	41

14.	Chondrite-normalized REE plots of model melts: hypothetical alkali-basaltic magma, hypothetical "ijolitic" magma .....	75
15a.	Chondrite-normalized REE plots of model rocks: malignite, feldspathoidal syenite, biotite syenite .....	77
15b.	Chondrite-normalized REE plots of model rocks: gabbro, pyroxenite, anorthosite .....	83
15c.	Chondrite-normalized REE plots of model rocks: nepheline syenite dikes and stocks .....	86
16.	Chondrite-normalized REE plots of model carbonatite melt and potential source melts .....	88
F-1.	Typical photopeak showing background, net peak area, and adjacent peak .....	136
F-2.	Spectra illustrating the interference of $^{59}\text{Fe}$ with $^{141}\text{Ce}$ .....	138

## A C K N O W L E D G E M E N T S

I would like to acknowledge first and foremost the assistance of my major professor, Dr. Robert L. Cullers for his guidance in all phases of this research. I would also like to thank Dr. Page C. Twiss, Dr. Sambhudas Chaudhuri and Dr. Kenneth G. Kay for serving on my supervisory committee and for their constructive editorial remarks.

The assistance of Mike McEwan, Dr. N. Dean Eckhoff, and the staff of the KSU Department of Nuclear Engineering is also gratefully appreciated. In addition I would like to acknowledge Dr. Donald O. Whittemore for his instruction in atomic absorption analysis, and Joseph P. Smalley for his assistance with the drafting of the figures.

A special thanks to my wife Christine for her assistance in the field, in the lab, and in typing and editing the rough drafts of this thesis. Her encouragement throughout this research was invaluable.

This research was partially supported by a Grant-in-Aid for Research from Sigma Xi, The Scientific Research Society of North America.



## I N T R O D U C T I O N

### STATEMENT OF THE PROBLEM

The McClure Mountain complex is a mafic-ultramafic and alkalic igneous complex (Parker and Hildebrand, 1963; Shawe and Parker, 1968) consisting of a series of major intrusive bodies and associated dikes. It, together with two other alkalic intrusions, the Gem Park and Democratic Creek complexes, collectively comprise a major alkalic province of Cambrian age located in the northern Wet Mountains of south-central Colorado. The three different complexes have been presumed to be genetically related based on proximity, petrologic similarities, and apparent similar ages (Shawe and Parker, 1968; Parker and Sharp, 1970; Parker and Hildebrand, 1963; Heinrich, 1977; Roden, 1977).

The main body of the complex consists of the following petrologic assemblages: biotite syenite, feldspathoidal syenite, malignite, and a layered gabbro-peridotite-dunite assemblage. Strong mineralogic similarities existing between the syenites and the malignites, and the undersaturated nature and alkalic affinity of the rocks of the layered assemblage suggest that they are all part of the same comagmatic series (Shawe and Parker, 1968; Parker and Hildebrand, 1963).

The primary purpose of this study was to examine in detail the relationship between the major rock units of the McClure Mountain complex and to formulate a model for the origin and subsequent modification of the magma(s) that produced it. Secondary goals of this research were to examine the relationship between the rocks at Gem Park and McClure Mountain and to refine existing isotopic ages for the McClure Mountain Complex.

Accordingly, this study focuses on the major and trace element contents and the Rb-Sr isotopic ratios of representative samples of the McClure Mountain complex. These data are used to test petrogenetic models for the origin of the complex. Rb-Sr isotopic ratios were used to establish relations between rock bodies, and to limit the potential source regions for the magmas which produced the complex. Mineralogy and trace element contents of the rocks of the source region are approximated using existing data and the trace element contents of melts derived from the source by different degrees of partial melting are calculated. Major element trends are used to suggest possible fractional crystallization sequences which may have further modified the derived melts. Using mineralogy similar to those of the rocks of the complex, trace element concentrations of rocks formed by fractional crystallization are calculated. Finally, the petrogenetic models are tested by comparing the calculated trace element contents with those of the rocks from the complex.

#### PREVIOUS INVESTIGATIONS

Initial publications of the McClure Mountain complex summarized the iron mine at Iron Mountain that is associated with the layered assemblage (Hayden, 1874; Putnam, 1886; Chauvenet, 1886, 1890; Kemp, 1899). The titanomagnetite ore of the deposit was the subject of a detailed study by Singwald (1913), and more recently was the subject of magnetic and gravity studies by the U.S. Bureau of Mines (Becker et al., 1961). A detailed geochemical and mineralogical study of the ore is being conducted at the University of Michigan (Spencer et al., 1978).

The alkalic nature of the McClure Mountain complex was first recognized by Parker and Hildebrand (1963), who described the major rock units occurring in the McClure Mountain and Gem Park complexes. These investigations suggested that the two complexes were related and probably belonged to the same comagmatic series. Studies by Reuss (1967) and Parker and Sharp (1970) of the Gem Park complex and its associated carbonatites

provided further evidence that the complexes at McClure Mountain and Gem Park are related. Roden and Cullers (1976) and Roden (1977), in recent studies of the Gem Park complex, have proposed a combination of partial fusion, fractional crystallization, and liquid immiscibility to explain the petrologic associations observed at Gem Park. They suggest that the rocks of the McClure Mountain complex may have formed by similar processes and that a comagmatic relationship may exist between the two bodies.

Studies of the presumably related Democrat Creek complex are less numerous (Christman et al., 1953; Christman et al., 1959) and have been resummarized in light of the new information obtained about the McClure Mountain and Gem Park complexes (Dahlem, 1965; Heinrich and Dahlem, 1966, 1969; Heinrich, 1966).

The McClure Mountain complex was further investigated by Dahlem (1965), Heinrich and Dahlem (1966, 1969), and Heinrich (1966), and an intense dike halo associated with the complex was described. Additional studies of the dikes occurring within and adjacent to the complex have been reported (Heinrich and Anderson, 1965; Staatz and Conklin, 1966; Heinrich and Shappirio, 1966; Heinrich and Dahlem, 1967; Moore, 1969; Heinrich and Moore, 1970; Alexander, 1974; Heinrich and Salotti, 1975; and Heinrich and Alexander, 1975). Shawe and Parker (1968) mapped and described in detail the mafic-ultramafic layered intrusion occurring at Iron Mountain and suggested, although it differed markedly in mineralogy, that it was genetically related to the associated syenite and malignite occurring at McClure Mountain. Alexander and Heinrich (1978) suggested that the McClure Mountain complex and associated dikes were formed by the fractional crystallization of an alkali basalt magma. The complex is now being studied by the U.S. Geological Survey (R.L. Parker, personal communication, 1977).

The first isotopic dates for the rocks at McClure Mountain were determined using K-Ar techniques by R.F. Marvin of the U.S. Geological Survey and indicated that the complex was Cambrian (Parker and Sharp, 1970). In the same year Fenton and Faure reported a late Precambrian - Cambrian age for the complex based on a Rb-Sr whole-rock isochron. Olson et al. (1977) recently reported K-Ar, Rb-Sr, and fission-track ages of minerals and whole rocks from the McClure Mountain, Gem Park, and Democrat Creek complexes. Their findings confirmed the Cambrian age reported by Parker and Sharp (1970). Earlier age determinations of the Democrat Creek complex reported by Christman et al. (1959) and Jaffe et al. (1959) were confirmed by the work of Olson et al. (1977).

Detailed discussions of the geologic history of the Northern Wet Mountains are provided by Logan (1966) and Dahlem (1965). The reader is referred to these works for further discussions of this topic.

Reports on the geologic investigations of alkaline complexes abound in the literature, and many have been summarized in the works of Heinrich (1966), Tuttle and Gittins (1966), and Sorensen (1974). Notable among these are the studies by Eby (1975), Mitchell and Brunfelt (1976), Cullers and Medaris (1977), and Roden (1977) which, like the present study, examine the REE (rare earth element) contents of the rocks associated with these complexes in an attempt to evaluate their genetic relationship.

## G E O L O G Y

### GENERAL

The McClure Mountain complex is the largest of three alkalic centers of Cambrian age which comprise the northern Wet Mountains alkalic province (Fig. 1), and it is followed in order of decreasing size and complexity by the Democrat Creek (McKinley Mountain) and Gem Park alkalic centers (Fig. 2). The McClure Mountain complex occupies an area of about 20 square miles and measures roughly 5 miles (N.E.) by 4 miles (N.W.) (Parker and Hildebrand, 1963). It is located in the south-central part of Fremont County, Colorado, approximately 13 miles north of Westcliffe and 11 miles southwest of Canon City.

Structurally, the McClure Mountain complex discordantly intrudes granite gneiss, amphibolite, and metasedimentary rocks of the Idaho Springs Formation and Precambrian granites of Boulder Creek age (1700 - 1800 M.Y.) (Dahlem, 1965; Shawe and Parker, 1968; Olson et al., 1977). Cross cutting relationships of the McClure Mountain complex with the metamorphic rocks and the absence of metamorphic textures in the McClure Mountain complex indicate that the regional metamorphism that affected the gneisses and related rocks predates the intrusion of the complex (Shawe and Parker, 1968).

The complex is roughly circular in plan and exhibits a poorly defined concentric distribution of the major rock bodies (Fig. 2). The U.S. Geological Survey (1971), on the basis of an anomalous magnetic high in the southwestern part of the complex, suggested that gabbroic material similar to that in the northeastern part of the complex may be located beneath the surface. They believed that the complex may be more symmetrical than field



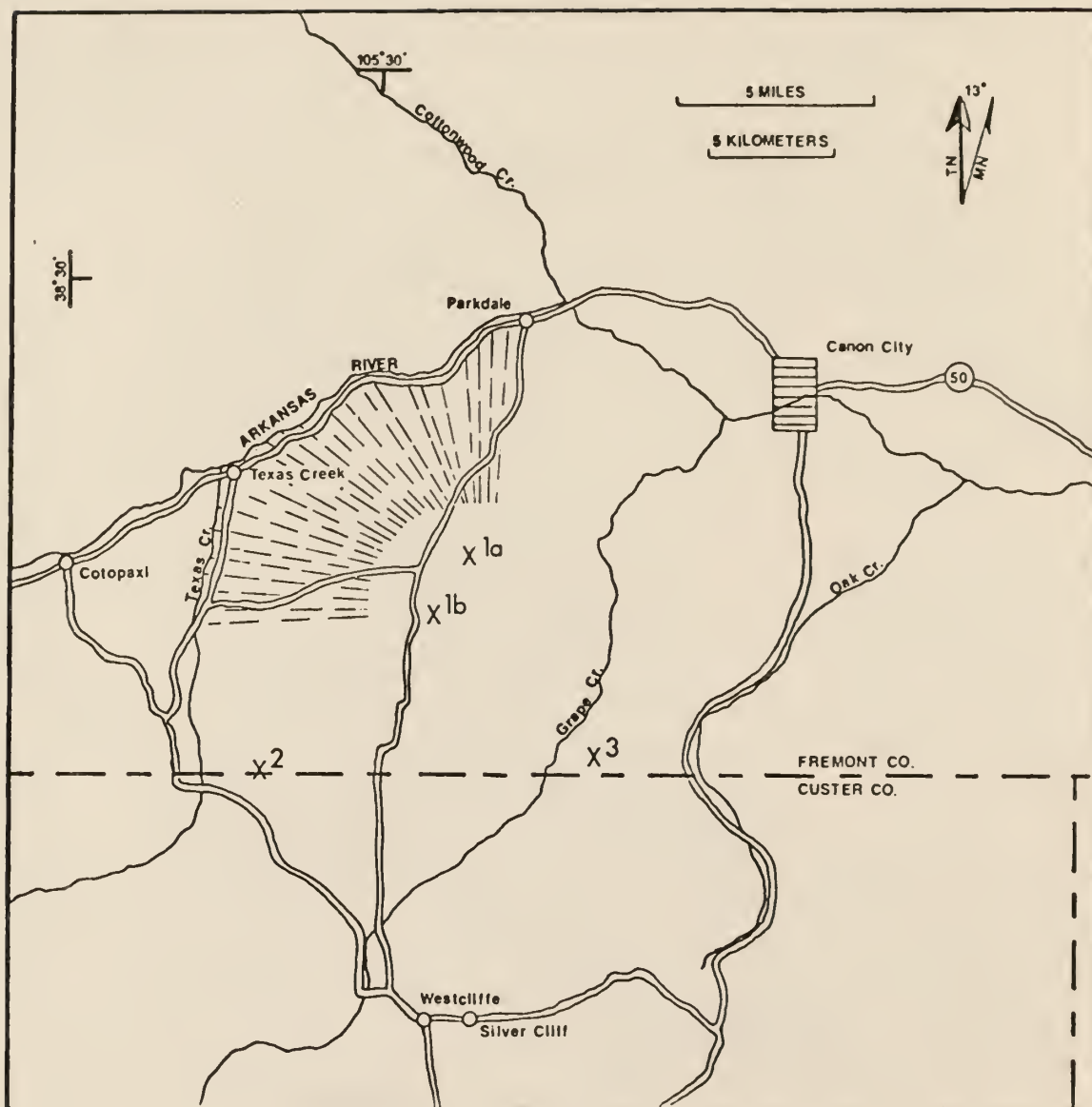


Figure 1. Index map of Fremont and Custer Counties, Colorado. 1a-1b, Iron Mountain-McClure Mountain mafic-alkalic complex; 2, Gem Park mafic-alkalic complex; 3, Democrat Creek alkalic complex. Radiating dashed lines represent dike halo associated with the McClure Mountain complex (From Heinrich, 1977).

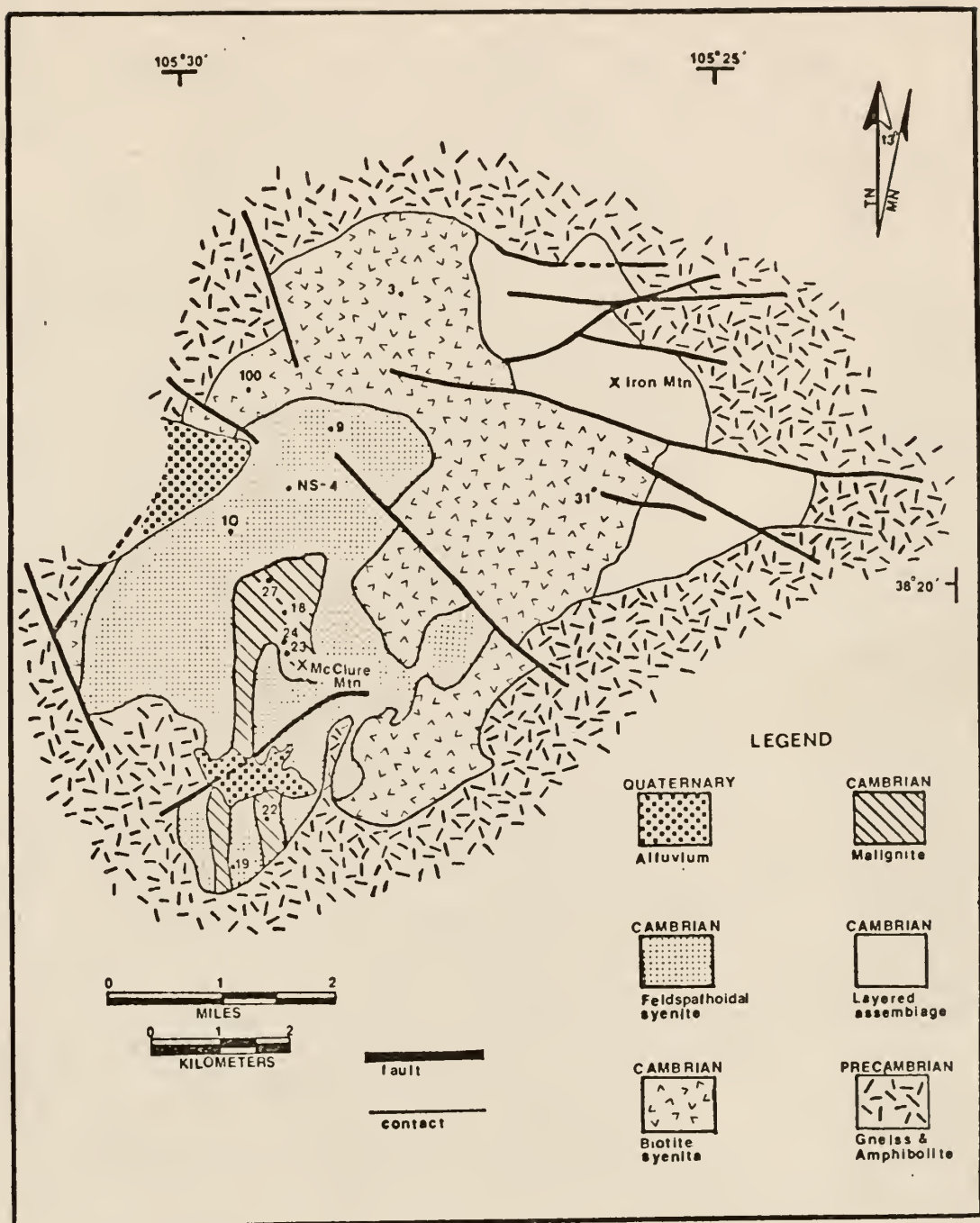


Figure 2. Generalized geologic map of the McClure Mountain complex showing locations of samples. The prefaces of the sample numbers have been omitted to conserve space (From Parker and Hildebrand, 1963).

relations indicate (Fig. 2). Unlike many reported alkalic complexes, the main body of the intrusion is not funnel-shaped, although the layered assemblage of the Iron Mountain complex to the northeast is funnel-shaped (Shawe and Parker, 1968). Heinrich and Dahlem (1969) proposed that this is the result of extensive erosion which has exposed the complex at a very deep level (mesozone-catazone). Several faults have dissected the complex and its Precambrian host rocks. Many faults are presumably a result of regional uplift during the Late Cretaceous to Early Tertiary Laramide orogeny (Reuss, 1967).

#### PETROLOGY

Four major petrologic assemblages comprise the McClure Mountain complex (Fig. 2). They are, in order of increasing age, feldspathoidal syenite, biotite syenite, ijolite (malignite), and the mafic-ultramafic layered intrusion (Alexander and Heinrich, 1978). Numerous dikes are both within the complex and in the surrounding Precambrian metasedimentary and igneous rocks (Heinrich and Dahlem, 1969). Minor fenitization of the country rock has occurred along the contact of the main intrusive body (Shawe and Parker, 1968; Heinrich and Dahlem, 1969). General features of each major body are summarized below, and detailed petrographic descriptions are in Appendix A.

Feldspathoidal syenite forms the core of the McClure Mountain complex and intrudes biotite syenite to the east and country rock to the north and west (Parker and Hildebrand, 1963). Dahlem (1965) estimated that feldspathoidal syenite is the most abundant nepheline-bearing rock, forming 25 percent of the complex. The feldspathoidal syenite is medium to coarse grained and locally porphyritic. Mineralogically it is highly varied and in local occurrences resembles its biotite syenite counterpart. It consists primarily of alkali-feldspar (perthite), highly varied amounts of nepheline, biotite,



and hornblende. Accessory minerals include Na-plagioclase, magnetite, apatite, and sphene. Cancrinite and sodalite are present in some varieties.

Biotite syenite, the most abundant rock unit in the McClure Mountain complex (~45 percent), composes an arcuate shaped body situated between the layered series (NE), the malignite (SW), and the Precambrian metamorphic rocks (NW, SE) (Parker and Hildebrand, 1963; Dahlem, 1965). It is coarsely crystalline and commonly displays a trachytoid texture attributed to flowage during intrusion (Parker and Hildebrand, 1963). Alkali feldspar (perthite) is the dominant mineral, and it is accompanied by Na-plagioclase, biotite, and hornblende. Sphene, apatite and minor amounts of muscovite are accessory minerals.

Malignite, previously referred to as mafic nepheline-bearing rock by Parker and Hildebrand (1963) and ijolite by Heinrich and Dahlem (1966, 1969), is surrounded by the younger feldspathoidal syenite on all sides except for two places where there are small protrusions of malignite into the country rock (Parker and Hildebrand, 1963). Malignite forms approximately 10 percent of the complex (Dahlem, 1965), is black, medium to coarse-grained, and commonly porphyritic. Hornblende is the most common mineral in the rock which also contains significant amounts of biotite, alkali-feldspar and nepheline. Sphene is a common accessory mineral and is accompanied, in lesser amounts, by augite, carbonates, sodalite, apatite, and magnetite.

The mafic-ultramafic layered intrusion at Iron Mountain occupies approximately 20 percent of the McClure Mountain complex (Dahlem, 1965). The layered intrusive rock forms the eastern intrusive contact of the complex with the country rock and is intruded by biotite-syenite to the west. The body, as described by Shawe and Parker (1968), is a funnel-shaped sequence of igneous rock layers several thousand feet in total exposed

thickness (Fig. 3). The layers range in thickness from a fraction of an inch to several tens of feet and in some massive units, extend laterally for thousands of feet (Shawe and Parker, 1968).

The rocks of the layered intrusion are medium-grained and consist of a series of gradational types composed principally of plagioclase, pyroxene, olivine, and magnetite in different proportions. Common accessory minerals include kaersutite, biotite, green spinel, pyrite, apatite, sphene, and rutile. Rock types in the complex include olivine gabbro, gabbro, dunite, pyroxenite, anorthosite, peridotite, troctolite, and titaniferous magnetite iron ore (Shawe and Parker, 1968). The rocks of the layered series were formed by cumulate processes within a crystallizing magma as evidenced by their cumulate textures in thin section and by other igneous structures such as scour and fill, graded bedding, and both compositional and rhythmic layering (Shawe and Parker, 1968). Alexander and Heinrich (1978) estimated that the average composition of the rocks is that of an alkalic gabbro with 1 - 2 percent normative nepheline. This is consistent with the findings of Shawe and Parker (1968) who suggested that the rocks of the layered series are undersaturated and alkalic.

Several larger intrusive plugs of pyroxenite and anorthosite occur within the layered assemblage complex. Mineralogically they resemble their layered series counterparts but are different in that they do not exhibit cumulate texture. Numerous dikes and small stocks of syenite and nepheline syenite, as well as two carbonatite dikes are also within the layered series.

Numerous dikes and sills are associated with the McClure Mountain complex and are particularly abundant in the area northwest of McClure Mountain (Fig. 1; Dahlem, 1965). Dikes occurring within the complex commonly are syenite or nepheline syenite and range from aphanitic to medium grained (Heinrich and Dahlem, 1969). Extracomplex dikes are chiefly

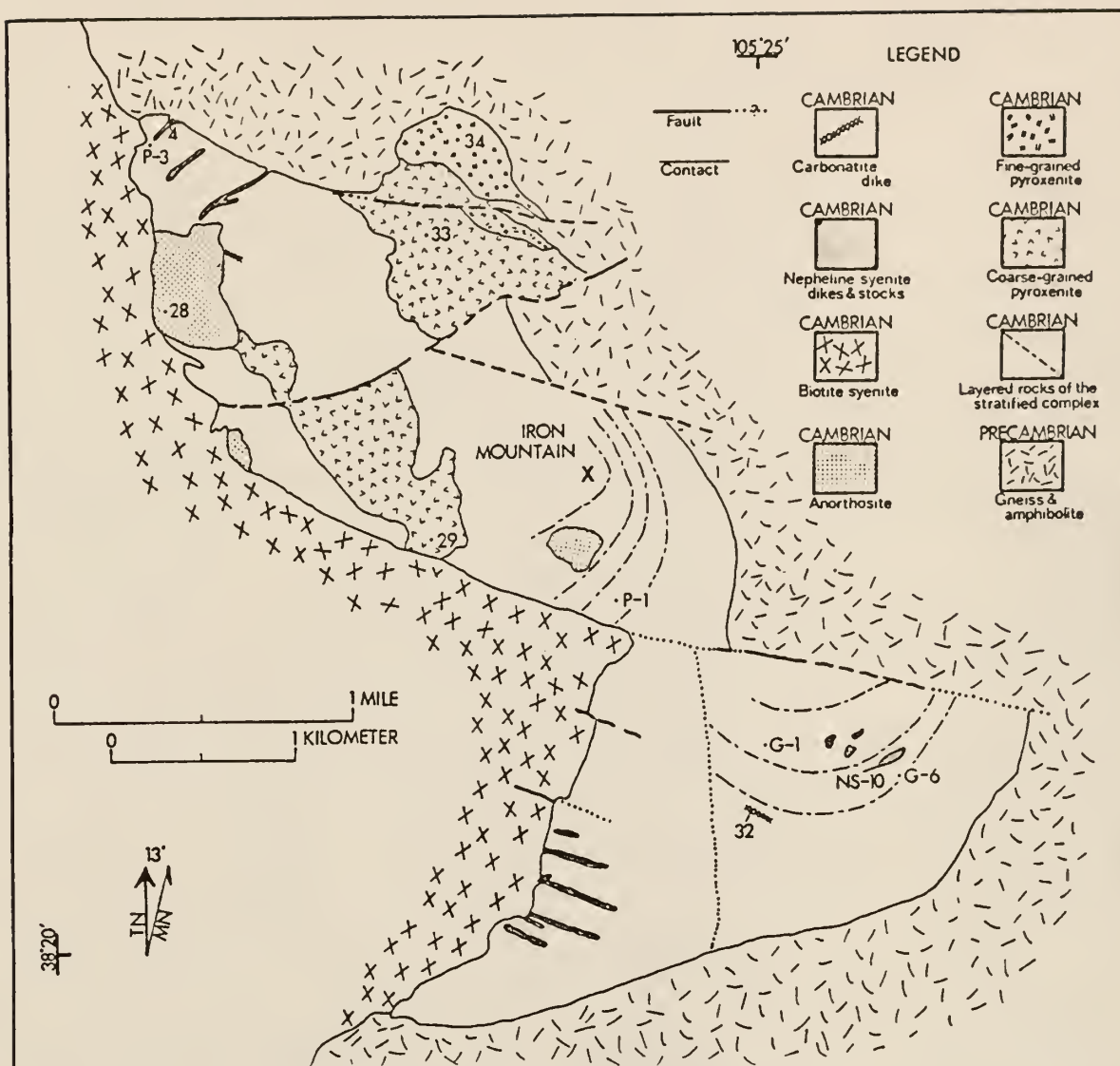


Figure 3. Geologic map of the mafic-ultramafic layered intrusion at Iron Mountain, Fremont, Colorado (After Shawe and Parker, 1968).

carbonatites and lamprophyres which, unlike the intracomplex dikes, are not represented by equivalent major units within the complex (Heinrich and Dahlem, 1969). The lamprophyric dikes commonly display extreme textural variation (Heinrich and Alexander, 1975). Cross cutting relations between the dikes, as determined by Dahlem (1965), indicate that the carbonatite dikes are the youngest and were preceded by the lamprophyric and syenitic dikes.

#### GEOCHRONOLOGY

Geochronologic studies by Olson et al. (1977) indicate that the rocks of the McClure Mountain complex are Cambrian. They obtained an age of 520 M.Y. using the combined results of K-Ar, Rb-Sr, and fission-track dating techniques. A less precise age of 495 M.Y. was reported by these same authors for red syenite dikes occurring within the complex. The results of Olson et al. (1977) are in excellent agreement with ages of 517 M.Y. obtained on an isochron reported by Fenton and Faure (1978) and 508 - 532 M.Y. obtained by the U.S. Geological Survey (Parker and Sharp, 1970) on rocks of the McClure Mountain complex.

## E X P E R I M E N T A L   M E T H O D S

Samples of the major rock units of the McClure Mountain complex and many of its associated dikes and stocks collected for laboratory analyses were cut so only the least weathered portions were used. Thin sections of the samples were prepared and described (Appendix A), and portions of the samples were ground to less than 200 mesh size and stored for chemical analyses (Appendix B).

The elements Si, Al, Fe, Mg, Ca, Na, K, Rb, and Sr were analyzed by atomic absorption using a Perkin-Elmer model 305B atomic absorption spectrophotometer (Appendix C). Powdered samples were dissolved similar to Buckley and Cranston (1971) and were diluted down to the concentration range necessary for analyses. A U.S. Geological Survey standard rock was analyzed relative to a synthetic standard in order to monitor the quality of the analyses (Table C-4). The values determined in this study are in excellent agreement with those reported in the literature.

The Rb and Sr concentrations and the  $^{87}\text{Sr}/^{86}\text{Sr}$  ratios of the samples were determined using a 6-inch, 60°, Nier-type mass spectrometer (Appendix D). Samples were dissolved using procedures similar to those of Chaudhuri (1966) and Methot (1973). X-ray spectrography was used to approximate the concentrations of Rb and Sr in the samples prior to their analyses (Appendix E). The  $^{87}\text{Sr}/^{86}\text{Sr}$  ratios were determined directly for some samples, whereas for others they were determined along with the Sr concentration. Rb and Sr concentrations were determined using isotope dilution techniques described by Chaudhuri (1966) and Faure (1977).



INAA (instrumental neutron activation analysis) was used to determine the REE (rare earth elements), Rb, Ba, Th, Hf, Ta, Co, Sc, Fe, Na, and Mn concentrations (Appendix F). The method was adapted from Gordon et al. (1968) and Jacobs et al. (1977). Samples and standards were irradiated in the Kansas State University Triga Mark II reactor, packaged and counted on a 25 cm<sup>3</sup>Ge (Li) detector coupled with a Northern Scientific 4096-channel analyzer and associated electronics. The ratio of standard to sample peak height ratios were calculated for the desired elements using a computer program adapted from Jacobs et al. (1977). Corrections for interfering peaks were made when necessary and are described in Appendix F.

A U.S. Geological Survey standard rock and a Canadian reference soil were analyzed at Kansas State University using INAA. The results, listed in Tables F-2 and F-3, are in good agreement with reported values for these standards. To determine the reproducibility of the analyses, a number of samples were analyzed repeatedly and are in Table B-4. The results indicate that the reproducibility of the determinations is generally within the range of the error resulting from the uncertainty in counting statistics.

Ignition was performed to determine the total volatile content of the samples. The procedure is in Appendix E.

## R E S U L T S

### MAJOR ELEMENTS

The major element content and the CIPW norms of representative samples of the major rock types in the McClure Mountain complex are reported in Table 1. The rock types analyzed include the following: feldspathoidal syenite, NK-10; biotite syenites, NK-100, NK-31, and FeNS-4; malignites, NK-18, NK-24, and NK-27; pyroxenites, NK-33 and FeP-1; gabbros, NK-34, FeG-1, and FeG-6; anorthosite, NK-28; nepheline syenite stock, FeNS-10; and carbonatite, NK-32. Samples of the feldspathoidal syenite, biotite syenite, malignite, pyroxenite, and gabbros were chosen so that the maximum range of mineralogy of these rock types was represented.

The major element contents of the rock units from McClure Mountain are similar to those in other alkalic complexes (Table 2; Tuttle and Gittins, 1966; Sorenson, 1974). In addition, analyses of rocks of the layered series and its associated intrusions are chemically similar to the older analyses of Shawe and Parker (1968) demonstrating the similarity of the chemical data among independent analysts (Table 2). Pyroxenites and gabbros at Gem Park (Parker and Sharp, 1970; Roden, 1977) also bear a strong chemical resemblance to their McClure Mountain counterparts (Table 2). The McClure Mountain carbonatite is similar to carbonatites from the Gem Park complex (Roden, 1977) but differs slightly from the average of a number of carbonatites reported by Gold (1963) (Table 2). This presumably is a result of the nonmineralogic nature of the McClure Mountain carbonatites.

Alumina saturation in the McClure Mountain samples ranges from peraluminous in the feldspathoidal syenites, biotite syenites, gabbros G-1 and

Table 1. Major element content (weight percent) and CIPW normative mineral composition (percent) of McClure Mountain major rock types.

	Feldspath- oidal Syenite NK-10	Nepheline Syenite Stock FeNS-10	Biotite Syenites		
			NK-100	NK-31	FeNS-4
SiO <sub>2</sub>	57.27	62.06	62.82	61.56	59.95
Al <sub>2</sub> O <sub>3</sub>	19.13	23.23	19.31	19.90	20.24
Fe <sub>2</sub> O <sub>3</sub>	6.48	3.84	3.09	2.49	3.58
MgO	1.79	0.09	0.66	0.51	0.75
CaO	3.68	0.72	1.02	1.29	2.52
Na <sub>2</sub> O	6.01	8.24	6.02	6.67	6.36
K <sub>2</sub> O	5.63	5.92	7.36	5.64	6.16
MnO	0.41	0.44	0.24	0.14	0.21
ignition	0.59	1.42	0.80	0.88	0.87
+H <sub>2</sub> O	0.21	0.67	0.19	0.27	0.18
TOTAL	101.20	106.63	101.51	99.35	100.82
C	---	1.77	---	0.48	---
Or	33.23	33.05	43.44	33.29	36.36
Ab	32.56	43.69	43.68	51.38	39.34
An	8.59	3.57	3.93	6.40	8.48
Ne	9.89	12.01	3.91	2.72	7.82
Di	7.97	---	0.94	---	3.33
Ol	3.49	1.81	2.15	2.04	1.71
Mt	4.23	2.75	2.24	1.69	2.47
Lc	---	---	---	---	---
Cs	---	---	---	---	---
Hy	---	---	---	---	---
Q	---	---	---	---	---
DI*	75.68	88.76	91.03	87.38	83.52

\*DI=Differentiation Index



Table 1. Major element content (weight percent) and CIPW normative mineral composition (percent) of McClure Mountain major rock types (Cont.)

	NK-34	Gabbros FeG-1	FeG-6	Anorthosite NK-28	Carbonatite NK-32
SiO <sub>2</sub>	45.05	45.46	40.95	46.84	0.98
Al <sub>2</sub> O <sub>3</sub>	13.78	18.55	16.20	23.81	---
Fe <sub>2</sub> O <sub>3</sub>	12.68	10.38	18.87	6.45	3.43
MgO	4.79	8.87	13.96	2.10	0.37
CaO	16.14	13.64	7.40	12.13	50.30
Na <sub>2</sub> O	1.90	1.99	1.99	3.89	0.07
K <sub>2</sub> O	1.87	0.11	0.14	0.25	---
MnO	0.13	0.13	0.19	0.17	3.75
ignition	1.58	0.52	0.17	0.51	42.94
+H <sub>2</sub> O	0.11	0.05	0.06	0.18	0.25
TOTAL	98.03	99.70	99.93	96.33	101.09
C	---	---	---	---	---
Or	6.47	---	---	1.49	---
Ab	---	12.49	12.74	23.16	---
An	23.53	41.65	35.24	46.73	---
Ne	8.71	2.35	2.22	5.27	---
Di	46.93	21.07	1.17	11.20	---
Ol	1.74	17.62	41.30	4.94	---
Mt	4.32	2.86	5.23	2.30	---
Lc	3.58	---	---	---	---
Cs	---	---	---	---	---
Hy	---	---	---	---	---
Q	---	---	---	---	---

DI\*

\*DI=Differentiation Index

Table 1. Major element content (weight percent) and CIPW normative mineral composition (percent) of McClure Mountain major rock types (Cont.)

	Malignites			Pyroxenites	
	NK-18	NK-24	NK-27	NK-33	FeP-1
SiO <sub>2</sub>	43.66	42.32	41.43	48.20	50.72
Al <sub>2</sub> O <sub>3</sub>	15.74	12.93	14.90	5.40	9.07
Fe <sub>2</sub> O <sub>3</sub>	10.62	11.71	9.84	7.25	8.70
MgO	4.43	8.96	7.55	13.30	9.91
CaO	9.00	10.46	9.68	18.96	18.40
Na <sub>2</sub> O	6.76	4.17	5.43	0.50	0.71
K <sub>2</sub> O	4.36	4.16	4.50	0.02	0.02
MnO	0.29	0.33	0.24	0.12	0.13
ignition	0.95	1.32	1.49	2.10	0.34
+H <sub>2</sub> O	0.23	0.47	0.24	0.14	0.10
TOTAL	96.07	96.82	95.30	95.99	98.1
C	---	---	---	---	---
Or	1.34	---	---	---	---
Ab	---	---	---	4.23	6.00
An	---	4.27	2.99	12.48	21.54
Ne	30.70	19.11	24.88	---	---
Di	36.23	28.97	22.52	65.02	56.18
Ol	---	16.15	15.38	4.74	---
Mt	6.70	6.09	5.74	1.57	1.93
Lc	19.13	19.25	20.83	---	---
Cs	---	3.59	5.24	---	---
Hy	---	---	---	4.91	8.61
Q	---	---	---	---	2.38
DI*	51.17	38.36	45.71	4.23	8.38

\*DI=Differentiation Index

Table 2. Major element analyses (weight percent) of rock types from selected alkaline complexes.

SAMPLE	Iron Mtn. WM-64-827 Gabbro (1)	Iron Mtn. WM-64-829 Pyroxenite (1)	Iron Mtn. IM-31-64 Anorthosite (1)	Gem Park GP-3 Pyroxenite (2)	Gem Park WM-64-859 Gabbro (2)	Gem Park Nepheline Syenite Pegmatite (2)
*REFERENCE						
SiO <sub>2</sub>	42.81	46.99	51.05	44.50	39.16	59.47
Al <sub>2</sub> O <sub>3</sub>	17.08	11.47	26.94	6.01	13.72	20.53
Fe <sub>2</sub> O <sub>3</sub>	13.85	8.35	2.0	8.87	18.38	2.86
MgO	6.53	10.68	1.29	12.23	6.68	0.15
CaO	13.59	20.02	12.47	20.52	12.12	0.97
Na <sub>2</sub> O	2.18	0.94	3.78	1.83	2.56	8.11
K <sub>2</sub> O	0.22	0.07	0.62	0.18	0.45	8.97
TiO <sub>2</sub>	2.57	1.71	0.28	2.97	4.42	3.25
MnO	0.15	0.13	0.03	0.14	0.21	0.05
CO <sub>2</sub>	0.78	0.03	0.48	---	0.99	---
H <sub>2</sub> O <sup>+</sup>	0.62	0.26	0.92	---	1.06	---
H <sub>2</sub> O <sup>-</sup>	0.07	0.03	0.08	---	0.10	---
	100.45	100.68	99.94	97.25	99.85	104.36

\*(1) Shawe and Parker (1968) (2) Roden (1977) (3) King and Sutherland (1966) (4) Garson (1966)  
(5) Barth and Ramberg (1966) (6) Floor (1974) (7) Gold (1963)

Table 2. Major element analyses (weight percent) of rock types from selected alkaline complexes (Cont.)

SAMPLE	Fenn Malignite (5)	Napak Nepheline Syenite N121 (3)	Average Carbonatite (7)	Glen Dessary Scotland, Biotite Hornblende Syenite (6)	Malawi Carbonatite (4)
*REFERENCE					
SiO <sub>2</sub>	43.75	51.32	11.99	60.43	0.88
Al <sub>2</sub> O <sub>3</sub>	15.77	21.92	3.52	14.45	0.37
Fe <sub>2</sub> O <sub>3</sub>	9.77	8.93	7.24	2.62	4.74
MgO	0.29	0.94	5.59	1.27	0.31
CaO	11.73	3.95	34.80	3.98	53.60
Na <sub>2</sub> O	7.36	7.60	0.42	4.31	0.09
K <sub>2</sub> O	4.17	5.10	1.48	6.47	0.03
TiO <sub>2</sub>	1.48	0.07	0.79	0.69	0.18
MnO	0.25	0.19	0.60	0.10	0.39
CO <sub>2</sub>	3.41	0.16	28.47	0.04	38.38
H <sub>2</sub> O <sup>+</sup>	0.32	0.11	---	0.35	---
H <sub>2</sub> O <sup>-</sup>	0.13	---	---	0.02	0.06
	98.43	100.29	94.9	99.85	96.85

\*(1) Shawe and Parker (1968) (2) Roden (1977) (3) King and Sutherland (1966) (4) Garson (1966)  
 (5) Barth and Ramberg (1966) (6) Floor (1974) (7) Gold (1963)

G-6, and the anorthosite, to metaluminous in the malignites, pyroxenites, and gabbro NK-34 (Hyndman, 1972). The feldspathoidal syenites are miaskitic, as expected in view of the associated carbonatites (Sorensen, 1974). The miaskitic and peraluminous nature of the McClure Mountain rock types is similar to that reported by Shawe and Parker (1968) in their study of the McClure Mountain complex and by Roden (1977) for rocks from nearby Gem Park.

The alkali-lime differentiation index, obtained by plotting ( $\sum \text{Na}_2\text{O} + \text{K}_2\text{O}$ ) versus  $\text{SiO}_2$  and also  $\text{CaO}$  versus  $\text{SiO}_2$  on the same graph and determining their intersection (Fig. 4), indicates that the rocks are alkalic (Peacock, 1931). The graph was constructed using the syenites and malignites and did not include the rocks of the layered series because of their extreme scatter when plotted in the diagram. This scatter is presumably a result of their pronounced cumulate textures and hence misrepresentation of changing magmatic composition.

The normative mineralogy and differentiation index (normative Q + Or + Ab + Ne + le + Kl) of the analyzed samples were calculated and are in Table 1. The FeO contents of the samples were approximated using the equation:

$$\text{Fe}_2\text{O}_3/(\text{FeO} + \text{Fe}_2\text{O}_3) = 0.0281 (\text{weight percent } \text{K}_2\text{O} + \text{Na}_2\text{O}) + 0.148$$

The equation was derived from a linear regression analysis of existing plutonic data (Anderson, personal communication, 1978).

Normative nepheline is present in the syenite, malignite, gabbro, and anorthosite. Both pyroxenites which were analyzed contain normative hypersthene. In addition, one of the pyroxenites, FeP-1, contains a small amount of normative quartz. The differentiation index of the samples increased in the order pyroxenites < gabbros < anorthosite stock < malignite < feldspathoidal syenites < biotite syenites. The nepheline syenite stock has a differentiation index in the range of that obtained for the biotite

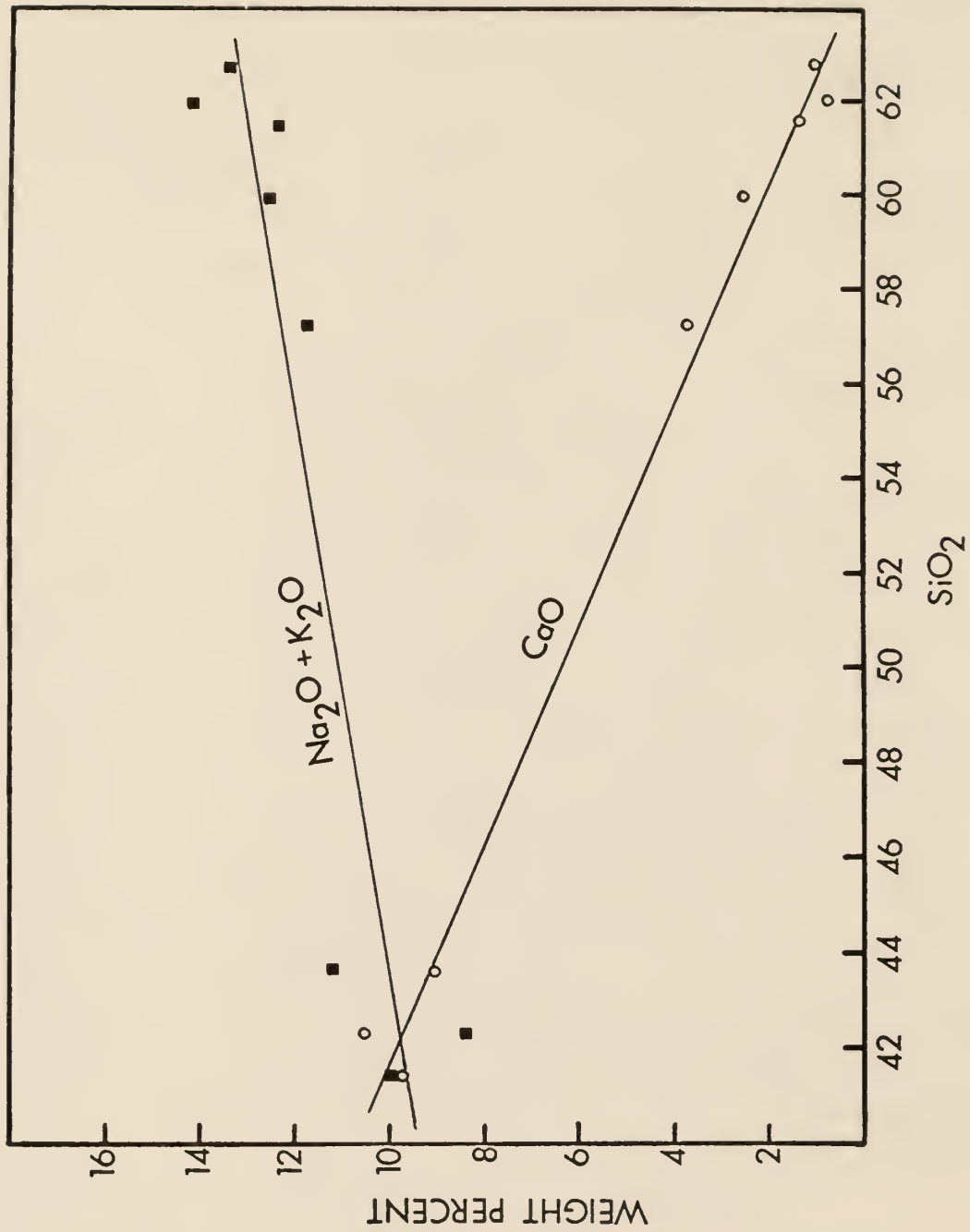


Figure 4. Alkali-lime differentiation index of the McClure Mountain Syenites and Malignites (weight percent) ( $\text{Na}_2\text{O} + \text{K}_2\text{O}$ ; (■);  $\text{CaO}$  (○)).

syenites. A large gap exists between the differentiation index obtained for the malignites and those obtained for the feldspathoidal and biotite syenites.

Major element variation diagrams for rocks of the McClure Mountain complex are obtained from the data both of this report and of Shawe and Parker (1968) (Figs. 5 to 8). Plots of the differentiation index versus the weight percent of the major oxides indicate that the syenites and malignites have smooth trends although some scatter of data is observed (Fig. 5). Trends of the rocks of the layered series are less well defined although in some cases the average trends appear to fall in line with those of the syenites and malignites. The syenites and malignites exhibit increasing  $K_2O$ ,  $Na_2O$ ,  $Al_2O_3$ , and  $SiO_2$ , and decreasing  $CaO$ ,  $MgO$ , and  $Fe_2O_3$  contents with increasing differentiation index. Increasing  $K_2O$ ,  $Na_2O$ , and  $Al_2O_3$ , and decreasing  $MgO$  and  $CaO$  contents are observed in the pyroxenites, gabbros, and anorthosite stock of the layered series with increasing differentiation index. Trends of the  $Fe_2O_3$  and  $SiO_2$  contents of these rocks are not readily discernible.

Plots of the  $CaO/(CaO + Na_2O)$  and  $Fe_2O_3/(Fe_2O_3 + MgO)$  versus  $Al_2O_3$  (Figs. 6 and 7) further exemplify the linear trend of the syenites and malignites and the highly scattered, although somewhat linear trends of the rocks of the layered series. These diagrams suggest increasing  $Na_2O$  and decreasing  $MgO$  contents with a concomitant increase in the  $Al_2O_3$  contents of the syenites and malignites. Similar, less pronounced trends are observed in the rocks of the layered series. Increasing  $Na_2O + K_2O$  contents in the order malignites < feldspathoidal syenites < biotite syenites are observed in the AFM diagram of Figure 8. Samples from the layered series exhibit considerable scatter and as a group do not define linear trends. Data from the analyzed carbonatite dike is also plotted in the diagram. It is highly enriched in



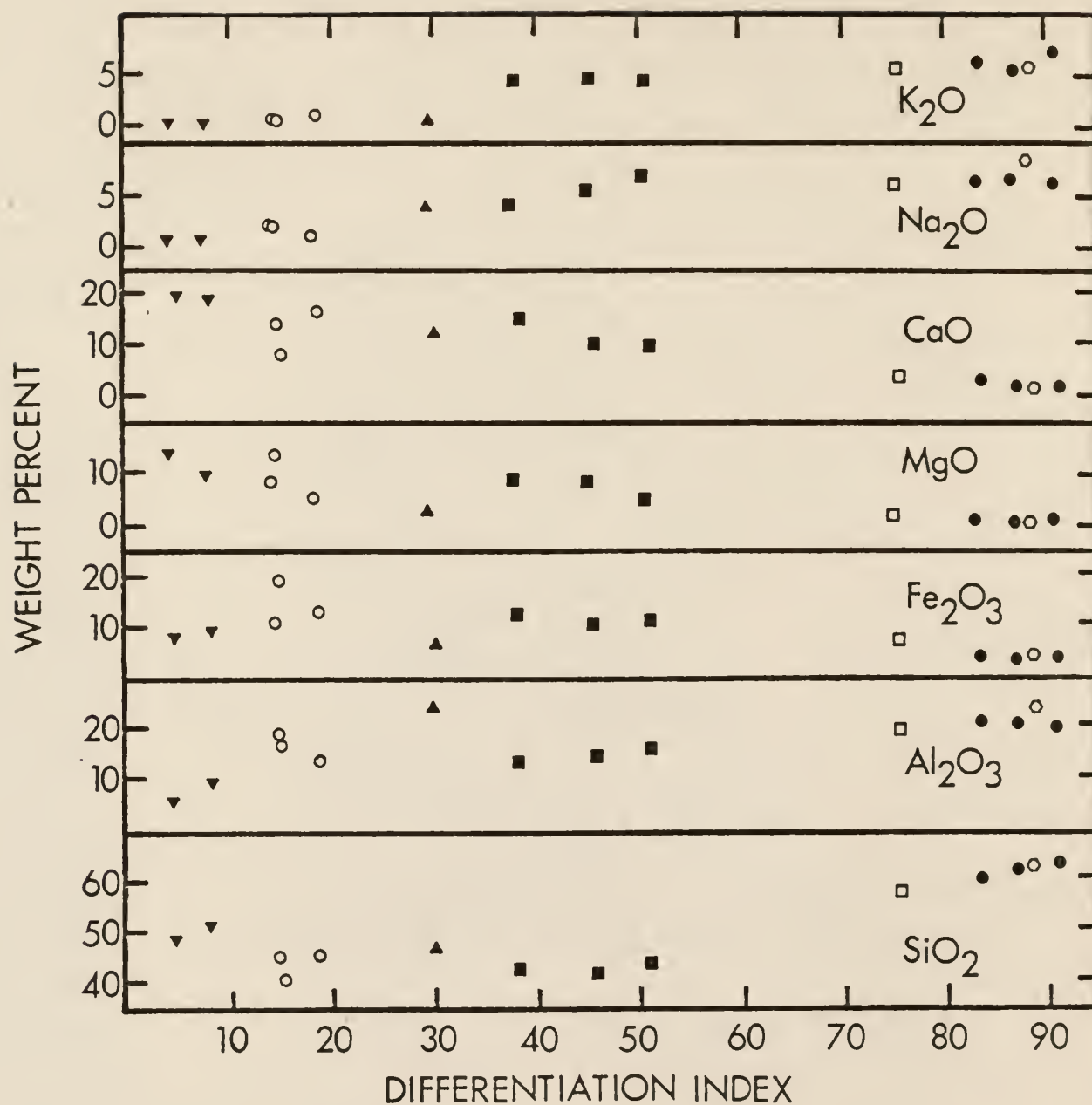


Figure 5. Major element variation diagram for the McClure Mountain complex. Weight percent oxide versus differentiation index. Feldspathoidal syenites ( $\square$ ); biotite syenites ( $\bullet$ ); malignites ( $\blacksquare$ ); pyroxenites ( $\blacktriangledown$ ); gabbros ( $\circ$ ); anorthosite stock ( $\blacktriangle$ ); nepheline syenites stock ( $\circ$ ).



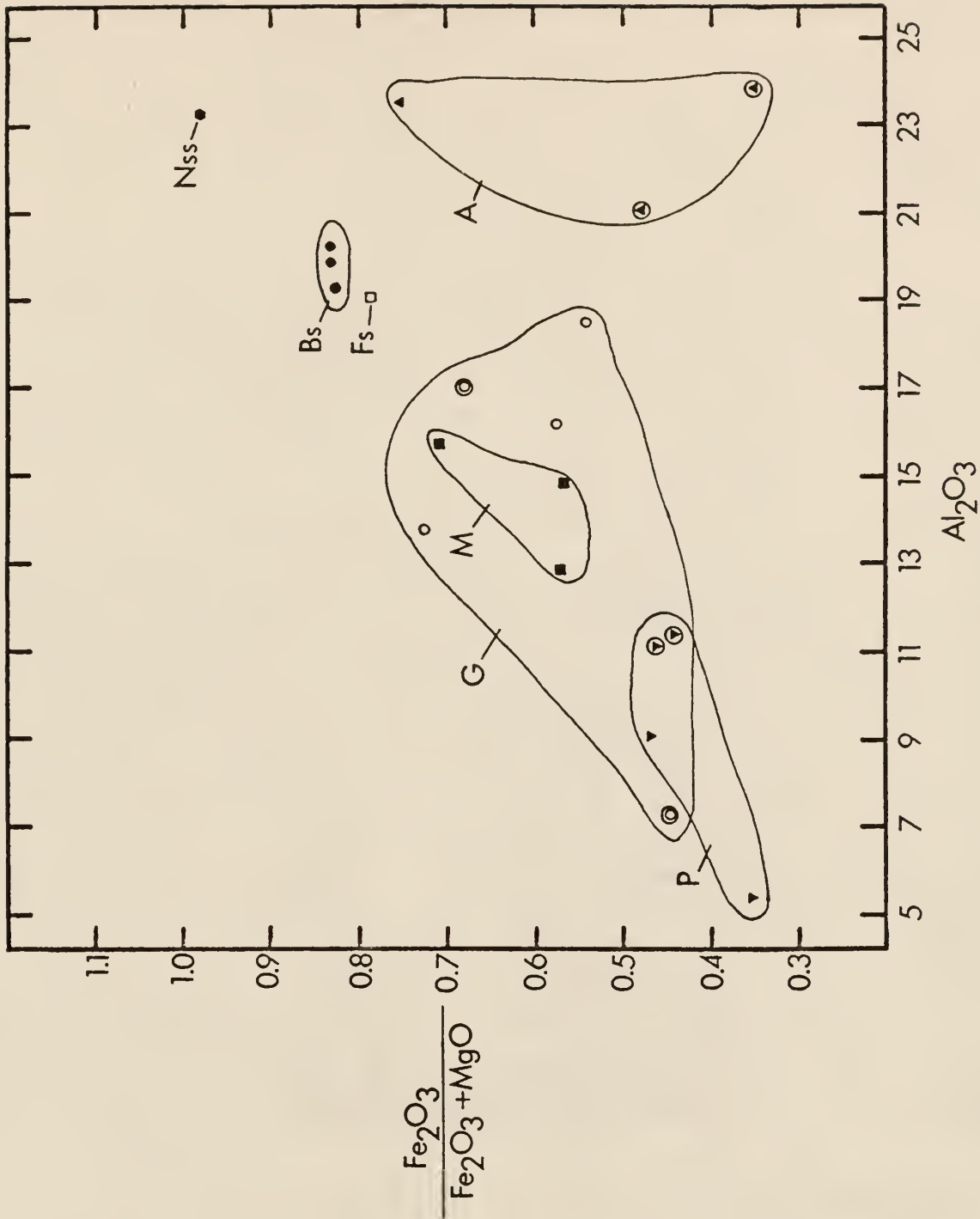


Figure 6. Major element variation diagram for the McClure Mountain complex.  $\text{Fe}_2\text{O}_3 / (\text{Fe}_2\text{O}_3 + \text{MgO})$  ratio versus  $\text{Al}_2\text{O}_3$ . Bs, feldspathoidal syenite ( $\square$ ); Fs, biotite syenites ( $\circ$ ); M, malignites ( $\blacksquare$ ); P, pyroxenites ( $\blacktriangledown$ ); G, gabbros ( $\circ$ ); Nss, nepheline syenite stock ( $\bullet$ ); A, anorthosite stock ( $\blacktriangle$ ). Additional samples from Shawe and Parker (1968) include pyroxenites ( $\odot$ ); gabbros ( $\otimes$ ); anorthosites ( $\triangle$ ).

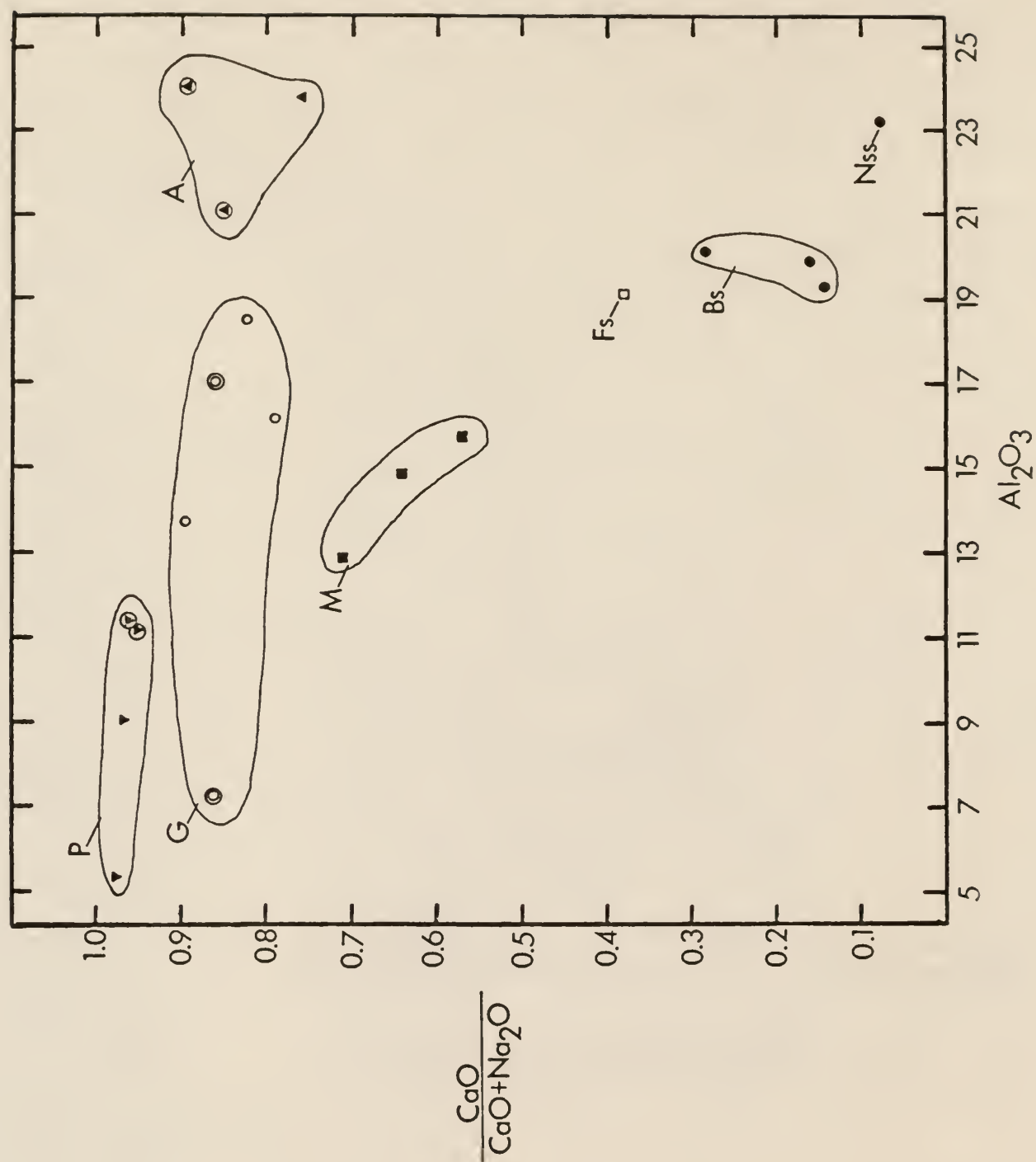


Figure 7. Major element variation diagram for the McClure Mountain complex.  $\text{CaO}/\text{CaO} + \text{Na}_2\text{O}$  ratio versus  $\text{Al}_2\text{O}_3$  (See Figure 6 for explanation of symbols).

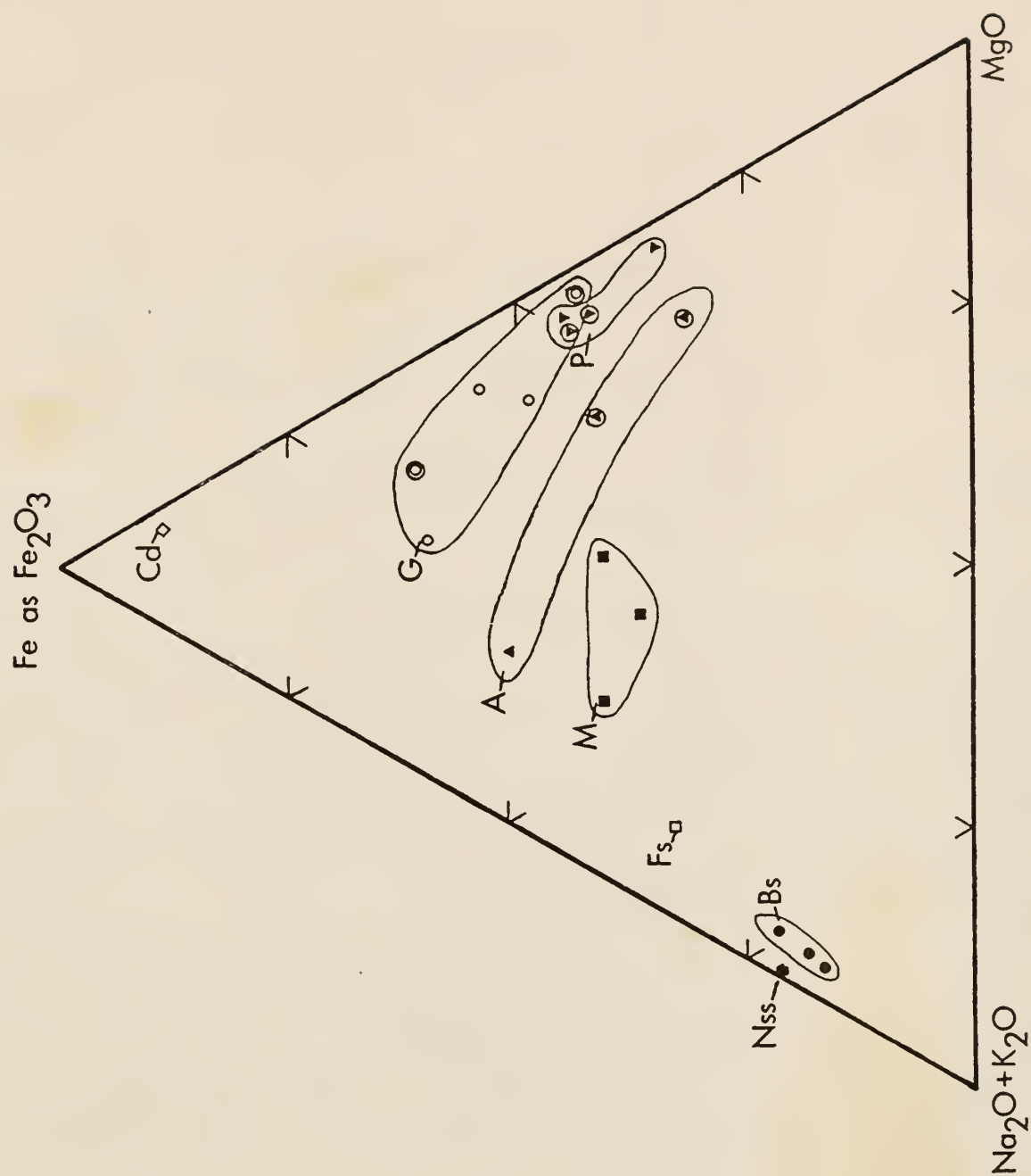


Figure 8. Major element variation diagram for the McClure Mountain complex. AFM diagram (mole percent Fe, Mg, and Na + K). (See Figure 6 for explanation of symbols) Cd, carbonatite dike (■).

Fe with respect to  $MgO$  and  $Na_2O + K_2O$ . The carbonatite dike does not exhibit an obvious chemical relationship with the other rock types.

### Rb-Sr ISOTOPIC RESULTS

The Rb-Sr isotopic data of the following samples from the McClure Mountain complex are in Table 3: pyroxenite, FeP-1; anorthosite, NK-28; carbonatite, NK-32; feldspathoidal syenite, NK-10; biotite syenite, NK-100; malignite, NK-18; and biotite separates, NK-18B and NK-10B from samples NK-18 and NK-10 respectively.

The  $^{87}Sr/^{86}Sr$  initial ratios of pyroxenite P-1, anorthosite NK-28 and carbonatite NK-32 are assumed to be represented by the  $^{87}Sr/^{86}Sr$  ratios of the samples because of their extremely low Rb/Sr ratio. There is considerable variability in the initial ratios of these samples with values ranging from  $0.7044 \pm 0.0005$  to  $0.7078 \pm 0.0005$ .

Initial ratios for samples from other alkalic complexes and from studies of the McClure Mountain complex by this and other investigators are in Table 4. The McClure Mountain carbonatite NK-32 is similar in initial ratio to other analyzed carbonatites from McClure Mountain and Gem Park. The initial ratio of this carbonatite is also similar to initial ratios reported for rocks of different alkalic complexes (Table 3). Initial ratios of  $0.7078 \pm 0.0005$  and  $0.7065 \pm 0.0005$  for pyroxenite P-1 and anorthosite NK-28 respectively are however, significantly greater than those reported for other alkalic complexes and reported values from similar rock types in the McClure Mountain and Gem Park complexes (Olson et al., 1977; Roden, 1977).

Isotopic data for the syenites, malignites, and biotite separates are plotted in a rubidium-strontium evolution diagram (Fig. 9). The carbonatite dike was not included in the diagram because of the potential age differences between it and the major intrusive bodies as suggested by Olson et al. (1977).

Table 3. Rb-Sr isotopic data of samples from the McClure Mountain complex.

Sample	Rb (ppm)	Sr (ppm)	Rb/Sr	$(^{87}\text{Sr}/^{86}\text{Sr})_{\text{corr.}}$ **	$^{87}\text{Rb}/^{86}\text{Sr}$
P-1 Pyroxenite	2.83	243*	0.01	$0.7080 \pm 0.0005$	0.0337
NK-28 Anorthosite	5*	1229*	---	$0.7065 \pm 0.0005$	---
NK-32 Carbonatite	5*	1597*	---	$0.7044 \pm 0.0005$	---
NK-10 Feldspathoidal Syenite	72*	1468*	0.05	$0.7057 \pm 0.0005$	0.14
NK-100 Biotite Syenite	125.0	85.8	1.46	$0.7354 \pm 0.001$	4.23
NK-18 Malignite	128.8	284.3	0.10	$0.7075 \pm 0.0005$	0.29
NK-18B Biotite separate from NK-18	494.1	216.5	2.28	$0.7515 \pm 0.001$	6.64
NK-10B Biotite separate from NK-10	495.6	122.1	4.06	$0.7864 \pm 0.001$	11.84

\*Values determined by X-ray fluorescence.

\*\*Corrected for isotopic fractionation assuming  $^{86}\text{Sr}/^{88}\text{Sr} = 0.1194$

Table 4.  $^{87}\text{Sr}/^{86}\text{Sr}$  initial ratios for select alkalic complexes.

Rock Type	Locality	Reference	$(^{87}\text{Sr}/^{86}\text{Sr})_0$
Pyroxenite (P-1)	McClure Mtn.	This study	$0.7078 \pm 0.0005$
Anorthosite (NK-28) (intrusive)	McClure Mtn.	This study	$0.7065 \pm 0.0005$
Carbonatite (NK-32)	McClure Mtn.	This study	$0.7044 \pm 0.0005$
Carbonatite	McClure Mtn.	Fenton and Faure (1970)	$0.7053 \pm 0.0005$
Anorthosite (layered series)	McClure Mtn.	Olson et al. (1977)	$0.7048$
Gabbro	McClure Mtn.	Olson et al. (1977)	$0.7041$
Anorthosite (layered series)	McClure Mtn.	Olson et al. (1977)	$0.7039$
Carbonatite	Gem Park	Roden (1977)	$0.7036 \pm 0.001$
Carbonatite	Gem Park	Roden (1977)	$0.7037 \pm 0.001$
Carbonatite	Gem Park	Roden (1977)	$0.7056 \pm 0.001$
Carbonatite	Gem Park	Roden (1977)	$0.7038 \pm 0.001$
Carbonatite	Gem Park	Roden (1977)	$0.7035 \pm 0.001$
Carbonatite	Uganda	Bell and Powell (1970)	$0.7035 \pm 0.001$
Carbonatite	Rocky Boy, Mt.	Powell et al. (1966)	$0.7057 \pm 0.0012$
Carbonatite	Oka, Quebec	Powell et al. (1966)	$0.7032 \pm 0.0012$
Nepheline Syenite	Magnet Cove, Ark.	Powell et al. (1966)	$0.7035 \pm 0.0006$
Gabbro	Gem Park	Roden (1977)	$0.7027 \pm 0.001$
Pyroxenite	Gem Park	Roden (1977)	$0.7028 \pm 0.001$
Pyroxenite	Iron Hill, Colo.	Powell et al. (1966)	$0.7013 \pm 0.0014$
Carbonatite	Iron Hill, Colo.	Fenton and Faure (1970)	$0.7051 \pm 0.0003$

In addition, pyroxenite P-1 and anorthosite NK-28 were excluded from the diagram because they did not exhibit colinearity with the other points.

Two separate isochrons were generated for the data in Fig. 9. The slopes of the lines were determined by a least squares analysis modified from York (1969). Ages were calculated from the slopes using the  $^{87}\text{Rb}$  decay constant of  $1.39 \times 10^{-11}$  per year. Isochron A was constructed using the three whole rocks and associated biotite separates, whereas isochron B was constructed using only the whole rocks. Ages of  $493 \pm 5$  M.Y. and  $514 \pm 11$  M.Y. were obtained from isochrons A and B respectively. The age of  $514 \pm 11$  M.Y. obtained using the whole rocks is in good agreement with ages reported for the complex by Olson et al. (1977).

Initial ratios of  $0.7055 \pm 0.0011$  and  $0.7051 \pm 0.0006$  are obtained from the rubidium-strontium evolution diagram. These are similar within the limits of analytical uncertainty, to the initial ratios obtained for McClure Mountain carbonatite NK-32 and anorthosite NK-28, but differ from that of pyroxenite P-1. The initial ratios are similar to those reported from other alkalic complexes (Table 3).

## TRACE ELEMENTS

### General

The trace element contents of the major rock types in the McClure Mountain complex are in Table 5. The calculated La/Lu ratios are obtained from the chondrite-normalized graphs and not from their actual concentration in the samples.  $\text{Eu}^*$  is determined by extrapolation of Sm and Tb on the chondrite-normalized curve to estimate the Eu present assuming no Eu was fractionated and is divided by the chondrite-normalized Eu to obtain  $\text{Eu}/\text{Eu}^*$ . The  $\text{Eu}/\text{Sm}$  and  $\text{Eu}/\text{Eu}^*$  ratios are indications of the degree of Eu depletion or enrichment relative to other REE. For this study an Eu concentration is



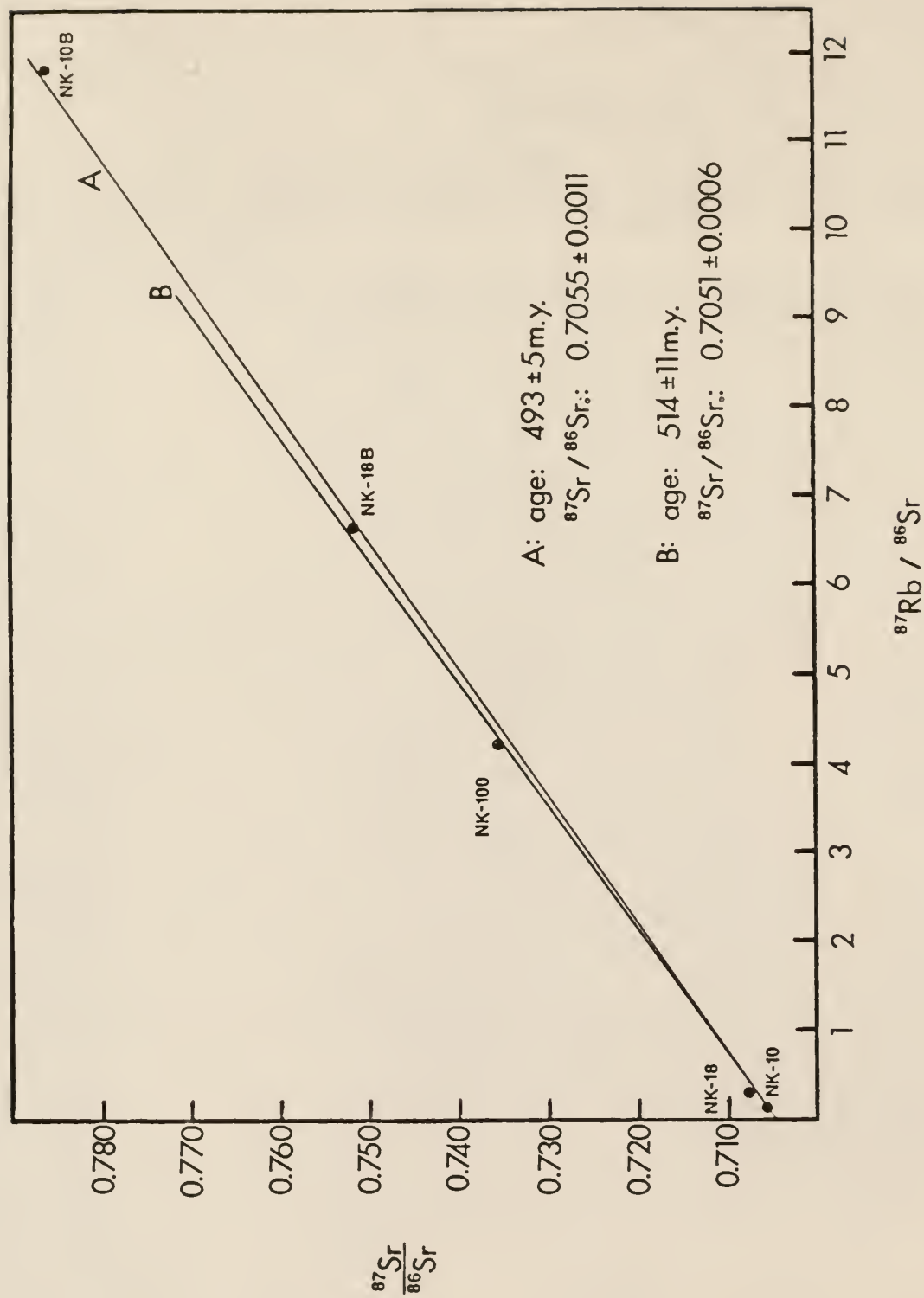


Figure 9. Rb-Sr evolution diagram for the McClure Mountain complex.



considered to be a negative Eu anomaly if the  $\text{Eu}/\text{Eu}^*$  ratio is greater than 1.2. A negative Eu anomaly is defined as an  $\text{Eu}/\text{Eu}^*$  ratio less than 0.8.

The chondrite-normalized plots of the REE contents of the analyzed rocks are in Figures 10 (a-c). The ranges of REE content in the major McClure Mountain rock types are in Figure 11. The REE concentrations of chondrites are considered to be equal to the average terrestrial REE distribution (Haskin et al., 1968). The ranges of the Rb, Ba, Sr, Co, Th, Hf, Ta, and Sc contents of the samples are plotted against the average differentiation index of the major McClure Mountain rock types in Figure 12. Table 6 summarizes the trace element characteristics of the McClure Mountain samples. The general chemical characteristics of the McClure Mountain rock types are stated below.

#### Major Intrusion

Rare Earth Elements.--Analyzed samples of the feldspathoidal syenite, biotite syenite, and malignite have similar relative REE distributions and are each characterized by a positive Eu anomaly (Fig. 10 a). The anomaly is most pronounced in the biotite syenites ( $\text{Eu}/\text{Eu}^* = 2.06$ ;  $\text{Eu}/\text{Sm} = 0.58$ ) and the feldspathoidal syenites ( $\text{Eu}/\text{Eu}^* = 1.86$ ;  $\text{Eu}/\text{Sm} = 0.54$ ), but is less positive in the malignite ( $\text{Eu}/\text{Eu}^* = 1.22$ ;  $\text{Eu}/\text{Sm} = 0.35$ ). The malignites have a similar absolute REE content ( $\sum \text{REE} = 329 \text{ ppm}$ ) as the feldspathoidal syenites ( $\sum \text{REE} = 319 \text{ ppm}$ ), but the biotite syenites are depleted in the REE ( $\sum \text{REE} = 204 \text{ ppm}$ ) with respect to the feldspathoidal syenites and the malignites (Fig. 11). The biotite syenites are more fractionated than the feldspathoidal syenites and malignites having an average La/Lu ratio of 32.0. Feldspathoidal syenites and malignites have similar La/Lu ratios averaging 25.0 and 23.6 respectively.

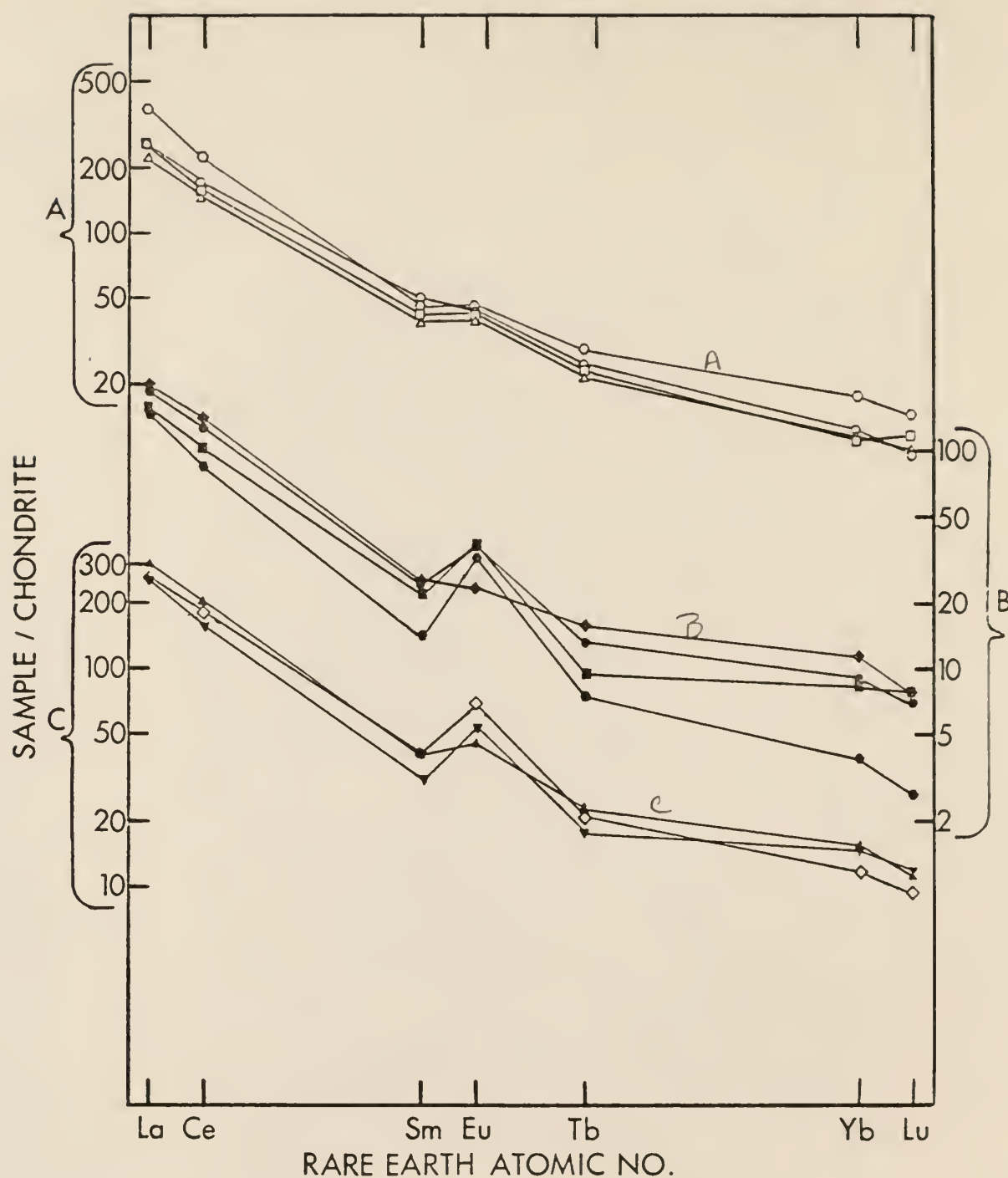


Figure 10a. Chondrite-normalized REE plots for the McClure Mountain complex. (A) Malignites, NK-18 (○), NK-22 (○), NK-24 (Δ), NK-27 (□); (B) Biotite syenites, NK-100 (◆), NK-3 (●), NK-31 (●), FeNS-4 (■); Feldspathoidal syenites, NK-19 (▼), NK-10 (▲), NK-9 (◇).

(C)

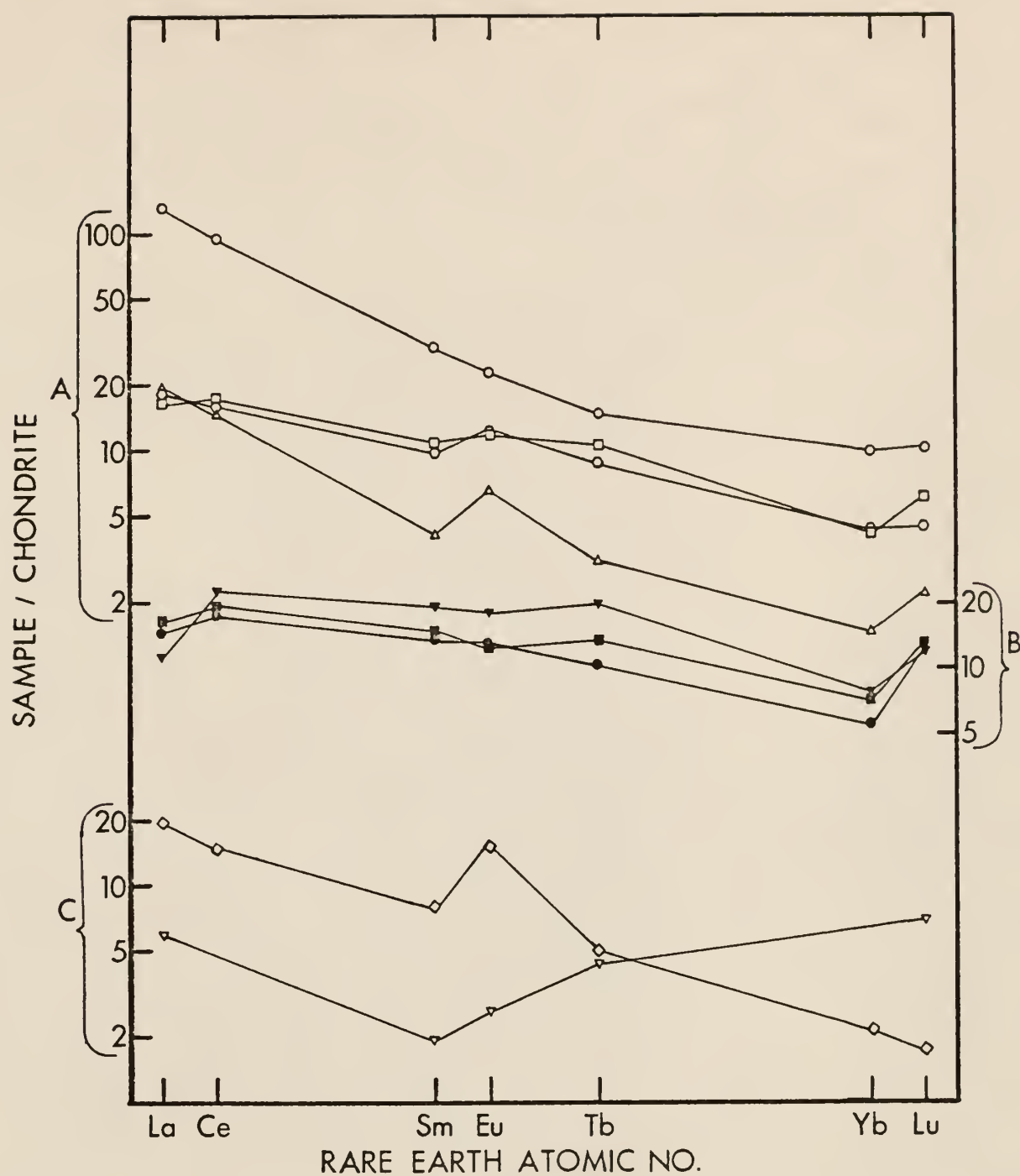


Figure 10b. Chondrite-normalized REE plots for the McClure Mountain complex. (A) Gabbros, NK-34 (○), FeG-1 (○), FeP-3 (□), FeG-6 (Δ); (B) Pyroxenites, NK-29 (●), NK-33 (■), FeP-1 (▼); (C) Anorthosite, NK-28 (◇); Magnetite ore, NK-1 (▽).

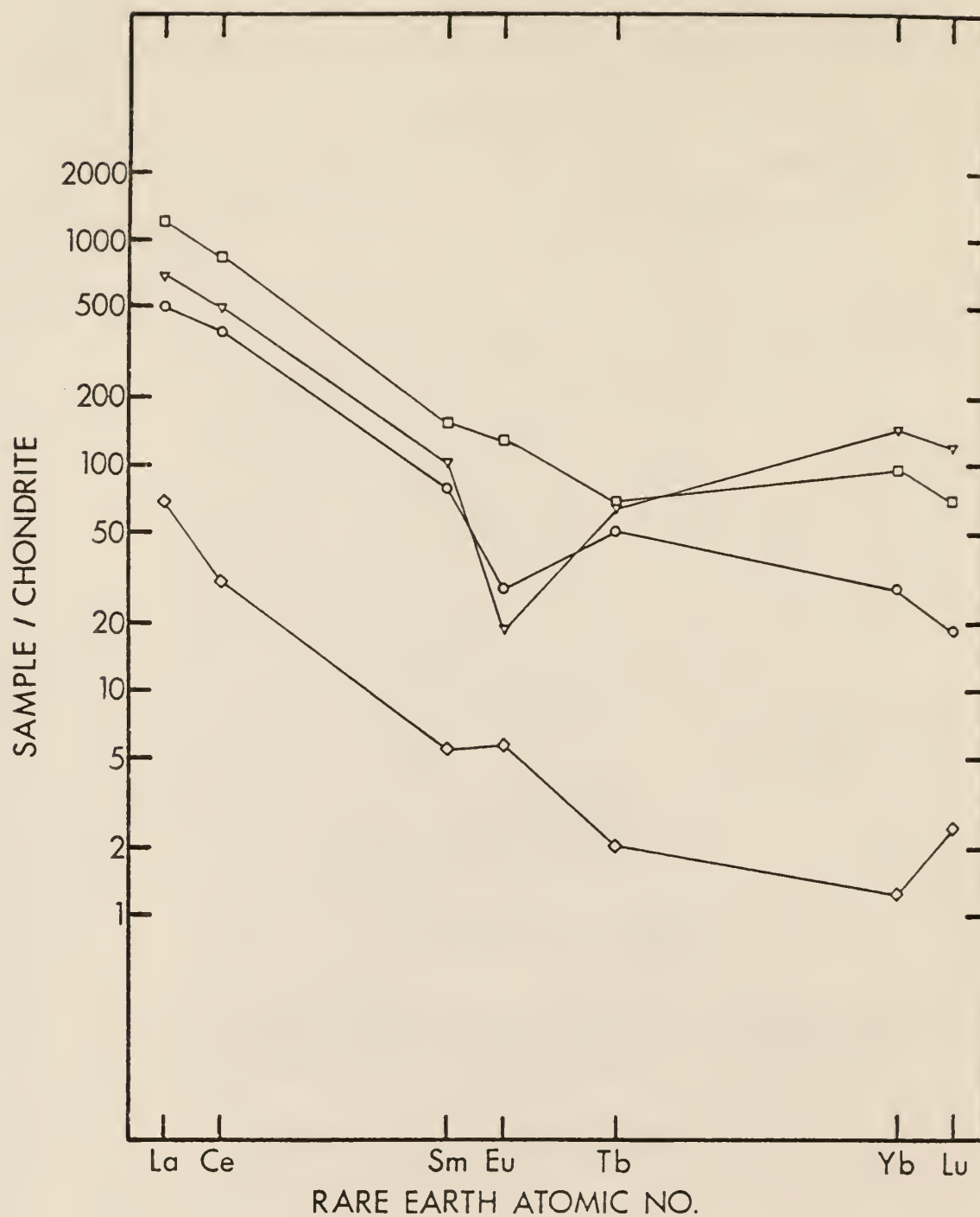


Figure 10c. Chondrite-normalized REE plots for the McClure Mountain complex. Carbonatite (□); nepheline syenite dikes and stocks, NK-4 (○), NK-23 (◇), FeNS-10 (▽).

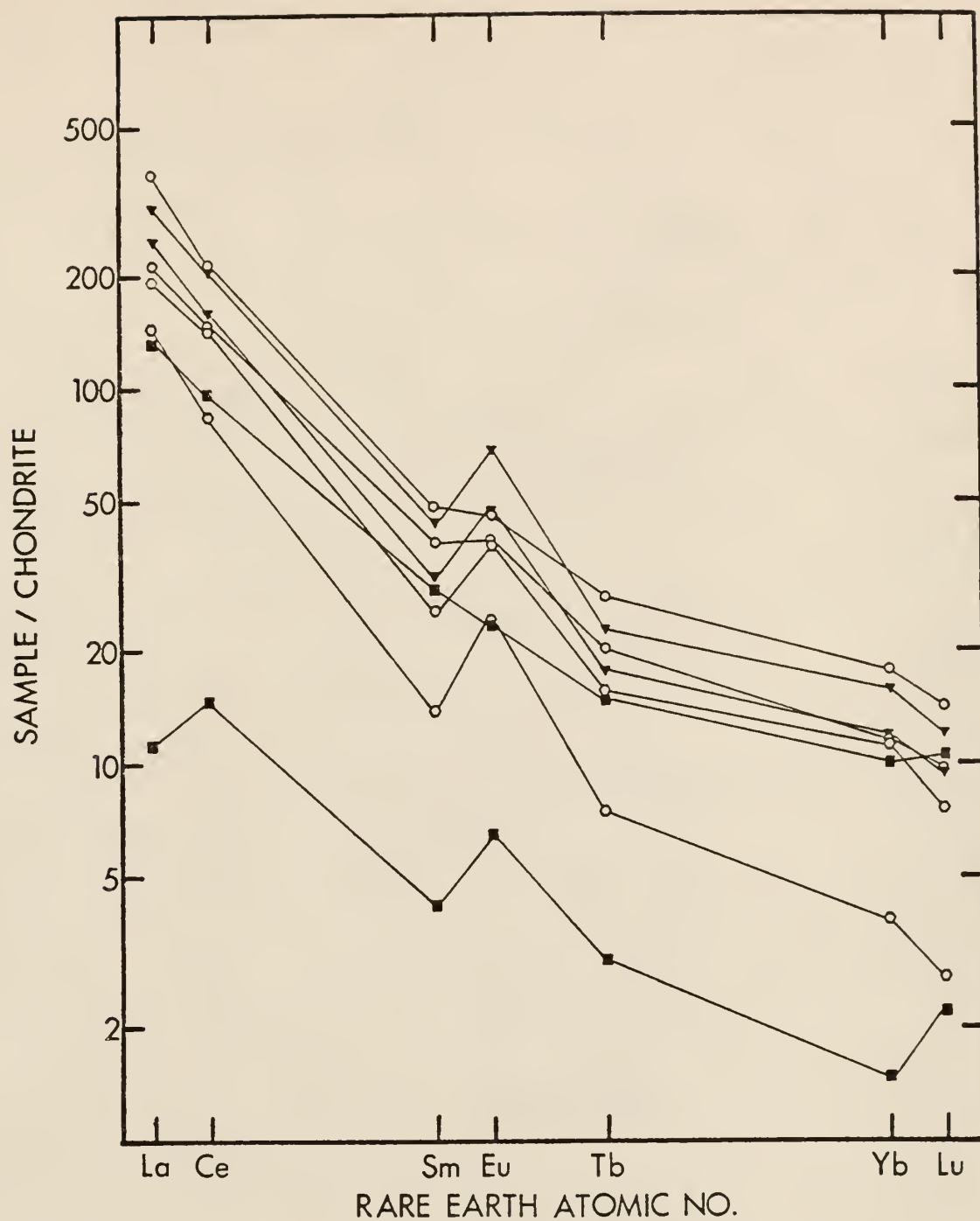


Figure 11. Chondrite-normalized ranges of the REE content in the major McClure Mountain rock types. Malignites (○), Biotite syenites (○), Feldspathoidal syenites (▼), Pyroxenites and Gabbros (■).

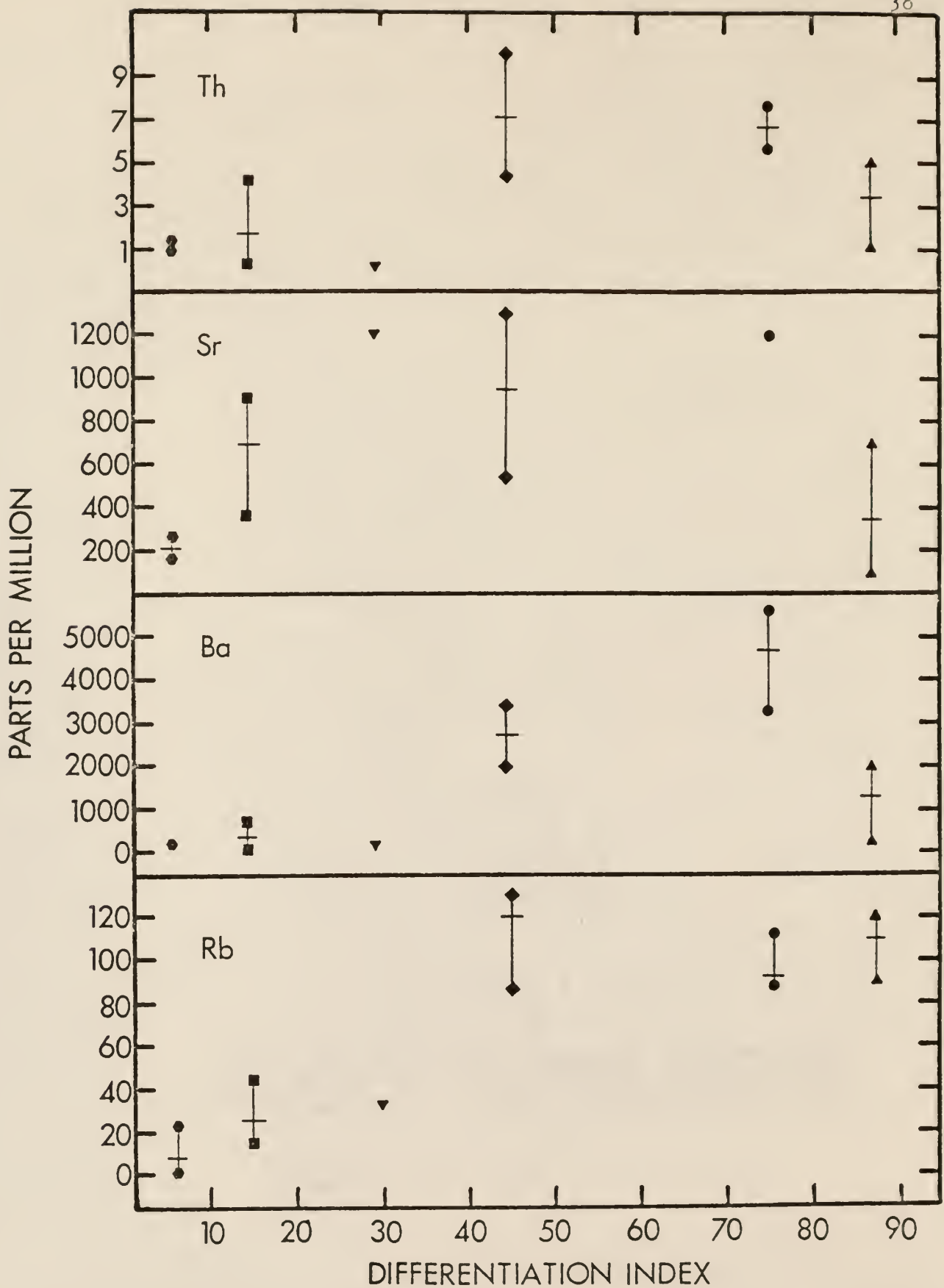


Figure 12. Range of trace elements plotted against average differentiation index for the McClure Mountain intrusives: Pyroxenites (●), Gabbros (■), Anorthosite stock (▼), Malignites (◆), Feldspathoidal syenites (●), Biotite syenites (▲). Perpendicular lines represent average values.



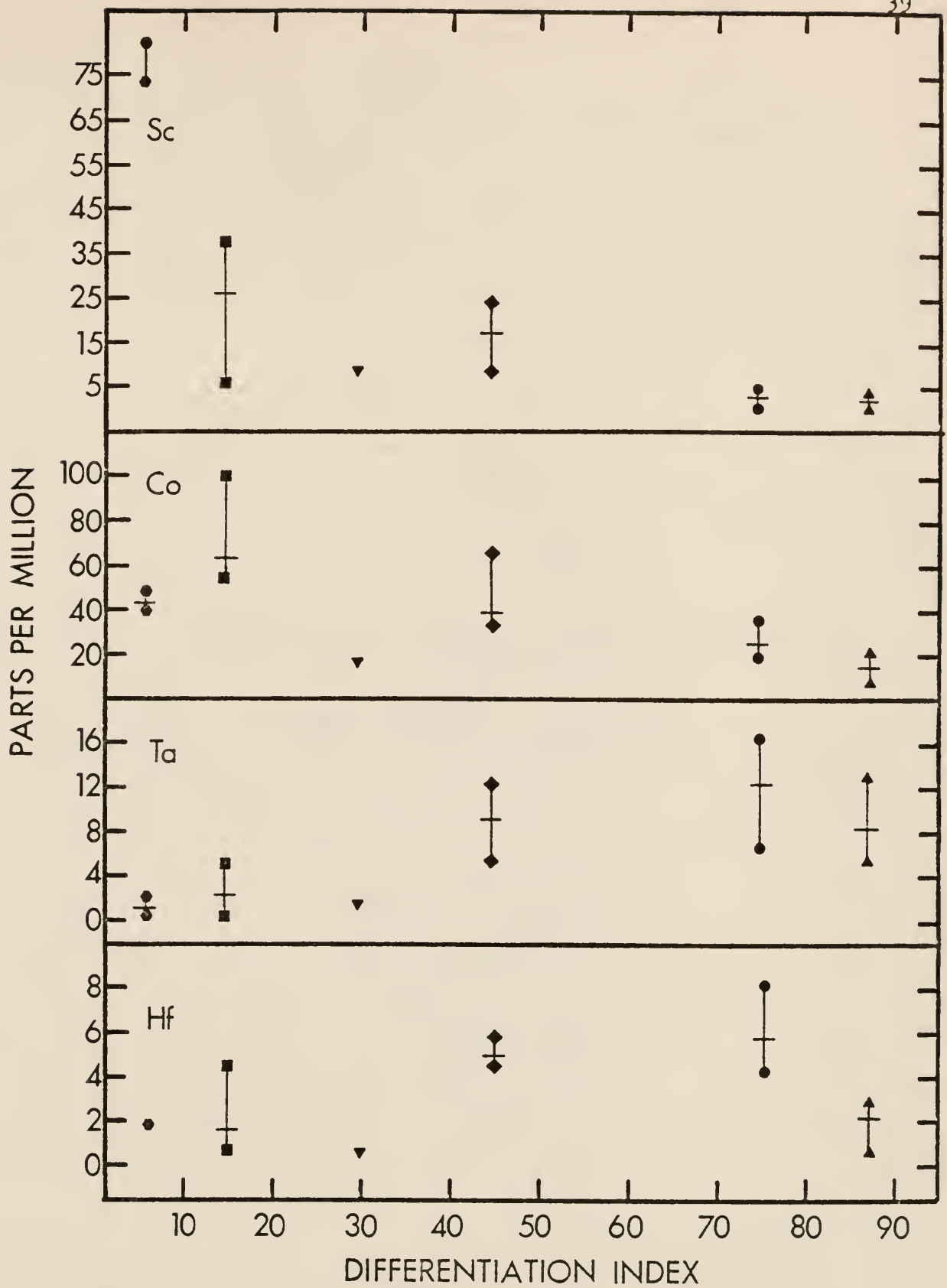


Figure 12. Range of trace elements plotted against average differentiation index for the McClure Mountain intrusives (Cont.)

Samples of the same rock type have similar REE contents, although one sample of biotite syenite was however depleted in heavy REE content with respect to other analyzed samples of this rock type. In addition, samples of the feldspathoidal syenites and biotite syenites exhibit some scatter in the size of their Eu anomalies.

McClure Mountain syenites and malignites have similar relative REE distributions to ijolites from both the Fen (Mitchell and Brunfelt, 1975) and Seabrook Lake (Cullers and Medaris, 1977) alkalic complexes (Fig. 13). They are also similar except for their Eu anomalies, to nepheline syenites and malignites from the Fen complex (Mitchell and Brunfelt, 1975) (Fig. 13). The feldspathoidal syenites differ markedly in relative and absolute REE content from a nepheline syenite pegmatite reported by Roden (1977) from the neighboring Gem Park complex.

Other Trace Elements.--Considerable scatter in the other analyzed trace elements among different samples of similar rock types is observed in the biotite syenites, feldspathoidal syenites, and malignites (Figs. 12 and 13). Ta and Rb contents are similar in the analyzed samples of the three rock types. The Sr, Th, and Hf contents of the malignites and feldspathoidal syenites overlap but are greater in these rocks than in the biotite syenites. Likewise, the feldspathoidal syenites and biotite syenites have similar Sc contents, but they are much less than Sc in the malignites. Co and Ba contents exhibit systematic changes among the rock types, Co increasing in the order biotite syenite < feldspathoidal syenite < malignite and Ba increasing in the order biotite syenite < malignite < feldspathoidal syenite.

Feldspathoidal syenites and biotite syenites from the McClure Mountain complex have Rb, Sr, Th, Ta, and Sc contents similar to nepheline syenites reported by Gerasimovsky (1974) (Table 7). Ba and Sc contents are greater and Hf contents lower in the McClure Mountain syenites than those reported

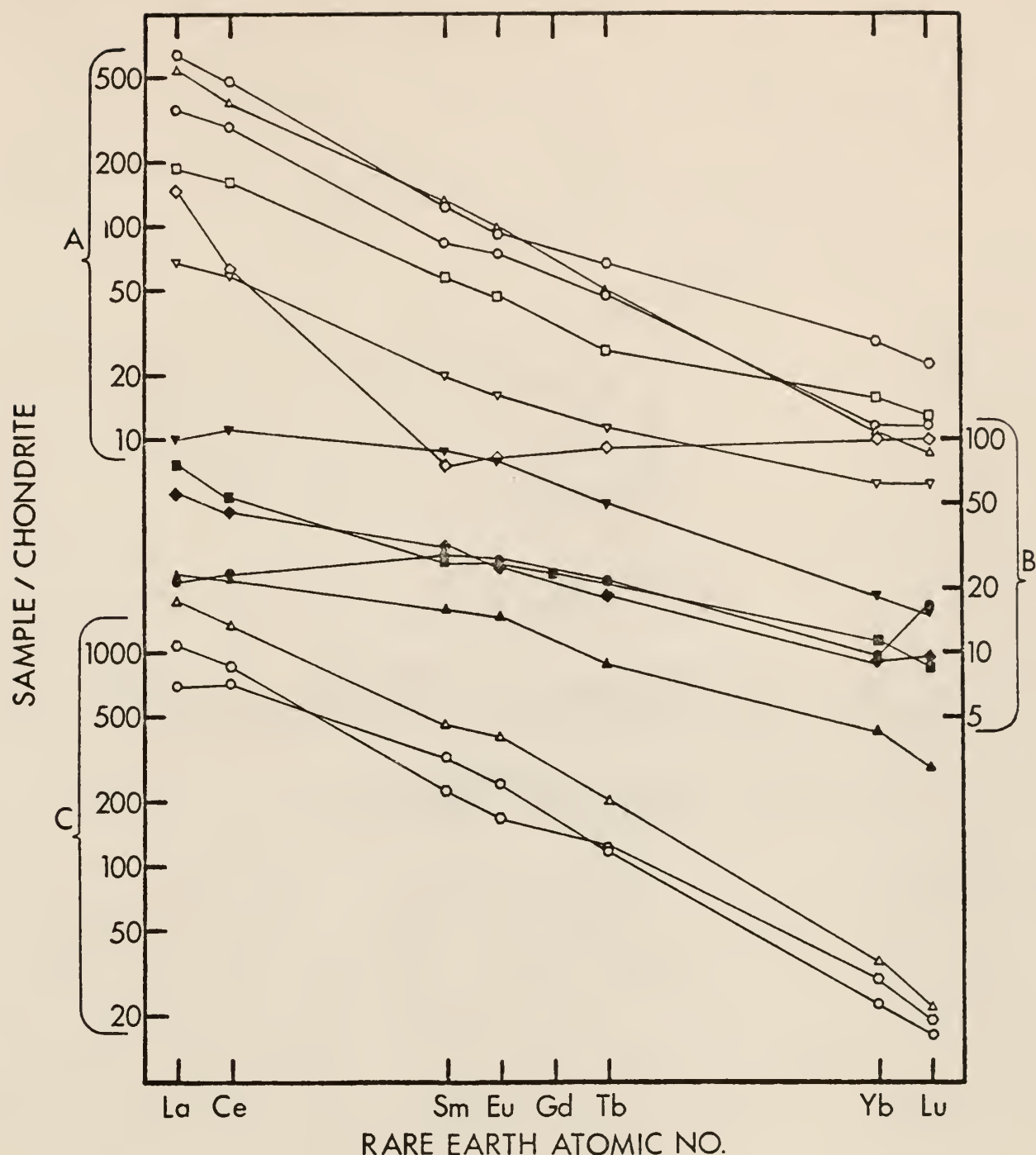


Figure 13. Chondrite-normalized REE distribution for rocks from select alkaline complexes. (A) From Mitchell and Brunfelt (1975) (Fenn Complex); Ijolites 34 (○) and 115 (□), Nepheline Syenite 203 (▽), Malignite 116 (○); From Roden (1977) (Gem Park Complex); Nepheline syenite Pegmatite GP-4 (◇); From Cullers and Medaris (1977) (Seabrook Lake Complex); Ijolite 19 (Δ). (B) From Roden (1977) (Gem Park Complex); Pyroxenites G-P-3 (▽) and G-P-6 (▲), Gabbros G-P-1g (●) and G-P-24 (◆); From Kay and Gast (1973); Alkali basalt 04 (■). (C) From Roden (1977) (Gem Park Complex); Carbonatite G-P-6b (○); From Cullers and Medaris (1977) (Seabrook Lake Complex); Carbonatite 5A (Δ); From Mitchell and Brunfelt (1975); Carbonatite 88 (○).

Table 5. Trace element contents of the McClure Mountain rock samples.

	FeNS-10 Nepheline Syenite Stock	NK-10 Nepheline Bearing Syenite	NK-9 Nepheline Cancrinite Syenite	NK-19 Foidal Syenite	NK-4 Sodalite Syenite Dike	NK-23 Nepheline Syenite	FeNS-4 Biotite Syenite	NK-3 Biotite Syenite
Rb	$2.0 \times 10^2$	89	77	$1.1 \times 10^2$	$1.7 \times 10^2$	$2.0 \times 10^2$	$1.1 \times 10^2$	$1.1 \times 10^2$
Ba	$4.9 \times 10^2$	$3.3 \times 10^3$	$5.6 \times 10^3$	$5.2 \times 10^3$	---	$5.7 \times 10^2$	$2.0 \times 10^3$	$1.9 \times 10^3$
Sr	$1.7 \times 10^2$	$1.2 \times 10^3$	---	---	52	---	$7.0 \times 10^2$	---
Th	118	7.1	7.5	5.6	11.9	3.0	5.0	3.2
Hf	51.4	5.1	4.3	8.0	8.2	1.0	2.8	2.8
Ta	90.2	14.0	16.5	6.9	49.5	4.0	5.7	12.8
Co	5.2	21.6	19.3	34.6	22.1	23.6	8.0	21.2
Sc	0.6	3.7	1.1	4.5	3.0	0.2	2.7	3.2
La	207	91.7	75.9	75.9	150	20.4	46.8	55.8
Ce	414	172	153	133	331	25.6	85.0	106.0
Sm	21.2	8.3	8.5	6.6	16.6	1.1	4.5	4.9
Eu	1.4	3.4	5.2	4.0	2.1	0.43	2.8	2.8
Tb	3.2	1.1	1.0	0.87	2.5	0.10	0.45	0.64
Yb	24.4	2.6	2.0	2.5	4.9	0.21	1.4	1.6
Lu	3.7	0.36	0.30	0.37	0.58	0.08	0.24	0.21
REE*	909.72	371.30	287.94	296.48	677.37	59.81	187.76	227.40
La/Lu**	5.72	26.64	27.13	21.17	26.94	27.90	20.36	27.05
Eu/Sm	0.06	0.41	0.61	0.60	0.13	0.38	0.62	0.56
Eu/Eu*	0.22	1.42	2.09	2.06	0.42	1.49	2.36	1.96

\*REE not analyzed were estimated from chondrite-normalized curves.

\*\*Chondrite-normalized ratio.

Table 5. Trace element contents of the McClure Mountain rock samples (Cont.)

	NK-31		NK-100		NK-18	NK-22	NK-24	NK-27	FeG-1	FeG-6
	Biotite Syenite	Syenite	Biotite Syenite	Syenite	Malignite	Malignite	Malignite	Malignite	Gabbro	Gabbro
Rb	89		$1.2 \times 10^2$	$1.3 \times 10^2$		86	$1.3 \times 10^2$	$1.2 \times 10^2$	15	19
Ba	$1.2 \times 10^3$		$2.9 \times 10^2$	$2.0 \times 10^3$		$2.5 \times 10^3$	$3.2 \times 10^3$	$3.4 \times 10^3$	$1.2 \times 10^2$	$1.2 \times 10^2$
Sr	$2.6 \times 10^2$		86	$1.3 \times 10^3$		---	$5.5 \times 10^2$	$1.0 \times 10^3$	$8.2 \times 10^2$	$8.7 \times 10^2$
Th	1.1		4.3	9.8		10.1	4.4	4.4	0.6	0.4
Hf	0.6		2.7	5.6		5.2	4.6	4.7	0.6	0.5
Ta	5.4		10.0	9.2		12.2	9.9	5.5	5.0	0.5
Co	11.0		20.7	34.5		46.3	42.2	33.7	54.8	99.4
Sc	0.4		3.3	8.3		21.4	23.4	15.2	24.3	5.6
La	43.7		59.4	111		75.2	63.9	75.5	5.4	5.7
Ce	70.4		117	180		139.7	124	136	13.3	12.4
Sm	2.9		5.2	9.7		10.2	8.1	8.7	2.0	0.87
Eu	2.4		1.7	3.4		3.2	2.9	3.2	0.89	0.48
Tb	0.36		0.76	1.4		1.2	1.0	0.98	0.43	0.15
Yb	0.66		1.9	3.0		2.1	2.0	2.0	0.73	0.25
Lu	0.08		0.24	0.44		0.30	0.31	0.37	0.14	0.07
REE*	154.96		246.24	410.09		321.38	277.99	307.22	39.22	28.53
La/Lu**	54.79		25.89	26.12		26.10	21.12	21.21	4.14	8.70
Eu/Sm	0.82		0.33	0.35		0.32	0.36	0.37	0.44	0.55
Eu/Eu*	2.85		1.09	1.17		1.15	1.24	1.33	1.28	1.98

\*REE not analyzed were estimated from chondrite-normalized curves. \*\*Chondrite-normalized ratio.



Table 5. Trace element contents of the McClure Mountain rock samples (Cont.)

	FeP-3 Gabbro	NK-34 Gabbro	FeP-1 Pyroxenite	NK-33 Pyroxenite	NK-29 Pyroxenite	NK-1 Magnetite Ore	NK-28 Anorthosite	NK-32 Carbonatite
Rb	---	43	2.8	1.7	21	---	32	---
Ba	84	$6.3 \times 10^2$	$1.6 \times 10^2$	---	$1.0 \times 10^2$	---	$1.5 \times 10^2$	$1.0 \times 10^3$
Sr	---	$3.6 \times 10^2$	$2.5 \times 10^2$	$1.7 \times 10^2$	---	---	$1.2 \times 10^3$	$3.1 \times 10^3$
Th	---	4.1	---	1.4	1.0	0.4	0.2	17.4
Hf	1.2	4.3	1.8	1.9	1.7	2.7	0.5	2.3
Ta	0.6	2.7	1.9	0.6	0.8	0.3	1.3	20.3
Co	60.1	35.0	43.2	46.6	40.3	235	15.9	3.9
Sc	34.9	37.8	81.0	80.6	73.9	14.6	8.7	3.4
La	4.9	49.3	3.4	4.9	4.3	1.8	6.0	360
Ce	14.3	80.1	18.8	16.2	14.6	---	12.6	706
Sm	2.3	6.1	3.9	3.1	2.8	0.40	1.7	31.8
Eu	0.88	1.7	1.3	0.92	0.94	0.19	1.1	9.5
Tb	0.51	0.71	0.96	0.65	0.51	0.21	0.25	3.3
Yb	0.71	1.7	1.3	1.2	0.94	---	0.37	16.0
Lu	0.19	0.33	0.38	0.41	0.39	0.22	0.06	2.2
REE*	41.76	182.26	58.88	49.83	43.91	14.19	34.86	1476.8
La/Lu **	2.67	12.36	0.91	1.24	1.15	0.84	11.27	17.11
Eu/Sm	0.39	0.28	0.34	0.30	0.34	0.47	0.67	0.30
Eu/Eu*	1.11	0.99	0.94	0.87	1.04	1.03	2.22	1.11

\*REE not analyzed were estimated from chondrite-normalized curves.

\*\*Chondrite-normalized ratio.



Table 6. Summary of trace element data (ppm); parentheses indicate average value.

Units	Rb	Ba	Sr	Th	Hf	Ta
Malignite	86 - $1.3 \times 10^2$ ( $1.2 \times 10^2$ )	$2.0 \times 10^3$ - $3.4 \times 10^3$ ( $2.8 \times 10^3$ )	$5.5 \times 10^2$ - $1.3 \times 10^3$ ( $9.5 \times 10^2$ )	4.4 - 10.1 (7.2)	4.6 - 5.6 (5.0)	5.5 - 12.2 (9.2)
Feldspathoidal Syenites	89 - $1.1 \times 10^2$ (92)	$3.3 \times 10^3$ - $5.6 \times 10^3$ ( $4.7 \times 10^3$ )	$1.2 \times 10^3$ -	5.6 - 7.5 (6.7)	4.3 - 8.0 (5.8)	6.9 - 16.5 (12.5)
Biotite Syenites	89 - $1.2 \times 10^2$ ( $1.1 \times 10^2$ )	$2.9 \times 10^2$ - $2.0 \times 10^3$	$86 - 7.0 \times 10^2$ ( $3.5 \times 10^2$ )	1.1 - 5.0 (3.4)	0.6 - 2.8 (2.2)	5.4 - 12.8 (8.5)
Gabbro	15 - 43 (26)	$84 - 68 \times 10^2$ ( $3.2 \times 10^2$ )	$3.6 \times 10^2$ - $8.7 \times 10^2$ ( $6.8 \times 10^2$ )	0.4 - 4.1 (1.7)	0.5 - 4.3 (1.6)	0.5 - 5.0 (2.2)
Pyroxenite	2 - 21 (8)	$1.0 \times 10^2$ - $1.6 \times 10^2$ ( $1.3 \times 10^2$ )	$1.7 \times 10^2$ $2.5 \times 10^2$ ( $2.1 \times 10^2$ )	1.0 - 1.4 (1.2)	1.7 - 1.9 (.18)	0.6 - 1.9 (1.1)
Magnetite Ore	---	---	---	0.4	2.7	0.3
Anorthosite Stock	32	$1.5 \times 10^2$	$1.2 \times 10^3$	0.2	0.5	1.3
Carbonatite Dike	---	$1.0 \times 10^3$	$3.1 \times 10^3$	17.4	2.3	20.3
Feldspathoidal Dikes, Stocks	$1.7 \times 10^2$ - $2.0 \times 10^2$ ( $1.9 \times 10^2$ )	$4.9 \times 10^2$ - $5.7 \times 10^2$ ( $5.3 \times 10^2$ )	$52 - 1.7 \times 10^2$ $1.7 \times 10^2$ ( $1.1 \times 10^2$ )	3.0 - 118 (44.3)	1.0 - 51.4 (20.2)	4.0 - 90.2 (47.9)

Table 6. Summary of trace element data (ppm); parentheses indicate average value (Cont.)

Units	Co	Sc	$\Sigma$ REE	La/Lu	Eu/Sm	Eu/Eu*
Malignite	33.7 - 64.3 (39.2)	8.3 - 23.4 (17.1)	278 - 410 (329)	21.1 - 26.1 (23.6)	0.32 - 0.37 (0.35)	1.15 - 1.33 (1.22)
Feldspathoidal Syenites	19.3 - 34.6 (25.2)	1.1 - 4.5 (3.1)	288 - 371 (319)	21.2 - 27.1 (25.0)	0.41 - 0.61 (0.54)	1.42 - 2.09 (1.86)
Biotite Syenites	8.0 - 21.2 (15.2)	0.4 - 3.3 (2.4)	155 - 246 (204)	20.4 - 54.8 (32.0)	0.33 - 0.82 (0.58)	1.09 - 2.85 (206)
Gabbro	54.8 - 99.4 (62.3)	5.6 - 37.8 (25.6)	29 - 182 (72.9)	2.7 - 12.4 (7.0)	0.28 - 0.55 (0.42)	0.99 - 1.98 (1.34)
Pyroxenite	40.3 - 46.6 (43.4)	73.9 - 81.0 (78.5)	44 - 59 (51)	0.9 - 1.2 (1.1)	0.30 - 0.34 (0.33)	0.87 - 1.04 (0.95)
Magnetite Ore	235	14.6	14	0.8	0.47	1.03
Anthrosite Stock	15.9	8.7	35	11.3	0.67	2.22
Carbonatite Dike	3.9	3.4	1477	17.1	0.30	1.11
Feldspathoidal Dikes, Stocks	5.2 - 23.6 (17.0)	0.2 - 3.0 (1.3)	60 - 910 (549)	5.7 - 27.9 (20.2)	0.06 - 0.38 (0.19)	0.22 - 1.49 (0.71)

by Gerasimovsky (1974). Malignites from McClure Mountain have trace element contents intermediate between those reported by Gerasimovsky (1974) for alkaline ultramafic rocks and nepheline syenites from other alkaline complexes (Table 7).

### Layered Series

Rare Earth Elements.--The relative distributions of the analyzed gabbros, pyroxenites, magnetite ore, and anorthosite stock of the layered series are generally different from one another (Table 6, Fig. 10b), although some similarities between rock types exist. Gabbros FeP-3 and FeG-1, for example, have relative REE distributions which resemble those of the analyzed pyroxenites. In addition, gabbro FeG-6 has a relative REE distribution similar to that of the anorthosite stock NK-28. A positive Eu anomaly is present in the anorthosite stock and also in two of the four analyzed gabbros, but the pyroxenites and the magnetite ore do not exhibit Eu anomalies. The pyroxenites have a similar absolute REE content as the anorthosite stock, but the pyroxenites are depleted in the REE with respect to the gabbros. The magnetite ore is strongly depleted in total REE.

The greatest amount of REE fractionation in the rocks of the layered series is exhibited by gabbro NK-34. As a group, however, the gabbros are not as fractionated as the anorthosite stock. The pyroxenites and the magnetite ore are not as strongly fractionated as the gabbros or the anorthosite stock. A trend of increasing  $\text{Eu}/\text{Eu}^*$  ratio with increasing  $\text{La}/\text{Lu}$  ratio is observed in the gabbros. This trend, however, was not recognized in the other rocks of the layered series or in the other units in the complex.

Scatter in relative and absolute REE content among different samples of the same rock type is a minimum in the pyroxenites but is of a considerable magnitude in the gabbros (Fig. 10b). Gabbro NK-34 is enriched in lightREE with respect to the other gabbros resulting in its having a higher

Table 7. Trace elements from other alkaline complexes.

	Nepheline Syenites (1)* (Range in 6 alkali centers)	Alkaline Ultramafic Rocks (1)* Kola Peninsula	Maimecha-Katuj Province	Alkali Basalts (2)* Formosa
Rb	85 - 950	80	---	20 - 67
Ba	19 - 2400	850	30 - 1500	---
Sr	47 - 3500	1300	10 - 3000	555 - 883
Th	0.55 - 38	90	1.4 - 180	4.0 - 7.2
Hf	8.5 - 97	5.1	---	4.2 - 7.1
Ta	1.7 - 60	34	---	---
Co	5 - 13	15	1 - 1000	27 - 60
Sc	---	24	5 - 30	11 - 27

\*(1) Gerasimovsky (1974) (2) Lo and Góles (1976)

absolute REE content and La/Lu ratio, and gabbro FeG-6 is depleted in the heavy REE with respect to the other gabbros.

The absolute and relative REE contents of the rocks of the layered series are different from those of the major intrusion (feldspathoidal syenite, biotite syenite, malignite), although some overlap exists. Rocks of the layered series are lower in total REE and light REE contents than the major intrusive syenites and malignites.

McClure Mountain pyroxenites have similar relative REE distributions but are depleted in absolute REE contents compared to pyroxenites from Gem Park (Roden, 1977) (Fig. 14). Two McClure Mountain gabbros (FeP-3, FeG-1) are similar to Gem Park gabbros (Roden, 1977) in relative REE distributions (Fig. 14). These McClure Mountain gabbros are strongly depleted in light REE contents when compared to alkali basalts reported by Kay and Gast (1973) (Fig. 14).

Other Trace Elements.--Other analyzed trace element contents usually exhibit considerable overlap among the rocks of the layered series (Figs. 12 and 13). Trends of these elements are, therefore, not as well defined as those of the syenites and malignites. Ba and Hf contents, for example, are similar in all rock types. Co is strongly enriched in the magnetite ore with respect to the gabbros and pyroxenites. The gabbros and pyroxenites are, however, more enriched in Co than the anorthosite stock. Rb is slightly more concentrated in the gabbros than in the pyroxenites and anorthosite. Sr, on the other hand, is more concentrated in the order anorthosite stock > gabbros > pyroxenites > magnetite ore. Rb and Sr were not detected in the magnetite ore. Sc is preferentially enriched and Th and Ta are preferentially depleted in one rock type with respect to the other rock types of the layered series. Sc is enriched in the pyroxenites and Th and Ta are depleted in the anorthosite stock and malignite ore respectively.

Rb, Ba, and Ta are depleted in the rocks of the layered series with respect to the other major intrusive bodies of the complex. Hf and Th are also depleted in the rocks of the layered series, except for the overlap that occurs with the major intrusive biotite syenites. Co and Sc, on the other hand, are preferentially enriched in the rocks of the layered series, with the exception of the slight overlap that occurs from Co being depleted in the anorthosite and Sc being enriched in the major intrusive malignites. There is considerable overlap in the Sr contents of the layered series rocks and in the major intrusive syenites and malignites.

The pyroxenites, gabbros and anorthosite stock from McClure Mountain have Rb, Ba, Sr, Th, Hf, Ta, Co, and Sc contents which are similar to alkali basalts (Lo and Goles, 1976) or the alkali ultramafic rocks (Gerasimovsky, 1974) reported in Table 7, although the limited data available for these rocks make detailed comparisons difficult.

#### Nepheline Syenite Dikes and Stocks

Rare Earth Elements.--The feldspathoidal syenitic dikes and stocks that were analyzed exhibit considerable variation in total REE content, La/Lu ratios, Eu enrichment, and heavy REE distributions (Fig. 10c). The syenitic dikes and stocks have both positive and negative Eu anomalies and a trend of increasing Eu/Eu\* with increasing absolute REE content. Two of the dikes (NK-4, FeNS-10) have large negative Eu anomalies, a characteristic not observed in any other rocks of the complex. Feldspathoidal dikes and stocks have absolute REE contents and La/Lu ratios which bracketed those of the major intrusive feldspathoidal syenites.

Other Trace Elements.--Extreme variability in other analyzed trace elements was observed in the feldspathoidal dikes and stocks. They appear to be depleted in Ba, Sr, and Co, and enriched in Rb when compared to major



intrusive feldspathoidal syenites. Th, Sc, Hf, and Ta overlap between the two groups of rocks.

#### Carbonatite Dike

The carbonatite dike is characterized by having a large absolute REE content, moderate La/Lu ratios, and no Eu anomaly. The carbonatite is similar in absolute REE content to carbonatites from Gem Park (Roden, 1977) (Fig. 14) but has lower La/Lu ratios. It is also lower in La/Lu ratios and in absolute REE content than carbonates reported by Cullers and Medaris (1977), Loubet et al. (1972), Mitchell and Brunfelt (1975), and Eby (1975) (Fig. 14).

The carbonatite dike is markedly different from other rocks in the complex in its extreme Sr enrichment and low Co content. It is also enriched in Th and Ta compared to the major rock units of the complex except for its overlap with the feldspathoidal dikes and stocks. Ba, Hf, and Sc contents in the carbonatite dike are similar to those in the other rock units of the complex. Rb was not detected in the carbonatite dike.

## D I S C U S S I O N

### INTRODUCTION

Many theories concerning the origin of alkalic rocks have been proposed and several are summarized by Hyndman (1972) and Sorensen (1974). Of particular importance, because of their preference among many present day petrologists, are the theories suggesting that alkalic rocks may be the product of differentiation (Barth, 1945; Turner and Verhoogen, 1960; Coombs and Wilkinson, 1969; Sorensen, 1970) or partial melting of an alkali olivine basalt or its magmatic equivalent (Bailey, 1964; Bailey and Schairer, 1966). Also significant are the theories suggesting that magmas other than alkali olivine basaltic magma (ultrabasic, nephelinite, diorite-monzonite) may give rise to alkalic rocks through fractional crystallization (Sood et al., 1970; Khalfin, 1961). Theories concerning the origin of the carbonatites frequently associated with alkaline rocks are also numerous (Tuttle and Gittins, 1966; Heinrich, 1966). Current thought focuses on their origin through the differentiation of an alkaline ultrabasic magma (alkali peridotite, nephelinite, ijolite) as a residual product of fractional crystallization (Wyllie and Haas, 1965, 1966; King and Sutherland, 1960; Watkinson, 1970; Watkinson and Wyllie, 1971) or as an immiscible liquid fraction of the original parent melt (Koster van Groos, and Wyllie, 1966, 1968, 1973; Wyllie and Huang, 1976; Mitchell and Brunfelt, 1975; Cullers and Medaris, 1977).

The preferred model proposed for the formation of the mafic-ultramafic and alkalic rocks of the McClure Mountain complex begins with a primary basaltic magma derived by small amounts (approximately 0.5 percent) of partial

melting of upper mantle peridotite (Table 8). Up to 5.0 percent melting of peridotite could be tolerated in this melting model to provide a somewhat more realistic volume of initial melt, but this would require minor modification in the percent crystallization of the fractional crystallization models. High pressure (15 - 23 Kb) fractional crystallization of clinopyroxene (approximately 70 percent) from a portion of this original magma, followed by the ascent and low total pressure-high water pressure fractionation of the remaining liquid formed (in order of increasing degrees of fractional crystallization) the malignite, feldspathoidal syenite, and biotite syenite. Quantitatively, the malignites were formed as cumulates by approximately 30 percent fractional crystallization of alkali feldspar (24 percent), hornblende (40 percent), biotite (26 percent), nepheline (8 percent), and sphene (1.5 percent) from the "ijolitic" magma and the incorporation of approximately 30 percent intercumulate liquid. Fifty percent fractional crystallization of alkali feldspar (74 percent), hornblende (14 percent), feldspathoids (7.6 percent), biotite (4 percent), sphene (0.6 percent), and apatite (0.0003 percent) from the remaining liquid plus the incorporation of approximately 20 percent intercumulate liquid produced the feldspathoidal syenites as cumulates. The biotite syenites were formed as cumulates from 35 percent fractionation of alkali feldspar, biotite, hornblende, and apatite in the proportions 84:9:0.5:0.3 from the liquid remaining after the formation of the feldspathoidal syenites. Layered series rocks were formed when portions of the original alkali basaltic parent magma rose to shallow depths and underwent low total and water pressure fractional crystallization of phases such as olivine, clinopyroxene, plagioclase, and magnetite. The nepheline syenite dikes and stocks of the McClure Mountain complex may have formed by the separation and subsequent crystallization of portions of the residual liquids formed

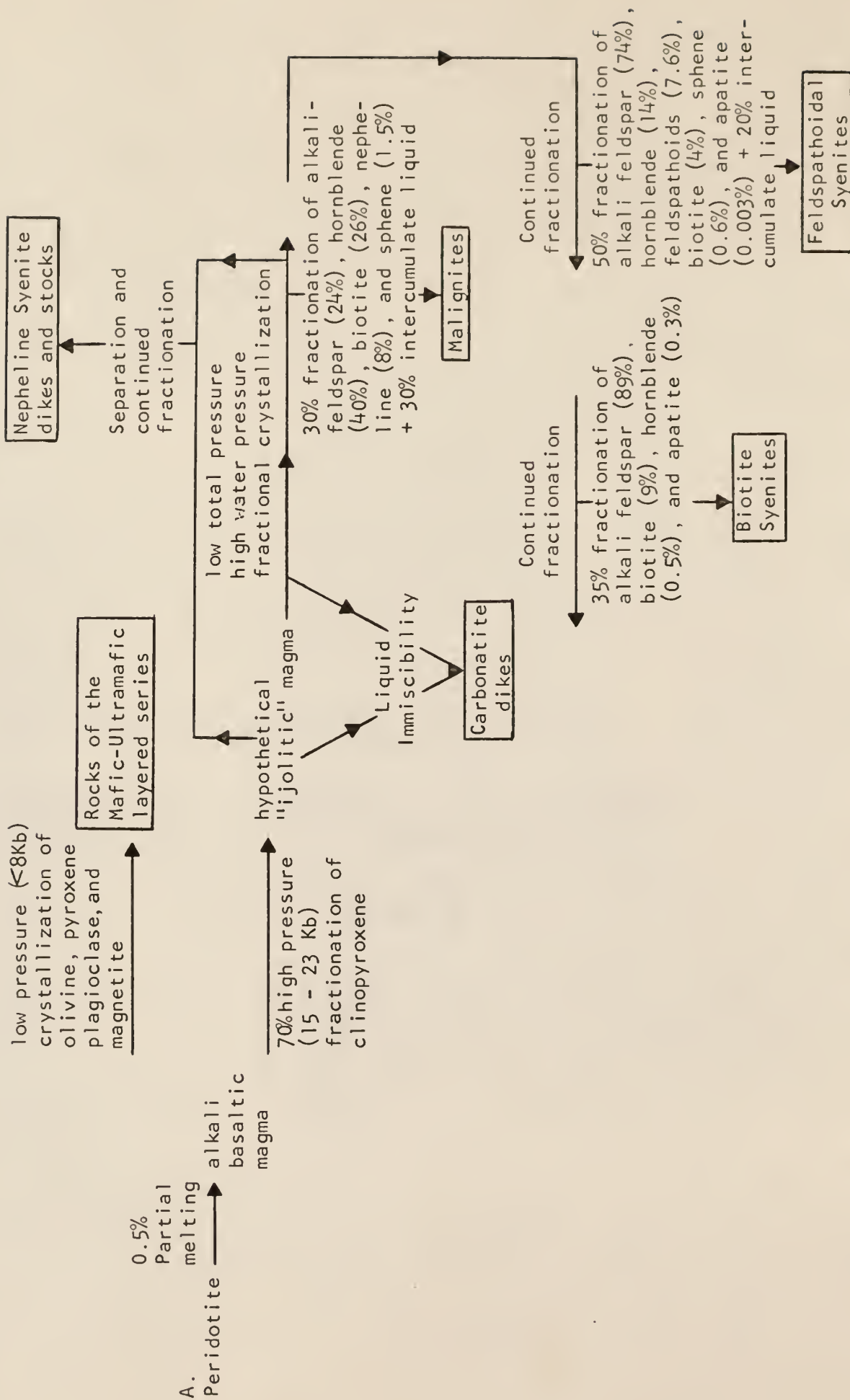


Table 8. Flow diagram summarizing the possible relations of the McClure Mountain rock types.  
A. Preferred model.

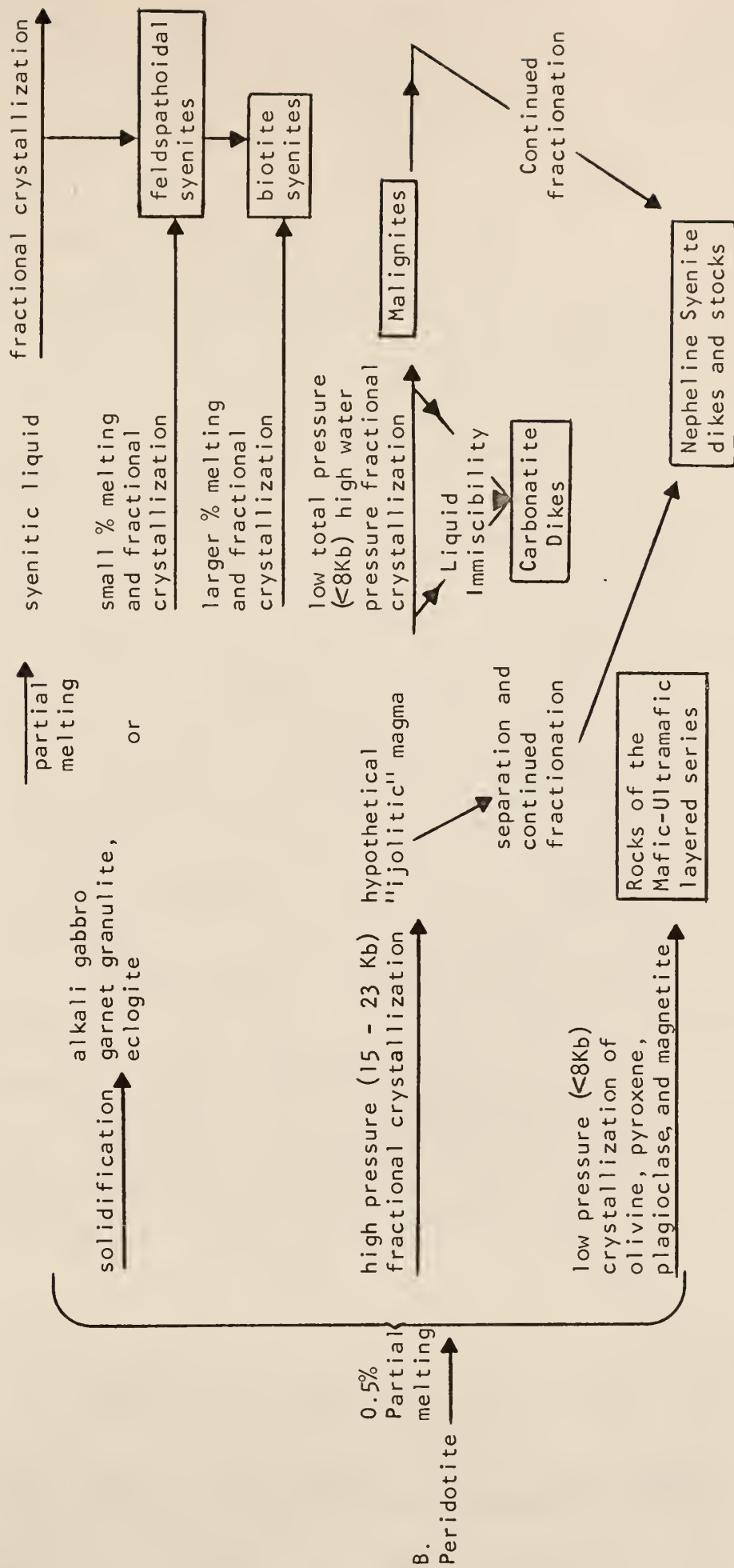


Table 8. Flow diagram summarizing the possible relations of the McClure Mountain rock types (Cont.)  
B. Alternate model

by the crystallization of the malignites and feldspathoidal syenites. The carbonatite dikes probably formed as an immiscible liquid fraction of the "ijolitic" magma or the residual liquid accumulating during the crystallization of the malignites.

An alternative model for the formation of the syenites is that a portion of the alkali basalt magma formed by the partial melting of peridotite solidified at depth, to produce as a function of pressure, an alkali gabbro, a garnet granulite, or an eclogite. The resulting solid was later fused to form through fractional crystallization the feldspathoidal syenites and the biotite syenites. An additional portion of the parental alkali basaltic magma underwent high pressure fractionation followed by the ascent and low pressure fractional crystallization of all or portions of the remaining liquid to form the malignites.

#### EXPERIMENTAL INVESTIGATIONS

Experimental studies of the origin of alkalic rocks have been summarized by Edgar (1974) and Bailey (1976). The effect of pressure on the minerals crystallizing from an alkali basaltic magma is of considerable importance (Green and Ringwood, 1967). Residual liquids produced by fractionation at intermediate and high pressures (12 - 23 Kb) would fractionate to greater amounts of normative nepheline and become enriched in alkali elements and total water content due to crystallization of clinopyroxene, orthopyroxene, olivine, and garnet. Lower pressures of crystallization formed the more traditional crystallization sequence of olivine, plagioclase, and clinopyroxene. Thus, the pressure dependent fractionation trends of basaltic liquids provide a mechanism for the generation of magma which could form the major intrusive malignites from a magma similar to that which formed the rocks of the layered series. In addition, hornblende, possibly replacing



pyroxene, becomes a stable phase in basaltic melts at low pressure and in the presence of excess water (Tilley and Yoder, 1968).

Investigation of Petrogeny's Residua System  $\text{NaAlSiO}_4$  -  $\text{KAlSiO}_4$  -  $\text{SiO}_2$  (nepheline - kalsilite - silica) by Schairer (1950) showed that rhyolites were residual magmas in the silica-saturated portions of the system and phonolites were residual magmas formed by crystallization in silica under-saturated portions of the system from the low pressure fractionation of various basalts. Investigation of the peralkaline part of the system  $\text{Na}_2\text{O}$  -  $\text{Al}_2\text{O}_3$  -  $\text{Fe}_2\text{O}_3$  -  $\text{SiO}_2$  by Bailey and Schairer (1966) illustrated a possible crystallization sequence from nephelinite (malignite or ijolite) to phonolite (nepheline syenite).

The application of experimental petrology to the McClure Mountain rock types is in some ways limited since the only studies were done on peralkaline systems (alkali/aluminum > 1) (Bailey and Schairer, 1966) or on subaluminous systems (alkali/alumina ratio = 1) (Schairer, 1950), but the McClure Mountain rock types have an excess of alumina over alkali. The general paucity in many experimental systems of mafic minerals similar to those in the McClure Mountain complex further limits the usefulness of experimental petrology in understanding the origin of the mafic-rich alkalic rocks of the complex.

Another significant feature of the investigations by Bailey and Schairer (1966) and Schairer (1950) is the presence of nepheline as a low temperature eutectic phase. In peralkaline systems nepheline crystallization begins at a very high temperature ( $1270^\circ\text{C}$ ) and continues throughout the crystallization sequence (Bailey and Schairer, 1966). In the subaluminous 'Petrogeny's Residua System' however, nepheline crystallization is confined to the low temperature ( $\sim 830^\circ\text{C}$ ) portion of the system (Schairer, 1950). In the McClure Mountain complex, however, nepheline is in the

malignites and feldspathoidal syenites but not in the biotite syenites. Rocks forming after the malignites and before or after the feldspathoidal syenites should, according to the above experimental evidence, contain nepheline.

### FIELD RELATIONS

Cross-cutting relationships of the major McClure Mountain rock types suggest that the order of emplacement of the rock bodies was, from oldest to youngest, mafic-ultramafic layered series, malignite, biotite syenite, feldspathoidal syenite, and associated dikes (Heinrich, personal communication, 1978). Although the order of intrusion frequently corresponds with the order of increased degree of differentiation numerous exceptions have been recorded (Hyndman, 1972), suggesting that fractionation sequences other than those corresponding to the order of emplacement, may have formed the McClure Mountain rock types.

The exposed areas and, thus, possibly the volumes of the major McClure Mountain rock types, as estimated by Dahlem (1965) are as follows: mafic-ultramafic layered series, 25 percent; malignite, 10 percent; feldspathoidal syenite, 25 percent; and biotite syentie, 45 percent. The uncertainties associated with volume estimates based on the areal extent of a rock type are, however, significant as the exposed level of the complex represents only one of an infinite number of planes through the complex. It is highly improbable that the exposed area of the different rock types should remain nearly constant along the horizontal axis of the complex and, therefore, the exposed areas of the rock types need not represent their relative volumes.

### MAJOR ELEMENTS

Major element variation diagrams, particularly when applied to volcanic rocks, can be used to suggest the formational sequence of a series of lavas.

The application of variation diagrams in determining the formational sequence of plutonic rocks may be limited if both residual liquids and cumulate phases are mixed. This often results in variation diagrams which do not clearly indicate the liquid line of descent of a crystallizing magma, but rather reflect the composition of varying cumulate phases mixed with the magma. This, in addition to the limited data available for the feldspathoidal syenite and the absence of precise composition of minerals in the rock types, makes it difficult to explain the major element variation of the McClure Mountain rock types. The trends in the variation diagrams, however, can be used to suggest sequences of crystallization which may be more precisely tested using trace element data.

The smooth linear trends of the major element variation diagrams of the malignites, feldspathoidal syenites, and biotite syenites suggest that these rocks may be part of the same comagmatic series (Figures 5 - 8). Field relations indicate that the rocks of the layered series are also comagmatic and exhibit extreme fractionation into pyroxenite, dunite, anorthosite, and gabbro cumulates and as expected, these cumulates have considerable scatter on the variation diagrams. The major element variation between the major intrusive (malignites, feldspathoidal syenites, and biotite syenites) and the rocks of the layered series suggest the possibility of a comagmatic relation between these two rock groups.

With increased differentiation index of the samples, there is an increase in  $K_2O$ ,  $Na_2O$ ,  $Al_2O_3$ , and  $SiO_2$  contents and a decrease in the  $CaO$ ,  $MgO$ , and  $Fe_2O_3$  contents of the rock types in the order malignite, feldspathoidal syenite, biotite syenite, suggesting that malignite was the first formed rock type and was followed by the formation of the feldspathoidal syenite and the biotite syenite. A similar sequence of differentiation is apparent

in the plots of  $\text{CaO}/(\text{CaO} + \text{Na}_2\text{O})$  and  $\text{Fe}_2\text{O}_3/(\text{Fe}_2\text{O}_3 + \text{MgO})$  versus  $\text{Al}_2\text{O}_3$  and from the AFM diagram.

Although the major element contents of the nepheline syenite stock differ slightly when plotted in the variation diagrams from the trends of the rocks of the major intrusion (malignite, biotite syenite, feldspathoidal syenite), it does appear to be comagmatic with them, being more differentiated than the feldspathoidal syenites (Fig. 5) and probably more differentiated than the biotite syenites (Figures 6 and 7). This suggests that although the nepheline syenite stock may be comagmatic with the major intrusions, the liquid which formed the nepheline syenite stock may have separated from the major intrusive magma and proceeded along a separate line of differentiation. A significant feature in the major element variations of the three major intrusive bodies is the break which exists between the major element content of the malignite and the biotite and feldspathoidal syenites, as any fractional crystallization sequence should have a continuum of magma composition from parent to most differentiated daughters. This break in major element content may be explained by the following: (1) the existence of rocks which are intermediate in composition, but are not exposed at the surface, or if they are exposed, were not analyzed because of the limited number of samples which were collected, or (2) the malignites are not related directly to the feldspathoidal and biotite syenites. The major element contents alone cannot be used to determine the exact cause of this gap although the other data available for these rocks, in combination with the major element trends, should help limit the number of possible explanations for this gap.

If we assume some gabbros best represent the composition of the original liquid in the layered series, an assumption which will be supported later, then rocks crystallizing from the parent melt should differ chemically from

the gabbros according to the type and relative amounts of their major minerals. Rocks rich in plagioclase with little trapped liquid, anorthosite for example, are expected to be enriched in  $Al_2O_3$  and  $Na_2O$  and depleted in  $MgO$  with respect to the gabbros. Similarly, rocks enriched in pyroxenes (pyroxenites) are expected to be more depleted in Al and more enriched in Ca than the gabbros. These trends are observed in the rocks in the complex, suggesting that their chemistry is strongly controlled by their major phases. Similar scatter among gabbros may also result from the mineralogical and trapped melt variations between the samples.

The relationship between the major intrusive malignites, feldspathoidal syenites, and biotite syenites, and the rocks of the layered series is not readily apparent from an examination of the variation diagrams. This results primarily from the scatter in the trends of the rocks of the layered series resulting from their cumulate origins and to a lesser extent to a similar scatter in the major intrusive rocks. Although the variation diagrams can in no way confirm a relationship between the two major rock suites, it is significant that weighted averages of the major rock types of the layered series, based on their relative abundance, tend to fall on the same line as the malignites and syenites. This indicates that the rocks of the layered series are less differentiated than the major intrusive biotite syenites, feldspathoidal syenites, and malignites, and thus, may be related to these rocks.

## Sr ISOTOPES

### Ages

Isotopic ages for the McClure Mountain complex are summarized in Table 9. The range of K-Ar ages (508 - 532 M.Y.) determined by R.F. Marvin and reported by Parker and Sharp (1970) are similar to the age of 517 M.Y.



Table 9. Isotopic ages for the McClure Mountain complex.

Reference	Kind of rock or mineral; Method	Age	$^{87}\text{Sr}/^{86}\text{Sr}$ Initial Ratio
A. Major intrusive rocks			
Parker and Sharp (1970)	Syenite; K-Ar	$508 \pm 15$ to $532 \pm 27$ M.Y.	---
Fenton and Faure (1970)	Feldspathoidal syenites, biotite syenites, malignites; Rb-Sr	$517 \pm 14$ M.Y. $704 \pm 70$ M.Y.	$0.7059 \pm 0.0003$ $0.7055 \pm 0.0004$
Olson et al. (1977)	Mineral (sphenes); fission track	$506 \pm 43$ M.Y.	---
Olson et al. (1977)	Mineral (hornblende); K-Ar	$520 \pm 13$ M.Y.	---
Olson et al. (1977)	Mineral (biotite); K-Ar	$508 \pm 14$ M.Y.	---
Olson et al. (1977)	Feldspathoidal syenites, biotite syenites, biotite separates; Rb-Sr	$521 \pm 10$ M.Y.	---
This study	Feldspathoidal syenites, malignites; Rb-Sr	$514 \pm 11$ M.Y.	$0.7051 \pm 0.0006$
This study	Feldspathoidal syenites, malignites, biotite separates; Rb-Sr	$493 \pm 5$ M.Y.	$0.7055 \pm 0.0011$
B. Dikes			
Olson et al. (1977)	Red syenite dikes; Rb-Sr	$495 \pm 10$ M.Y.	$0.7048$



calculated from one of two isochrons reported by Fenton and Faure (1970). These same authors also reported an age of 704 M.Y. for the complex and suggested that the two isochrons define the limits of the age of the intrusion. Olson et al. (1977) reported multi-technique age determinations for the complex which are in excellent agreement with each other. Their results, which include the earlier findings reported by Parker and Sharp (1970), indicate that the complex is approximately 510 M.Y. old. These results agree closely with the younger age of  $517 \pm 14$  M.Y. calculated from one of the two isochrons reported by Fenton and Faure (1970).

Ages of  $493 \pm 5$  M.Y. and  $514 \pm 11$  M.Y. were calculated from the two isochrons in Figure 9. The age of  $493 \pm 5$  M.Y. was calculated from the isochron constructed through three whole rocks and two biotite separates, whereas the age of  $514 \pm 11$  M.Y. was obtained from an isochron constructed through the three whole rocks. Because of the information obtained by Olson et al. (1977) and Fenton and Faure (1970), there is reason to suspect that the age of  $493 \pm 5$  M.Y. may be erroneous and that the age of  $514 \pm 11$  M.Y. is reflective of the magmatic event which formed the complex.

The discordance in ages obtained from the two isochrons presumably is related to the Rb-Sr isotopic content of the biotite separates. As a test of their isotopic content "model" ages were calculated for the biotite separates (Table 9). "Model" ages for two biotites reported by Olson et al. (1977) were also calculated (Table 10). Biotite WM-471 (B) was chosen because it fell a distance from their isochron, whereas biotite WM-12-71 (B) was chosen to represent the biotites on or very near the isochron. Ages were calculated using the equation:

$$\frac{87\text{Sr}}{86\text{Sr}} = \frac{87\text{Sr}}{86\text{Sr}_0} + \frac{87\text{Rb}}{86\text{Sr}} e^{\lambda t - 1}$$

and solving for  $t$ . Values of  $87\text{Sr}/86\text{Sr}$  and  $87\text{Rb}/86\text{Sr}$  were calculated from measured Rb and Sr contents and Sr isotopic ratios (Faure and Powell, 1972;

Faure, 1977). The Rb decay constant ( $\lambda$ ) equals  $1.39 \times 10^{-11}$ /yr. Values of the  $^{87}\text{Sr}/^{86}\text{Sr}$  initial ratio of the rock were estimated using calculated initial ratios of the complex (Table 11).

Calculated "model" ages indicate that some biotite separates are isotopically younger than ages determined using Rb-Sr evolution diagrams and other radiometric techniques. Biotite WM-12-71 (B), however, has a

---

Table 10. "Model" ages of McClure Mountain biotite separates.

---

<u>Sample</u>	<u>Assumed IR</u>	<u>Age</u>
NK-18 B	0.7055	497 M.Y.
NK-10 B	0.7055	486 M.Y.
WM-471 (B)	0.7055	483 M.Y.
WM-12-71 (B)	0.7055	518 M.Y.

---

"model" age very similar to reported ages for the complex. This is to be expected because it and two other biotites analyzed by Olson et al. (1977) fall on or very near their isochron. "Model" age calculations therefore indicate that some biotites are isotopically younger, whereas others are similar to reported ages for the complex. Differences in the isotopic character of the biotites can be explained by a loss of radiogenic  $^{87}\text{Sr}$  as a result of either heating during metamorphism or incipient weathering.

The lack of regional or contact metamorphic textures in the analyzed rocks suggests that metamorphism was not important in determining the present isotopic composition of the biotites. In addition, it is expected that a regional metamorphic event would affect all biotites equally, whereas biotites affected by contact metamorphism would be confined to a localized area. Neither of these trends is observed in the McClure Mountain biotites suggesting that a metamorphic event had not altered the isotopic character of the biotites. Furthermore, the good agreement in ages determined using Rb-Sr, fission track, and K-Ar dating techniques (Table 9), which

collectively have a wide range of temperature dependence, further suggests that a significant metamorphic event has not affected the complex.

Dasch (1969) showed that small degrees of incipient weathering can cause the rapid release of radiogenic strontium from a rock. This is facilitated by the smaller size of Sr in comparison to the Rb parent and by the small amount of structural site damage in the crystals that results from the decay of Rb (Faure, 1977). In biotite, this effect is further enhanced by the location of the radiogenic strontium in the crystal structure. This results from the Rb parent concentrating in the interlayer positions of the biotite structure. These interlayer positions are thought to have a very high capacity for ion exchange (Dasch, 1969). Incipient weathering, therefore, could have produced the anomalous isotopic character of the biotites. This mechanism would be consistent with the fact that not all biotites were of an anomalous nature, as different degrees of weathering would be responsible for the range of "model" ages exhibited by the biotites. Although some biotites may have been affected by radiogenic Sr loss, the whole rocks from which they were separated were not. This is also consistent with the above explanation for the anomalous biotite ages. Petrographic analyses of the samples from which the biotites were separated indicate that the whole rock samples had not been subjected to large degrees of weathering. Radiogenic Sr release, therefore, may have been confined to the more susceptible biotite. The isotopic content of the rocks as a whole may not have been affected significantly by release of Sr from its biotite, because biotite comprises only a small portion of the total mineralogy. It is also possible that the radiogenic Sr, once released, may have been incorporated by other phases present in the rock.

### Initial Ratios

Initial  $^{87}\text{Sr}/^{86}\text{Sr}$  ratios have in recent years been used as petrogenetic tracers in the study of igneous rocks (Faure and Hurley, 1963; Powell et al., 1966). Besides indicating a possible genetic relationship between rock types, initial  $^{87}\text{Sr}/^{86}\text{Sr}$  ratios can be used to determine the nature of the source region from which the rocks were generated.

The initial  $^{87}\text{Sr}/^{86}\text{Sr}$  ratios of the syenites and malignites obtained from Rb-Sr evolution diagrams (0.7036 - 0.7059), the initial ratios obtained for the McClure Mountain carbonatite dikes (0.7044 - 0.7053), and the initial ratios obtained for the mafic rocks of the layered series by Olson et al. (1977) (0.7039 - 0.7048) are broadly similar to each other suggesting a comagmatic origin for these rock types (Table 11). In addition, Faure and Hurley (1963) indicated that rocks with initial ratios in the range of those obtained for the McClure Mountain complex may be derived from the upper mantle.

Initial ratios for rocks from the Gem Park complex range from 0.70293 to 0.70433 (Roden, personal communication, 1978) (Table 11). The majority of the reported initial ratios are similar, within the limits of analytical uncertainty, to their McClure Mountain counterparts suggesting the possibility of a genetic relationship between the two complexes.

The initial  $^{87}\text{Sr}/^{86}\text{Sr}$  ratios of the pyroxenite and the anorthosite determined in this study are distinctly different from those of the syenites and malignites and the carbonatites. In addition, they differ from those reported by Olson et al. (1977) for the mafic rocks of the layered series. Because of the low Sr content of the pyroxenite and anorthosite, and, as indicated by petrographic study, alteration of their minerals, it is possible that their high  $^{87}\text{Sr}/^{86}\text{Sr}$  ratios are related to post-magmatic alteration. The low  $^{87}\text{Sr}/^{86}\text{Sr}$  ratios of the pyroxenite and anorthosite could easily

Table 11. Initial ratios of rocks in the McClure Mountain and Gem Park Complexes.

Initial Ratio	Rock Type	Reference
A. McClure Mountain		
0.7059 $\pm$ 0.0003	Feldspathoidal syenite, biotite syenite, malignite Rb-Sr isochron diagram	Fenton and Faure (1970)
0.7053 $\pm$ 0.0005	Carbonatite	Fenton and Faure (1970)
0.7036	Feldspathoidal syenite, biotite syenites, biotite separate Rb-Sr isochron diagram	Olson et al. (1977)
0.7048	Anorthosite	Olson et al. (1977)
0.7041	Gabbro	Olson et al. (1977)
0.7039	Anorthosite	Olson et al. (1977)
0.7051 $\pm$ 0.0006	Feldspathoidal syenite, biotite syenite, malignite Rb-Sr isochron diagram	This study
0.7078 $\pm$ 0.0005	Pyroxenite	This study
0.7065 $\pm$ 0.0005	Anorthosite stock	This study
0.7044 $\pm$ 0.0005	Carbonatite	This study
B. Gem Park		
0.70433 $\pm$ 0.000023	Gabbro	Roden (personal comm., 1978)
0.70390 $\pm$ 0.000011	Pyroxenite	Roden (personal comm., 1978)
0.7038 $\pm$ 0.001	Nepheline syenite, pegmatite	Roden (1977)
0.7036 $\pm$ 0.001	Carbonatite	Roden (1977)
0.7037 $\pm$ 0.001	Carbonatite	Roden (1977)
0.70293 $\pm$ 0.00003	Carbonatite	Roden (personal comm., 1978)
0.7038 $\pm$ 0.001	Carbonatite	Roden (1977)
0.7036 $\pm$ 0.001	Carbonatite	Roden (1977)



be increased by their interreaction with subsurface fluids which are reported to have  $^{87}\text{Sr}/^{86}\text{Sr}$  ratios as high as 0.7341 (Chaudhuri, 1978).

In addition to the above explanation for the high initial  $^{87}\text{Sr}/^{86}\text{Sr}$  ratio of the anorthosite stock, it is possible that it was derived from an isotopically different source than the other rocks in the complex. Its intrusive nature with respect to the rocks of the layered series indicates that it is possible that the anorthosite stock may have formed through processes separate from those which formed the other rocks in the complex and was emplaced subsequent to the rocks of the layered series.

## TRACE ELEMENTS

### General

Trace elements are used to test and modify the possible relationships suggested by the major element contents of the McClure Mountain rock types. The behavior of a trace element in a melting solid or in a crystallizing magmatic fluid is predicted by its distribution coefficient ( $D$ ), which is defined as its concentration in the solid phase divided by its concentration in the melt (Gast, 1968; Ewart and Taylor, 1969; Philpotts and Schnetzler, 1970a; Drake and Weill, 1975; Haskin et al., 1970). Trace element concentrations in phases of evolving magmatic systems in fractional crystallization are further modified by the percent of parental magma which has crystallized and in partial melting by the percent of original material which has melted.

The equations used in this study to predict trace element partitioning between co-existing phases are from Haskin et al. (1970), and represent a simplification of the equations derived by Gast (1968) and Shaw (1970). In using the equations of Haskin et al. (1970) it is assumed that in partial melting, the proportions of minerals melted remains the same and for both fractional crystallization and partial melting that the distribution coefficients remain constant.



The trace element contents of derived phases (solid in fractional crystallization; liquid in partial melting) can be generated using the following equation from Haskin et al. (1970):

$$C_D/C_A = 1 - (1 - X)^D$$

Where,

$C_D/C_A$  = the average concentration of the derived phase to the average concentration for the system for a particular element

$X$  = the fraction of completion of the process (percent solidified or melted)

$D$  = the distribution coefficient for the particular element.

The elemental concentrations of the residual phases (liquid in fractional crystallization, solid in partial melting) are calculated using another equation of Haskin et al. (1970):

$$C_R/C_A = (1 - X)^{D - 1}$$

Where,

$C_R/C_A$  = the average concentration of a particular element in the residual phase divided by the average concentration of that element in the system

$X$  = the fraction of completion of the process

$D$  = the distribution coefficient for the particular element.

The above equations, together with published distribution coefficients for the elements (Appendix H), are used to formulate a model for the formation of the rock types in the McClure Mountain complex.

It will be shown in the following sections that the proposed origin for the complex is consistent with the trace element contents of the McClure Mountain rock types. Although in the proposed model particular degrees of partial melting and fractional crystallization are assumed, the significance of the trace element models lies not in their ability to predict precise values of these parameters but rather in their ability to predict the likelihood of a general sequence of events having formed the rock types. Different values of distribution coefficients, source mineralogy, source

REE content, degrees of partial melting and fractional crystallization, and the relative proportions of the phases that crystallize, could produce hypothetical products with REE contents similar to rocks in the McClure Mountain complex. Alternative models for the complex also will be discussed in light of trace element data, although a rigorous quantitative treatment of these models will not be presented.

Distribution coefficients for the elements Co, Sc, Sr, Ba, and Rb are available so that these elements can be used as a further test of the proposed model for the origin of the complex. Unlike the REE, these elements will be used qualitatively because of the uncertainty surrounding the published distribution coefficients, particularly in alkalic rocks, although some general predications can be made. Petrogenetic modelling of Th, Hf, and Ta, even in a qualitative sense, is limited by the paucity of distribution coefficients available for these elements.

#### Derivation of the Model

The normative alkali basaltic composition and the low  $^{87}\text{Sr}/^{86}\text{Sr}$  initial ratios of the rocks of the layered series suggest that they may have formed by direct partial melting of upper mantle material (O'Hara and Yoder, 1967; Gast, 1968; Philpotts and Schnetzler, 1970a,b; Kay and Gast, 1963). Furthermore, the close physical association of the rocks of the layered series with the major intrusive feldspathoidal syenite, biotite syenite, and malignite, as well as their similar  $^{87}\text{Sr}/^{86}\text{Sr}$  initial ratios suggests that the magma which formed the layered series may be similar to the parent material which formed the major intrusive rocks.

The major intrusive biotite syenites, feldspathoidal syenites, and malignites may be related and may be comagmatic because they have a close spatial association and similar mineralogy. In addition, smooth chemical trends and the colinearity of the rock types when plotted in a Rb-Sr

evolution diagram further support a comagmatic origin for the major intrusive rocks. The apparent cumulate nature of the rock types, as suggested by petrographic examination and geochemical data (the Eu anomaly), further suggest that fractional crystallization was operative in the formation of the rocks.

There are two fractional crystallization sequences which may have formed the major intrusive malignites, feldspathoidal syenites, and biotite syenites. The order of intrusion, as inferred from field relations, indicates that the malignite, biotite syenite, and feldspathoidal syenite were emplaced in that order (Heinrich, personal communication, 1978). Mineralogical variations, major element variation diagrams and, as will be discussed later, the Ba and Sr distribution between the major intrusives indicate, however, that the sequence of crystallization may have been, from first to last, malignite, feldspathoidal syenite, and biotite syenite.

The large gap in silica concentration that exists between the malignites and the syenites warrants the examination of an alternative hypothesis for the origins of these rocks. The field relationships, Sr isotopic data, and the major element contents of the major intrusive malignites, feldspathoidal syenites, and biotite syenites are consistent with the possibility that these rocks were initially comagmatic but that the malignites and the syenites formed as a result of separate evolutionary paths. This model is consistent with existing theories that suggest that syenites may form as a result of direct partial melting of lower crustal alkali basalt (Bailey, 1964; Bailey and Schairer, 1966).

The close spatial association of the McClure Mountain dikes, and their mineralogical similarity to major intrusive rocks suggests that the dikes are related to the major intrusives. In addition, major element contents in the analyzed nepheline syenite dike indicate that it may be

comagmatic with the major intrusive malignites, feldspathoidal syenites, and biotite syenites.

As summarized in the Introduction and in Table 8, it is proposed that the rocks of the McClure Mountain complex formed from an alkali basaltic magma produced by small amounts of partial melting of upper mantle peridotite. The mafic-ultramafic rocks of the layered series crystallized directly from the parental alkali basaltic magma, whereas the major intrusive malignite, feldspathoidal syenite, and biotite syenite formed by the progressive fractional crystallization of portions of the parental alkali basaltic magma. An alternative model for the formation of the syenites is that they were produced by the partial fusion and subsequent fractionation of an alkali gabbro or its magmatic equivalent, formed when portions of the parental alkali basalt crystallized at depth. The nepheline syenite dikes and stocks were formed by the crystallization of portions of the residual liquids accumulating during the formation of the major intrusive rocks, and the carbonatites may have formed by liquid immiscibility from portions of these same liquids.

#### Rare Earth Elements

General.--Textural criteria impose significant constraints on the modelling of the REE in fractional crystallization sequences. Of prime importance is the percent of residual liquid that may have been trapped in interstitial areas during the fractional crystallization process. Petrographic examination of the malignite, feldspathoidal syenite, and biotite syenite indicate that in addition to the cumulate phases, trapped intercumulate liquid may have been present in some of the rock types. Accordingly, in the model that follows, different amounts of trapped intercumulate liquid are assumed to have been present during the formation of some rock types in order to explain the trace element characteristics of the rocks.

For example, assuming there is 20 percent trapped intercumulate liquid with the cumulate, the observed REE concentration for a particular REE cumulate,  $C_{\text{REE}}$ , is equal to 80 percent times the concentration of the solid plus 20 percent times the concentration of the liquid, assuming equilibrium concentrations of REE in the solid and liquid (Haskin et al., 1970).

Petrographic examination revealed that the percent of trapped liquid was greatest in the malignites (approximately 30 percent) and the feldspathoidal syenites (approximately 20 percent). The biotite syenites, however, may have incorporated only small amounts ( $< 5$  percent) of trapped liquid during their formation. Interestingly enough, the relative percent of trapped liquid correlates well with the percent of nepheline in the samples, suggesting as does the petrographic evidence, that nepheline might be a product of intercumulate crystallization. This mechanism of intercumulate nepheline crystallization offers a possible explanation of the anomalous nepheline distribution in the McClure Mountain rock types. If the nepheline crystallization temperature had not been reached prior to the formation of the cumulate phases in the rock types, then it would be a phase only in rock types which incorporated significant intercumulate liquid during their formation. Thus nepheline would be present in the malignite and feldspathoidal syenite and absent from the biotite syenite.

Primary Melt.--Most petrologists now believe that the upper mantle is composed primarily of peridotite, although some speculate that some eclogite may also be present (Ringwood, 1975). Trace element models for the formation of alkali basaltic magma produced by small degrees ( $< 5$  percent) of partial melting of upper mantle peridotite, consistent with the results of experimental petrology, have been proposed by Gast (1968) and Kay and Gast (1973). Similarly, it will be shown that the hypothetical alkali



basaltic parent magma which differentiated to form the rocks in the McClure Mountain complex can be generated by small degrees of partial melting of upper mantle peridotite.

Studies of South African kimberlites by Mathias et al. (1970) revealed that garnet lherzolite may be at all depths below the Mohorovicic discontinuity. Accordingly, a garnet lherzolite peridotite consisting of approximately 20 percent olivine, 50 percent clinopyroxene, 28.5 percent orthopyroxene, and 1.5 percent garnet is chosen as the upper mantle source. Based on the results of Reid and Frey (1971) and Haskin et al. (1968) the initial REE contents of the source peridotite is assumed to be five times the chondritic REE contents. The chondrite-normalized REE content of the hypothetical alkali basaltic magma produced by 0.5 percent partial melting of the source peridotite is similar to REE contents observed by Gast (1968) in alkali basalts, indicating that the REE characteristics of the hypothetical primary melt are similar to those of other materials presumed to have upper mantle sources (Fig. 14).

Major intrusive biotite syenite, feldspathoidal syenite, and malignite.--If a portion of the hypothetical alkali basaltic magma formed by the partial melting of upper mantle peridotite were to undergo extensive high pressure fractional crystallization, the resulting liquid would have a major element and REE content similar to the liquid which is believed to have formed the major intrusive sequence. Consistent with the results of Green and Ringwood (1967), it is theorized that the hypothetical alkali basaltic magma, at pressures ranging from 15 - 23 Kb (52 - 80 Km), underwent approximately 70 percent fractionation of clinopyroxene to generate the hypothetical "ijolitic" magma (Figure 14). The residual liquid produced by this fractionation would contain greater amounts of normative nepheline and be more



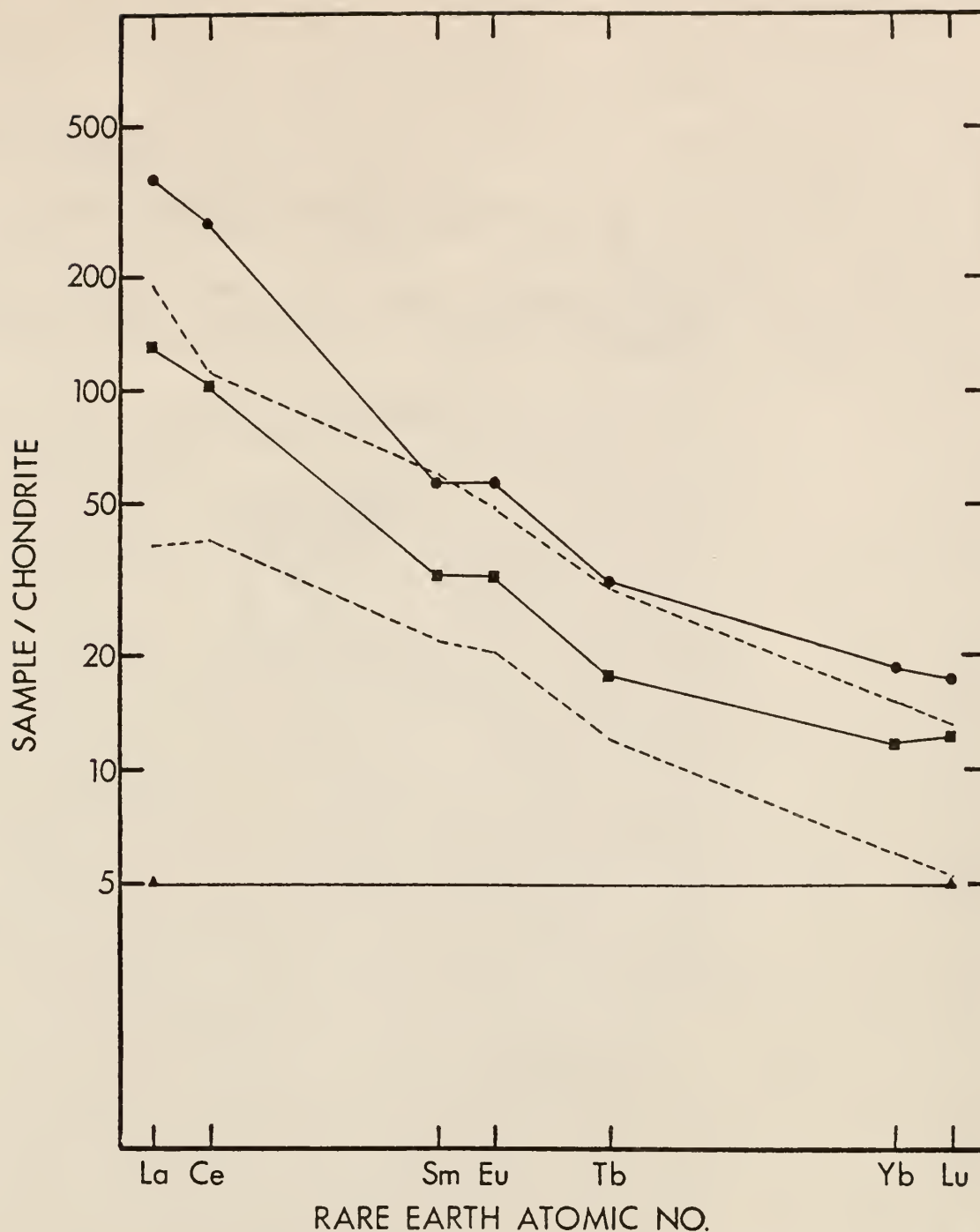


Figure 14. Chondrite-normalized REE plots of model melts. (■) Hypothetical alkali basaltic magma produced by 0.5 percent partial melting of peridotite (20 percent olivine, 50 percent clinopyroxene, 28.5 percent orthopyroxene, and 1.5 percent garnet) having an initial REE content of 5 times chondrites. Dashed lines represent range in REE contents of alkali basalts (Gast, 1968). (●) Hypothetical "ijolitic" magma formed when alkali basaltic magma underwent 70 percent fractionation of clinopyroxene.

enriched in alkali elements and water content than the original alkali basaltic magma, making it a highly potential parent material for the alkali-rich major intrusive malignites, feldspathoidal syenites, and biotite syenites (Green and Ringwood, 1967).

Following the crystallization of clinopyroxene, the hypothetical  $H_2O$ -rich "ijolitic" magma ascended to shallower depths where decreasing temperatures and pressures resulted in the fractionation of hornblende, biotite, alkali feldspar, and other minor phases. The alkali element concentration of the melt was presumably great enough to allow eventually the direct crystallization of alkali feldspar. Although this has not been observed experimentally in systems with alkali/alumina ratios less than one, similar crystallization sequences have been observed experimentally in peralkaline systems. The McClure Mountain malignite may have formed by a combination of both the crystallization of 30 percent of the following phases from the hypothetical "ijolitic" melt and the incorporation of 30 percent of the residual liquid: alkali feldspar (24 percent), hornblende (40 percent), biotite (26 percent), nepheline (8 percent), sphene (1.5 percent), and carbonate (1 percent). (Fig. 15a). The mineral proportions chosen are similar to those present in the actual malignites, and although the nepheline may have crystallized from the interstitial liquid, the REE contents in this phase are low enough that the REE content of the resulting solid should not be significantly affected. With the exception of a slight enrichment in Eu, the model malignite is identical in REE content to the range of REE contents in the natural malignites. The Eu anomaly could result from a portion of the alkali feldspar having crystallized from the trapped intercumulate liquid, thus being more depleted in Eu than the model melt which was calculated assuming that all of the alkali feldspar was of a cumulate origin. It is also possible that the alkali feldspar distribution coefficient for Eu is too high.

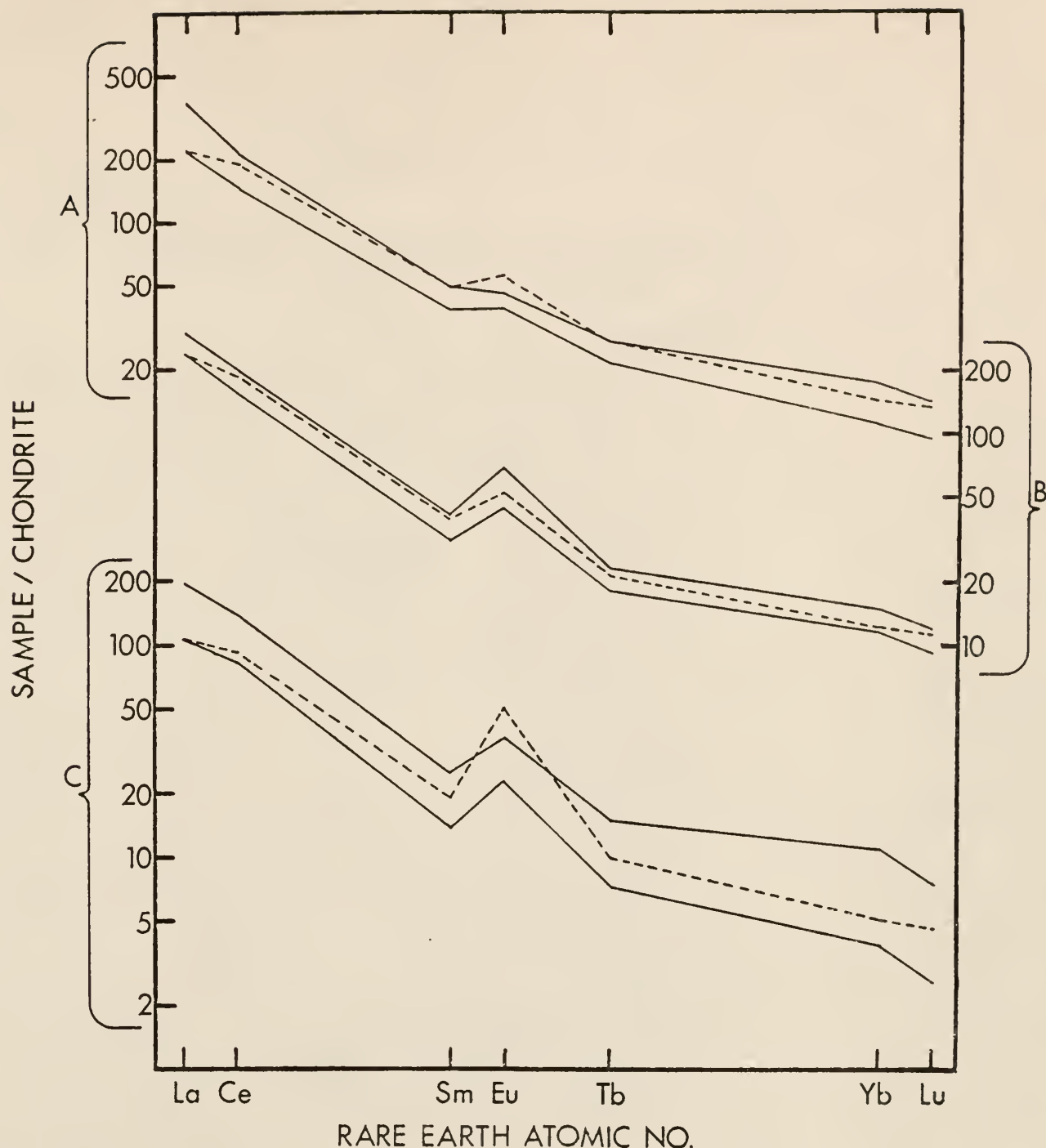


Figure 15a. Chondrite-normalized REE plots of model rocks. (A) Malignites formed as a cumulate by a combination of 30 percent crystallization from the hypothetical "ijolitic" magma and the incorporation of 30 percent of the residual liquid. (B) Feldspathoidal syenite formed as a cumulate by the combination of 50 percent crystallization from the residual liquid of the malignite formation and the incorporation of 20 percent of the residual liquid. (C) Biotite syenite formed as a cumulate by 30 percent crystallization from the residual liquid of feldspathoidal syenite crystallization. Model rocks are represented by a dashed line. Also plotted are the range in chondrite-normalized REE contents of the malignites, biotite syenites and feldspathoidal syenites (solid lines).

The residual liquid produced when portions of the "ijolitic" magma crystallized to form the malignites would be different chemically from the original "ijolitic" magma. An increase in the silica concentration of the residual liquid is expected because of the relatively large amount of silica-deficient phases (hornblende, biotite) which crystallized to form the malignites. Although it is difficult to show, it appears possible that significant crystallization of these silica-deficient phases from the "ijolitic" magma could increase the silica concentrations of the residual liquid to the level necessary to form the syenites.

With decreasing temperature and increasing degrees of fractionation, the percent of felsic phases crystallizing from the residual liquid should increase with respect to the percent of mafic phases. The McClure Mountain feldspathoidal syenites could have formed from a combination of both the accumulation of 50 percent of the following minerals from the residual liquid produced by the malignite fractionation and the incorporation of approximately 20 percent of the trapped residual liquid: alkali feldspar (74 percent), hornblende (14 percent), feldspathoids (7.6 percent), biotite (4 percent), sphene (0.6 percent), and apatite (0.003 percent) (Fig. 15a). As in the case of the malignites, although the trapped intercumulate liquid could have crystallized the interstitial nepheline present in the feldspathoidal syenites, the REE contents of the resulting solid should not be affected. The model feldspathoidal syenite is nearly identical in REE content to the range of REE contents observed in the McClure Mountain feldspathoidal syenites.

If the residual liquid formed by the crystallization of the feldspathoidal syenites was to undergo 30 percent crystallization of alkali feldspar, biotite, hornblende, and apatite in the proportions 89:9:0.5:0.3, the resulting solid would have a REE content similar to that of the McClure

Mountain biotite syenites (Figure 15a). Although the model biotite syenite was calculated assuming no intercumulate liquid, the incorporation of up to seven percent residual liquid would still be consistent with the above origin for the biotite syenites. The model biotite syenite has a REE content similar to the range observed in the actual biotite syenites, although it is slightly enriched in Eu with respect to the latter.

REE models indicate that it is possible to generate the major intrusive crystallization sequence of, in order of increasing degree of fractionation, malignites, biotite syenites, feldspathoidal syenites, although mineralogical variations, major element variation diagrams, and as will be discussed later, some trace element distributions are inconsistent with such a formational sequence. The model necessitates a greater amount of high pressure crystallization of clinopyroxene ( $>85$  percent) and requires that smaller amounts of trapped residual liquid be incorporated during the formation of the malignites and the feldspathoidal syenites. In addition, the model favors the incorporation of larger quantities of trapped intercumulate liquid during the formation of the biotite syenites. Although the amount of trapped intercumulate liquid required by the above model appears to be inconsistent with textural criteria, the uncertainties involved in the estimation of the percent of intercumulate liquid present during the formation of a rock type makes it impossible to use REE criteria as a positive indication of the validity of either crystallization sequence.

A significant feature of the chemical character of the major intrusive rocks is the large gap in silica concentration that exists between the malignites and the feldspathoidal syenites. As previously mentioned, the gap in the preferred model can be explained by the existence of rocks intermediate in composition between the malignites and the feldspathoidal syenites that are not exposed at the surface. Alternately, the intermediate rocks at



the surface could have been missed because of the limited number of samples which were collected.

An alternative explanation for the gap in silica concentrations is that the malignites are not related directly to the feldspathoidal and biotite syenites. If this were true, then, as previously proposed, the malignites could form by fractional crystallization of an "ijolitic" magma at low total pressure and high water pressure which was produced by the crystallization of alkali basalt at high pressure. As suggested by many (Bailey, 1964; Bailey and Schairer, 1966; Hyndman, 1972), the syenites could possibly form from partial melting of a solid with an alkali basaltic composition. The textural evidence is not, however, consistent with the theory that the feldspathoidal syenites and biotite syenites formed directly from partial fusion of an alkali gabbro, garnet granulite or eclogite, although fractional crystallization of the liquid produced by the partial fusion of eclogite might form these rock types.

Liquids produced by partial fusion of the feldspar-bearing alkali gabbro or garnet granulite are expected to be significantly depleted in Eu with respect to the other REE. As can be seen in Figure 10a, however, both the feldspathoidal syenites and the biotite syenites are not depleted in Eu, but are rather significantly enriched in this element with respect to the other REE. This, in addition to the textural evidence, indicates that the feldspathoidal syenites and biotite syenites could not have possibly formed directly through the partial fusion of a feldspar-bearing source.

Because the crystallization of significant amounts of plagioclase from an Eu depleted melt could increase the Eu concentration of the resulting cumulate, it might appear possible that the syenites could form as cumulates from a melt produced by the partial fusion of an alkali gabbro or garnet granulite. It is doubtful, however, that the resulting cumulate would have



an Eu anomaly similar to that present in the syenites. This is illustrated by the model syenites calculated above having Eu anomalies that are similar to those of the natural rocks but were formed as cumulates from a melt with no Eu deficiency.

Liquids derived by partial fusion of the feldspar-free eclogite are not expected to contain anomalous concentrations of Eu. The positive Eu anomalies in the feldspathoidal syenites and the biotite syenites indicate that they could not be formed by direct partial fusion of eclogite, although a combination of partial fusion followed by fractional crystallization of the resulting liquid at low pressure could produce the Eu anomaly present in the feldspathoidal syenites and biotite syenites. In addition, melts produced by partial fusion of eclogite are expected to be significantly depleted in heavy REE with respect to light REE. This results from the high garnet concentration in eclogite, a mineral which has a large affinity for the heavy REE. The absence of heavy REE depletion in the syenites, as suggested by somewhat similar La/Lu ratios to the malignites, suggests that the syenites may not have formed by the partial fusion of an eclogite.

Layered series.--If a portion of the original alkali basaltic parent magma used to generate the malignite-syenite sequence were to rise rapidly to relatively shallow depths and dehydrate much more rapidly, undergoing extensive low pressure fractional crystallization, the resulting solid phases would have a mineralogy similar to those of the rocks in the McClure Mountain layered series. This is consistent with experimental studies by Green and Ringwood (1967) which indicated that the major phases to crystallize from an alkali basaltic magma in the pressure range of 1 - 5 Kb are olivine, plagioclase, and clinopyroxene.

The REE content of the McClure Mountain gabbros can be represented by the cumulate of similar mineralogy observed in these gabbros consisting of

57 percent plagioclase, 25 percent clinopyroxene, 12 percent olivine, 4 percent magnetite, and 2.3 percent amphibole which crystallized from the alkali basaltic magma (Fig. 15b). Assuming that the alkali basaltic magma does not change composition with crystallization, i.e., that the percent crystallization of the original magma is very small, the equation of Haskin et al. (1970) reduces to:

$$\text{distribution coefficient} = \frac{\text{solid}}{\text{melt}}$$

and the concentration of the cumulate solid is readily calculated. The REE content of the calculated model gabbro, assuming it is all cumulate (dashed line in Figure 15b, part A), is within the lower range of REE contents observed in the McClure Mountain gabbros. The large range in REE contents of the McClure Mountain gabbros results from the differences in mineralogy and from the incorporation of differing amounts of residual liquid. The REE content of gabbro NK-34, for example (Fig. 10b and upper line of the range in REE contents of gabbros in Fig. 15b, part A), is similar to that of the presumed parental alkali basaltic magma, suggesting that this sample may have crystallized rapidly without significant fractionation directly from the parental magma. The absence of a cumulate texture in the sample also supports this theory for its origin.

The REE content of the model pyroxenite formed by the accumulation of 86 percent clinopyroxene, 13 percent plagioclase, 0.4 percent olivine, and 0.4 percent amphibole from the parental alkali basaltic magma, is similar to the REE content of the measured pyroxenites (Fig. 15b, part B). The relative proportions of the accumulating phases are similar to those observed in the sampled pyroxenites.

Textural evidence suggests that the anorthosite stock may have formed by the incorporation of approximately five percent of the residual liquid in addition to the cumulate phases present in the rock. The chondrite-normalized

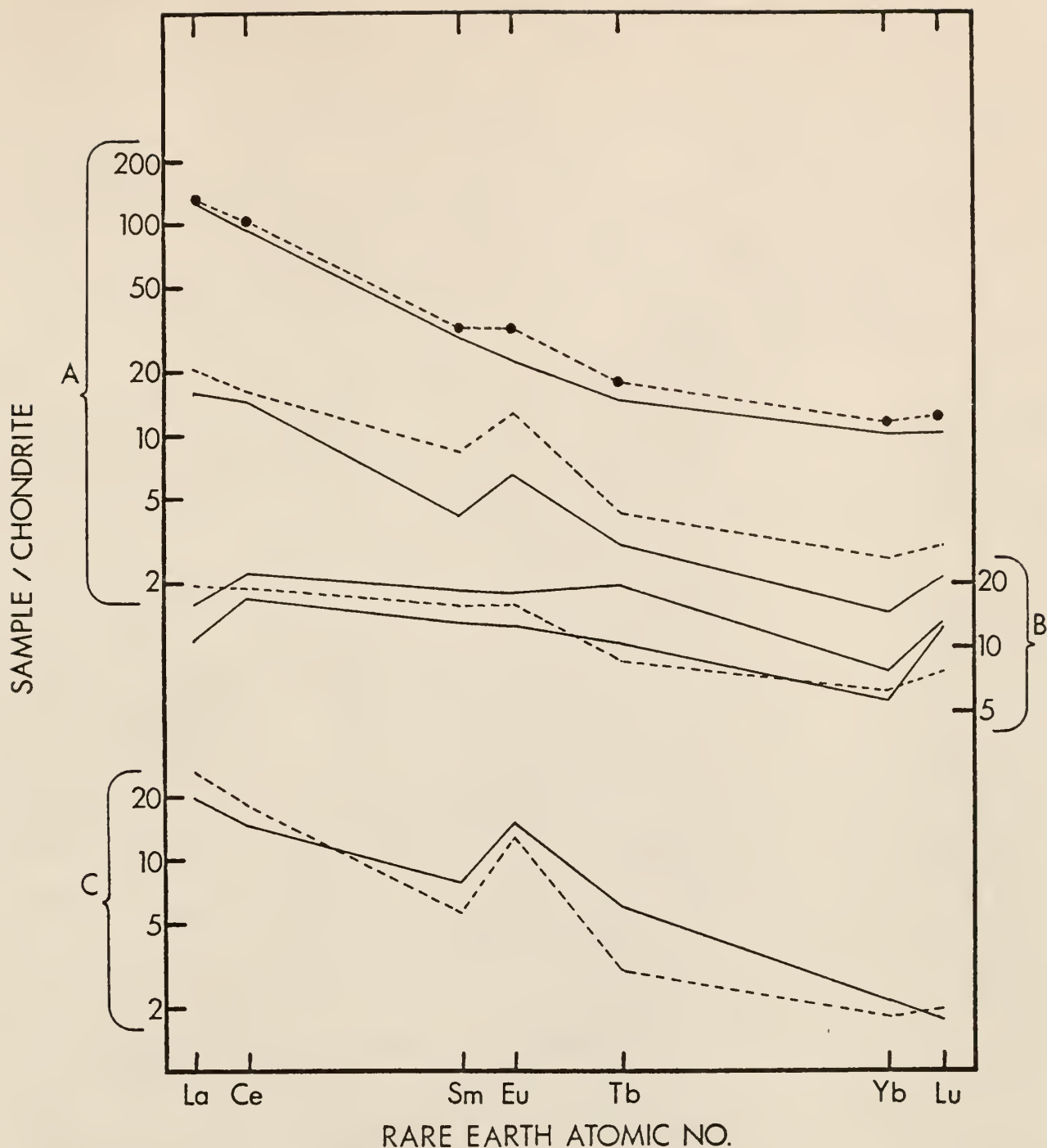


Figure 15b. Chondrite-normalized REE plots of model rocks. (A) Model gabbro (dashed line only) formed by the accumulation of plagioclase, clinopyroxene, olivine, magnetite, and amphibole in the proportions 57:25:12:4:2:3 from parental alkali basaltic magma (●). Range of gabbros is represented by solid lines. (B) Model pyroxenite (dashed line) formed by the accumulation of clinopyroxene, plagioclase, olivine, and amphibole in the proportions 86:13:0.4:0.4 from the parental alkali basaltic magma. Range of pyroxenites is represented by solid line. (C) Model anorthosite (dashed line) formed by the accumulation of plagioclase, clinopyroxene, magnetite, and biotite in the proportions 87:10:2.3:1 from the alkali basaltic parent magma. Anorthosite stock is represented by solid line.

REE contents of a model anorthosite formed by the accumulation of plagioclase, clinopyroxene, magnetite, and biotite in the proportions 87:10:2.3:1 from the alkali basaltic parent magma and the incorporation of five percent of the residual liquid is similar to the REE content observed in the McClure Mountain anorthosite stock (Fig. 15b Part C).

The preponderance of large positive Eu anomalies in the plagioclase-enriched samples from the layered series and the belief that many of the layered series rocks were formed by small degrees of fractionation of a parental magma suggests that a large portion of the layered series is not exposed at Iron Mountain. Density stratification relations of the major mineral phases (Shaw and Parker, 1968) indicate that the unexposed portions of the layered series may have been removed by erosion.

Dikes and Stocks.--Consistent with their close spatial association and similar mineralogy, REE evidence suggests that the nepheline syenite dikes and stocks of the McClure Mountain complex may have formed from portions of the residual liquids produced during the formation of the rocks of the layered series.

The low REE content and positive Eu anomaly suggest that dike NK-23 may have formed as a cumulate of direct fractional crystallization from liquids which produced the rocks of the layered series. Attempts to quantify such an origin, however, resulted in calculated model melts that were greatly enriched in Eu with respect to the dike. Additional attempts to decrease the size of the Eu anomaly by incorporating portions of the residual liquid along with the cumulate phases present in the dike resulted in absolute REE contents that were larger than those observed in sample NK-23.

The REE content of dike NK-23, however, can be generated by the indirect crystallization from the liquid which produced the major intrusive rocks. If a portion of the hypothetical "ijolitic" magma which formed the major

intrusives was to undergo approximately 60 percent crystallization of alkali feldspar, hornblende, biotite, and sphene in the proportions 24:40:26:9, the residual liquid would have a REE content significantly lower than that of the ijolitic liquid. Except for a greater concentration of sphene, the phases assumed to have crystallized from the ijolitic magma are similar in mineralogy and relative percent to those in the malignites. Nepheline syenite dike NK-23 could then have formed by a combination of 80 percent crystallization of alkali feldspar (86 percent), nepheline (11 percent), muscovite (3 percent), and the incorporation of 20 percent of the residual liquid (Fig. 15c, Part A). Although the calculated model dike is slightly different in REE content from dike NK-23, the overall similarity suggests the possibility of such a process having formed the dike.

The REE content of dikes FeNS-10 and NK-4 can also be generated from the liquid which produced the major intrusive rocks. If a portion of the residual liquid produced by the crystallization of the malignites was to separate from the main magma body and undergo approximately 35 percent fractionation of alkali-feldspar, biotite, sphene, and apatite in the proportions 90:9:0.3:0.3, the residual liquid, with the exception of a slight enrichment in Eu, would have a REE content similar to that of nepheline syenite dike NK-4 (Fig. 15c, Part B). The Eu enrichment in the calculated model dike may be a result of the Eu-alkali feldspar distribution coefficients being a little too low.

The REE content of dike FeNS-10 could be generated by similar processes as those which formed dike NK-4 except that a greater percentage of sphene may have crystallized prior to its formation. Although the crystallization of greater amounts of sphene would decrease the overall REE content in the residual liquid, it would also increase the Yb and Lu concentrations with respect to the other REE. To counteract the decrease in the REE content of



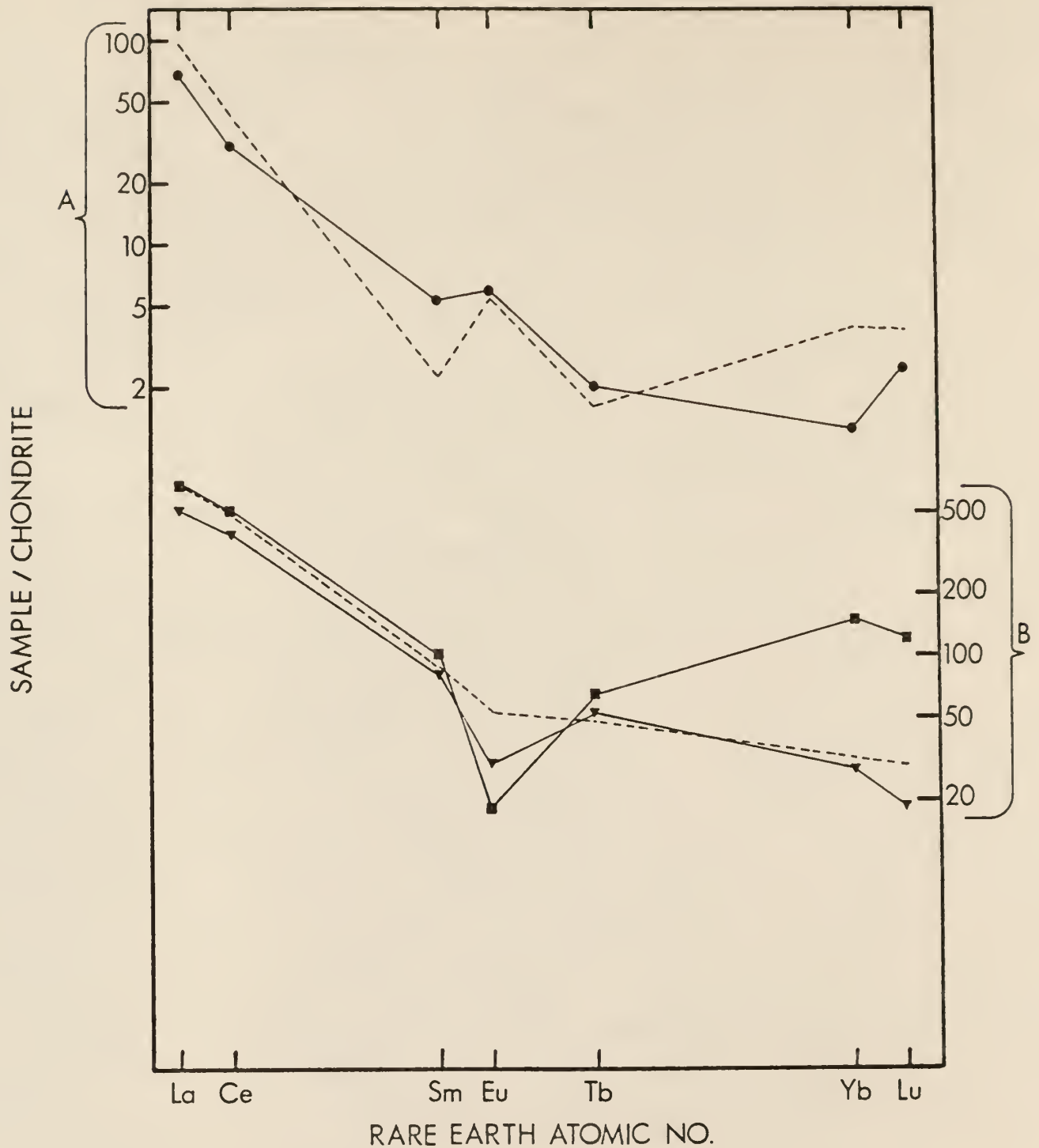


Figure 15c. Chondrite-normalized REE plots of model rocks (A) Dike NK-23 (●) and the calculated model rock produced by 80 percent crystallization of alkali-feldspar (86 percent) nepheline (3 percent) and muscovite (3 percent), and the incorporation of 20 percent residual liquid from a melt formed by 60 percent crystallization of alkali-feldspar (24 percent), hornblende (40 percent), biotite (26 percent), and sphene (9 percent) from the hypothetical "ijolitic" magma. (B) Nepheline syenite dikes FeNS-10 (■) and NK-4 (▼) and the calculated model melt produced by 35 percent fractionation of alkali-feldspar (90 percent), biotite (9 percent), sphene (0.3 percent), and apatite (0.3 percent) from the residual liquid produced by the crystallization of the malignites. Calculated model rocks are represented by dashed lines.



the residual melt, a lesser amount of fractional crystallization of the original magma is necessary.

Partial fusion of peridotite has been offered as a possible explanation for the origin of carbonatites (Wyllie and Huang, 1975). As they are difficult to generate by direct partial melting, the high REE contents in the McClure Mountain carbonatite do not suggest such an origin. Uncertainties, however, in the distribution coefficients at high pressure and in systems with a high  $\text{CO}_2$  content render it impossible to rule out such an origin. Although the REE evidence indicates that the carbonatites could possibly have formed by the fractional crystallization of the residual liquids resulting from the formation of the major intrusive rocks, the non-linear trends of the major element variations in the carbonatites with respect to those of the major intrusive rocks do not support such an origin. It is proposed rather that the carbonatites present in the McClure Mountain complex may have formed as an immiscible liquid phase of the hypothetical "ijolitic" magma or the residual liquid accumulating during the crystallization of the malignites. Using the carbonate melt/silicate melt distribution coefficients of Cullers and Medaris (1977), the range in REE content of the source magma from which the carbonatite may have separated was calculated (Fig. 16). The REE contents of both the hypothetical "ijolitic" magma and the residual liquid of malignite crystallization generally fall within the range of the REE contents in the calculated source magma (Fig. 16). This suggests that either the "ijolitic" magma or the residual liquid accumulating during malignite crystallization could act as a possible carbonatite source magma. In addition, the carbonate minerals in the McClure Mountain malignite suggests that carbonate immiscibility may have been operative during its formation.

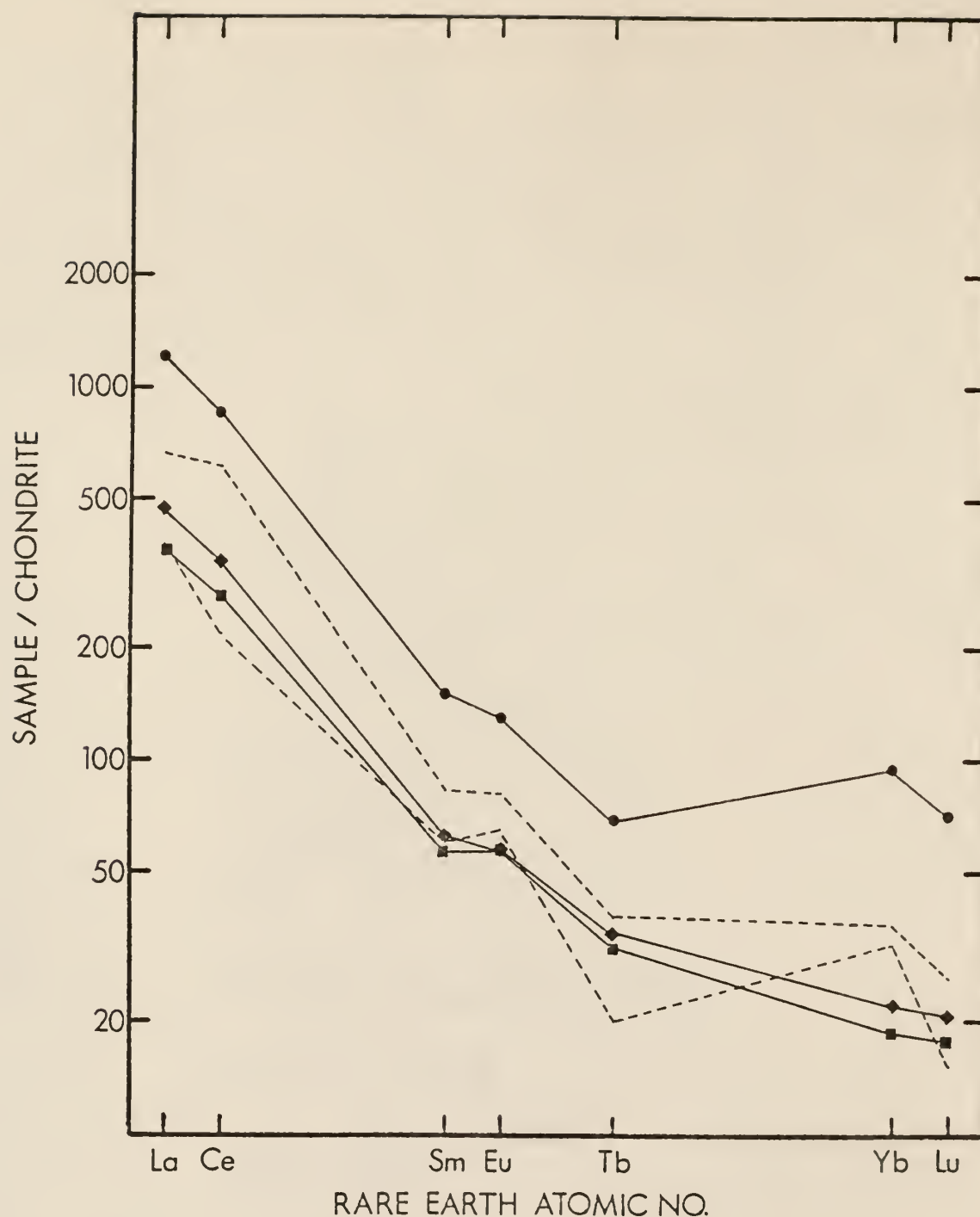


Figure 16. Chondrite-normalized REE plots of the model carbonatite melt and potential source melts. Chondrite-normalized REE content of the McClure Mountain carbonatite dike (●). The range in REE content of potential source melt calculated assuming liquid immiscibility and using carbonate melt/silicate melt distribution coefficients are represented by dashed lines. Possible source melts of the carbonatite dikes include hypothetical "ijolitic" magma formed by high pressure fractional crystallization of alkali basaltic parent magma (■) and liquid remaining after the formation of the malignites as cumulates from approximately 30 percent crystallization of hypothetical "ijolitic" magma (◆).

### Other Trace Elements

General.--The elements Co, Sc, Ba, Sr, and Rb can be used to test the validity of portions of the proposed model. Several factors however render these elements unreliable as quantitative indicators in the petrogenetic study of the rocks in the McClure Mountain complex. Notable among these are the following: (1) unavailability and uncertainties in the published distribution coefficients of these elements in alkalic and ultramafic rocks, (2) absence of reliable trace element data, particularly Co and Sc in peridotites, (3) high concentrations of Co and Sc in the early formed biotite, a phase which does not appear to have separated completely from the residual liquids, and (4) incomplete Sr data for many of the rock types. Sufficient data are available however for Co, Sc, Ba, Rb, and Sr that they can be used as qualitative indicators in testing portions of the proposed model. Th, Hf, and Ta are not used in this respect because of the general unavailability of distribution coefficients for these elements.

Primary melt.--Because it is not extensively exposed at the surface, the trace element content of the primary alkali basaltic parent magma is represented by sample NK-34 which, on the basis of REE and textural evidence, is believed to have formed by the rapid cooling of a portion of the parental magma. The trace element contents of sample NK-34, consistent with the belief that the sample represents a portion of the alkali basaltic parent magma, are, with the exception of a slight depletion in Sr and enrichment in Sc, within the range of similar elements reported for 11 alkali basalts by Lo and Goles (1976) (Table 12).

Assuming that sample NK-34 is representative of the parental alkali basaltic magma, its REE content is generally consistent with the belief that the parental alkali basaltic magma was generated by the partial melting of

Table 12. Trace element contents in peridotites and alkali basalts.

Element	Range in undepleted peridotite (Helmke et al., 1972)	Range in Formosan alkali basalts (Lo and Goles, 1976)	Presumed McClure Mountain alkali basaltic parent material (NK-34)
Co	35-120	27-60	35
Sc	5-15	11-27	37.8
Sr	10-40	555-883	360
Ba	4-5	---	630
Rb	2-8	20-67	43

upper-mantle peridotite. Examination of existing distribution coefficients for Rb, Ba, and Sr indicates that these elements have a strong tendency to fractionate into the liquid phase during the melting of peridotite. Consistent with this prediction, the Rb, Ba, and Sr concentrations of sample NK-34 are greater than those reported by Helmke et al. (1978) for undepleted peridotites (Table 12). Distribution coefficients for Co and Sc suggest that these elements should be slightly depleted in melts derived from the partial fusion of peridotite. The Co concentration of sample NK-34, as predicted, was similar to the lower limit of Co concentrations reported in undepleted peridotites (Helmke et al., 1978) (Table 12). Sc, however, being more enriched in sample NK-34 than in the source peridotite, is not consistent with its predicted distribution (Table 12). Although this suggests the possibility that sample NK-34 may not represent the parental alkali basaltic magma, similar anomalous Sc distributions between peridotite and derived melts have been noted by Helmke et al. (1978). They suggest that the Sc distribution coefficients may be strongly pressure dependent and could decrease, resulting in increased Sc concentrations in derived melts, with increasing pressure.

Major intrusive biotite syenite, feldspathoidal syenite, and malignite.--

Based on existing distribution coefficients for the elements, the fractionation of clinopyroxene from the parental alkali basaltic magma would result

in the strong depletion of Sc, moderate depletion of Co, moderate enrichment of Sr, and the strong enrichment of Ba and Rb in the residual "ijolitic" magma. The subsequent fractionation of mafic and felsic phases from the "ijolitic" magma to form the major intrusive series would have a profound effect on the distribution of these elements in the resulting solids.

Co and Sc, because of their strong tendency to concentrate in biotite and hornblende, should be depleted in rocks containing lesser quantities of these phases, and because they tend to crystallize early, in melts or solids formed through increased degrees of fractionation. Consistent with the proposed model for the origin of gabbro NK-34 and the major intrusives, average Co and Sc contents decrease in the order gabbro NK-34 > malignites > feldspathoidal syenites > biotite syenites, although some overlap in the Sc contents of the feldspathoidal syenites and biotite syenites does exist (Fig. 12).

The overlap in the Rb concentrations of the major intrusive malignites, feldspathoidal syenites, and biotite syenites and its depletion with respect to these same rocks in gabbro NK-34 is also consistent with the proposed model for their origin. Because the Rb distribution coefficients for gabbro NK-34 and the malignites, feldspathoidal syenites and biotite syenites are less than one, both the residual melt and solids formed through fractional crystallization should become increasingly enriched in Rb. This, balanced by the fact that the Rb distribution coefficients for the malignites are slightly greater than those of the feldspathoidal syenites and biotite syenites, results in the overlapping Rb concentrations of the major intrusives and its relative depletion in gabbro NK-34.

Because of the strong affinity of alkali feldspar for Ba and Sr, these elements are more concentrated in the feldspathoidal syenites than in the malignites, since little alkali feldspar is removed from the melt prior to the formation of the feldspathoidal syenites. After the large amounts of



alkali feldspar fractionation involved with the feldspathoidal syenite crystallization, the melt should be sufficiently depleted in Ba and Sr that the biotite syenites would contain smaller amounts of Ba and Sr than the other rock types. This results in average Ba and Sr concentrations which decrease in the order feldspathoidal syenites malignites biotite syenites.

The possibility that the biotite syenites may have crystallized before the nepheline syenites is refuted by their Ba and Sr distributions. Because feldspathoidal syenites and biotite syenites have Ba and Sr distribution coefficients of solid melt equilibria which are much larger than one owing to their high concentration of alkali feldspar, the residual liquids and co-existing solids resulting from the progressive crystallization of these phases are expected to be continually depleted in these elements. Because Ba and Sr concentrations of the biotite syenites are significantly lower than those of the feldspathoidal syenites, the biotite syenites must have formed after the feldspathoidal syenites.

In addition to the REE contents, the trace element contents of the feldspathoidal syenites and the biotite syenites are not consistent with their having formed by the fractional crystallization of a melt produced by partial fusion of an alkali gabbro or its high pressure equivalents, garnet granulite and eclogite. Because of the number of variables involved, however, trace elements cannot be used to test the possibility that the feldspathoidal syenites and the biotite syenites formed by the crystallization from two different melts produced by progressive partial fusion of an alkali gabbro or its high pressure equivalent.

If it is assumed that the alkali gabbro, garnet granulite, or eclogite source has a trace element distribution similar to sample NK-34, which is believed to represent the original alkali basaltic parent material, then certain predictions concerning the composition of melts derived by partial



fusion of these source rocks can be made. Because of the tendency of pyroxene and garnet, the major mineral phases in eclogites, to preferentially incorporate Co and Sc and reject Sr, Ba, and Rb as indicated by the distribution coefficients listed in Appendix H, melts derived from the feldspar-free eclogite are expected to have contents of Co and Sc which are less and Sr, Ba, and Rb contents which are greater than those in sample NK-34. Similar distributions are expected in melts derived from the feldspar-bearing garnet granulite and alkali gabbro except that Sr, an element preferentially incorporated by feldspar, would be more depleted in the derived melt than in sample NK-34. Assuming that they form from the same melt, the fractionation of the feldspathoidal syenites and the biotite syenites from the melt produced by the fusion of the alkali gabbro or its high pressure equivalent would further modify their trace element concentrations with respect to NK-34.

Because of the two-step formational sequence of the feldspathoidal syenites and biotite syenites, the elements Co, Sc, Sr, and Rb cannot be used to test the validity of the alternate model. This results from their being concentrated in one step and depleted in the other and there being no way of determining which step has the greatest effect. For example, during fusion, Rb increases in the melt with respect to its concentration in NK-34; it decreases, however, in the cumulate during fractional crystallization.

Because Ba is fractionated into the liquid during fusion and into the alkali feldspar-rich solid during fractional crystallization its concentration should be much greater in the syenites than in sample NK-34. The Ba concentration of one of the analyzed biotite syenites being less than that of sample NK-34 is, however, not consistent with its having formed by such an origin.

It is also possible that the feldspathoidal syenites and biotite syenites formed by fractional crystallization from two different melts produced by progressive partial fusion of an alkali gabbro or its high pressure equivalent. The number of variables involved in such a formational sequence, however, render the elements Ba, Rb, Sr, Co, and Sc useless as precise quantitative indicators of the validity of such a process.

Layered Series.--Unlike the major intrusive bodies, the rocks of the layered series are assumed to have formed by small degrees of crystallization from the same magmatic body, thus alleviating the problems resulting from changing magmatic concentrations as a result of extensive fractionation. If the calculated distribution coefficient for a particular element in a cumulate is greater than one, then it is to be expected that the concentration of that element in the cumulate would be greater than the concentration of the same element in sample NK-34, which represents the original parent magma. Similarly, if the distribution coefficient for a particular element in a particular rock is less than one, then its concentration in the cumulate is expected to be less than that in the parental magma.

The Rb and Ba distribution coefficients of the gabbros, pyroxenites, anorthosite stock, and magnetite ore, for example, being significantly less than one suggest that the concentrations of these elements should be significantly lower in these rocks than in the assumed parental magma represented by sample NK-34 (Appendix H). As predicted, Rb and Ba are significantly enriched in sample NK-34 compared to their concentrations in the gabbros, pyroxenites, anorthosite stock, and magnetite ore. Similarly the Sr, Co, and Sc concentrations of the gabbros, pyroxenites, anorthosite stock, and magnetite ore are greater in the appropriate cumulates compared to NK-34, consistent with their concentrating in plagioclase (Sr), pyroxene (Co, Sc), olivine (Co), and magnetite (Co, Sc).

The Th, Hf, and Ta concentrations of the gabbros, pyroxenites, anorthosite stock, and magnetite ore were consistently lower than those of the assumed parental magma NK-34. These elements seem to concentrate in residual liquids with respect to the mafic phases crystallizing during the formation of the rocks of the layered series.

Dikes and Stocks.--The low Th, Hf, and Ta contents and the positive Eu anomaly of dike NK-23 compared to other alkalic rocks in the complex are consistent with the previously proposed model that it formed as a cumulate product of fractionation from a melt produced by the crystallization of a portion of the "ijolitic" magma. These trends result because the elements Th, Hf, and Ta, and the REE, with the exception of Eu, are generally enriched in residual liquids. The high Rb and low Ba, Sr, and Co contents of dike NK-23, compared to the other nepheline syenite dikes, suggest that the magma from which it crystallized had previously undergone extensive fractionation as Rb increases and Ba, Sr, and Co decrease with increasing degree of fractionation. The low Ba and Sr contents indicate that alkali feldspar may have been one of the phases to crystallize prior to the formation of the dike, in as much as these elements would otherwise be concentrated in the alkali feldspar-rich dike. The high Co content of the dike is probably a result of its high magnetite and muscovite contents, phases which have a large affinity for this element.

Consistent with their having formed by the crystallization of residual liquids with little or no cumulate minerals being present, dike NK-4 and stock FeNS-10 are significantly enriched in Rb, Th, Hf, and Ta with respect to the other rocks in the complex. Also consistent with the model for their formation, the low Ba and Sr contents and the negative Eu anomalies of the dikes, as in the case of dike NK-23, suggest that the parental melt may have previously crystallized significant amounts of alkali feldspar.

Higher Th, Hf, Rb, and Ta, and lower Co and Sc contents in dike NK-4 suggest that it may have formed from more fractionated magma than stock FeNS-10.

The trace element character of the carbonatite dike is inconsistent with its having formed as a result of extensive fractional crystallization of a silicate magma. In a general sense, the concentrations of the elements Th, Hf, Ta, and Rb are expected to increase while the concentrations of Ba, Sr, Co, and Sc are expected to decrease with increasing degrees of fractionation of a silicate magma precipitating alkali feldspar, hornblende, biotite, and feldspathoids. The residual liquid of this fractionation is therefore expected to be enriched in Th, Hf, Ta, and Rb and depleted in Ba, Sr, Co, and Sc. Although enriched in Th and Ta, and depleted in Co and Sc, as expected, the low Rb and Hf and high Sr and Ba contents of the dike are inconsistent with this mode of origin.

Because of the unavailability of data concerning the partitioning of elements between silicate melts and immiscible liquid phases, it is difficult to use the trace element contents of the carbonatite dike to test the possibility that liquid immiscibility may have been responsible for its formation. It seems probable, however, that a mechanism other than partial melting or fractional crystallization of silicate phases was responsible for the formation of the carbonatite dikes.

#### RELATION TO THE GEM PARK COMPLEX

The occurrence of mafic-ultramafic and alkalic rocks, in addition to carbonatite dikes, at both McClure Mountain and Gem Park, and their similar geographic locations and ages suggest that a genetic relationship may exist between the two complexes (Olson et al., 1977).

Roden (1977), in a petrogenetic study of the Gem Park complex proposed that different degrees of partial melting of upper mantle peridotite both

with and without low temperature fractional crystallization produced the gabbros and pyroxenites there. In addition, she theorized that the nepheline syenite pegmatite that crops out in the complex is a late-stage product of the same fractionation sequence. Carbonatite dikes in the complex were assumed to have formed either by partial fusion of peridotite or as an immiscible liquid fraction of a hypothetical "ijolitic" magma.

The similarities in processes which are proposed to have formed the rocks at McClure Mountain and Gem Park warrant a comprehensive model for the origin of the complexes. A possible explanation for the mafic-ultramafic rocks in the two complexes is that they formed by small degrees of partial melting of upper-mantle peridotite followed by low temperature fractional crystallization. The extreme difference in mineralogy and REE content of the rocks results from their having incorporated different amounts of residual liquids along with the cumulate fractionation products. In addition, some rocks could have crystallized from melts enriched in the REE due to their previously having crystallized significant amounts of low REE-bearing phases.

Although there are some differences in texture and mineralogy, the nepheline syenite pegmatite dike at Gem Park may be related to the nepheline syenite dikes in the McClure Mountain complex and possibly formed as a result of similar processes. The Gem Park nepheline syenite dike has a REE content which is intermediate between the range of REE contents observed in the McClure Mountain nepheline syenite dikes. The occurrence of several nepheline syenite dikes in the area within and surrounding the McClure Mountain complex is a testament to the mobility of the magmas which formed the dikes.

The similarities in REE content of the McClure Mountain and Gem Park carbonatite dikes suggests that they too may have formed as a result of similar processes. Although the most probable mechanism for the formation



of the dike appears to be as a result of liquid immiscibility from an alkali-rich mafic magma, the possibility that they formed by very small degrees of partial melting of upper mantle peridotite does exist. In either case it seems almost certain that the dikes in the McClure Mountain and Gem Park complexes are closely related.



## S U M M A R Y

The field relations, petrographic criteria, major element contents, Sr isotopic data, REE distributions, and other trace element contents of the major rock bodies are consistent with the theory that the rocks of the McClure Mountain complex are comagmatic. Existing data available for the rocks in the nearby Gem Park complex suggest that a genetic relationship may exist between the rocks at Gem Park and at McClure Mountain. The following model is proposed for the formation of the rocks in the McClure Mountain complex:

- 1.) The alkali rocks in the McClure Mountain complex, as indicated by Rb-Sr isotopic studies, were formed approximately 520 million years ago. A similar age of emplacement for the mafic-ultramafic rocks of the layered series is assumed, although age dates for the rocks have not been reported.
- 2.) An alkali basaltic parent magma was formed by approximately 0.5 percent partial melting of upper mantle peridotite.
- 3.) Part of the alkali basaltic parent magma underwent extensive (approximately 70 percent) high pressure fractional crystallization (15 - 23 Kb) of clinopyroxene to generate a hypothetical "ijolitic" magma. The magma ascended to shallow depths where it underwent 30 percent low temperature crystallization at high water pressure to generate a cumulate which, along with the incorporation of 30 percent of the residual liquid, formed the malignite. Fifty percent fractional crystallization of the remaining liquid along with the incorporation of 20 percent of the residual liquid produced the feldspathoidal syenite. The biotite syenite was formed

as cumulates from 35 percent fractionation of the liquid remaining after the formation of the feldspathoidal syenite.

- 4.) Part of the alkali basaltic parent magma rose rapidly to shallow depths and underwent small degrees of low temperature fractional crystallization at low water pressure to produce the gabbro, pyroxenite, anorthosite, and magnetite ore of the layered series. Rocks formed by the residual liquid of this fractionation are believed to have been mostly removed by erosion.
- 5.) The nepheline syenite dikes and stocks of the McClure Mountain complex may have formed from portions of the residual liquids produced during the formation of the malignite and feldspathoidal syenite. Some dikes represent cumulate portions of the residual liquids.
- 6.) The carbonatite dikes in the McClure Mountain complex probably formed as an immiscible liquid fraction of the "ijolitic" magma or the residual liquid accumulating during the crystallization of the malignite. It is possible, however, that partial fusion of peridotite may have formed the carbonatite magma.

Although the details are not presented in this study the proposed model is believed to explain the formation of the rocks at Gem Park.

## A P P E N D I X

## A. Petrographic Descriptions

Thin sections of analyzed samples are petrographically described below. Mineral percentages were obtained by counting 1000 points (Table A-1). Approximate size ranges of minerals are listed in parentheses. Included with each summary is a brief discussion of the order of crystallization of the minerals. A more generalized discussion based on the results of this and other studies is included in the main body of the text. Table A-1 gives the modal analysis of the samples described.

### NK-4 Sodalite Syenite dike:

This is a holocrystalline, medium grained, hypidiomorphic-granular sodalite syenite. It contains 68.9% euhedral to subhedral perthite (2.0 - 3.5 mm), 21.4% subhedral to anhedral sodalite (0.1 - 3.5 mm), and 7.5% subhedral hornblende (0.2 - 1.6 mm). Also present, in minor amounts, are 0.7% anhedral biotite (0.1 - 0.3 mm), 0.8% euhedral sphene (.35 mm), 1.0% subhedral magnetite (0.6 mm), and 0.5% anhedral plagioclase (0.35 mm). Traces of apatite and cancrinite are also present. The perthite is slightly altered to kaolinite and magnetite displays a slight alteration to iron oxide. Sodalite appears to be a secondary mineral after nepheline. Alkali feldspar probably was the first major mineral to crystallize followed by nepheline (sodalite) and hornblende.

### NK-9 Nepheline - Cancrinite Syenite:

This is a holocrystalline, medium grained, xenomorphic-granular nepheline-cancrinite syenite. It contains 67.1% anhedral perthite (1.2 - 2.6 mm), 7.8% anhedral nepheline (0.6 - 1.5 mm), 7.5% anhedral cancrinite (0.5 - 1.5 mm), 12.1% anhedral to subhedral hornblende (1.2 - 1.8 mm), and 4.6% anhedral biotite (0.7 mm). Subhedral sphene (0.7 mm) is present as a

minor (0.7%) constituent. Traces of apatite and magnetite are also present. The perthite is moderately altered to kaolinite and nepheline is strongly altered to zeolite. Hornblende is partially replaced by biotite. Alkali feldspar crystallized first followed by hornblende, feldspathoids, and finally biotite.

#### NK-10 Hornblende Nepheline Syenite:

This is a holocrystalline, medium grained, xenomorphic-porphyritic, nepheline bearing hornblende syenite with perthitic feldspar and hornblende phenocrysts. It contains 70.7% anhedral perthite (0.05 - 0.8 mm and 2.0 - 4.5 mm), 18.0% hornblende in euhedral to subhedral cross sections (1.0 - 2.0 mm) and anhedral tabular grains (1.5 - 3.0 mm), 6.2% anhedral biotite (0.4 - 0.8 mm), 2.6% interstitial subhedral nepheline (0.2 mm), and 3.0% interstitial anhedral plagioclase. Accessory minerals include sphene, magnetite, and apatite. The perthite is moderately altered to kaolinite. Alkali feldspar and hornblende appear to have been the earliest formed phases to crystallize followed by biotite and nepheline.

#### NK-19 Feldspathoidal Syenite:

This is a holocrystalline, medium grained, allotriomorphic-granular nepheline and sodalite bearing feldspathoidal syenite. It contains 80.0% anhedral perthite (1.5 - 3.5 mm), 12.4% anhedral hornblende (1.5 - 2.5 mm), and 4.0% anhedral nepheline. Also present in minor amounts are 1.0% interstitial, anhedral sodalite (0.4 mm), and 1.0% anhedral biotite (1.2 mm). Other, less abundant minerals include cancrinite, muscovite, apatite, carbonate, and opaques. Perthite is moderately altered to kaolinite. Biotite occurs primarily as a replacement of hornblende. Cancrinite and muscovite were formed by the deuteric alteration of nepheline. The primary mineral crystallization sequence appears to be alkali feldspar followed by hornblende and nepheline.

FeNS-4 Biotite Syenite:

This is a holocrystalline, coarse grained, xenomorphic-granular cancrinite bearing biotite syenite. It contains 87.0% anhedral perthite (4.0 - 8.0 mm), 7% anhedral biotite (0.3 - 0.7 mm), and 2.9% anhedral cancrinite (0.2 - 0.4 mm). Anhedral hornblende (0.7 - 1.3 mm) is present as a minor (1.6%) constituent. Also present are limited amounts of muscovite, sphene, plagioclase, apatite, and opaques. Perthite grains are extensively altered to kaolinite. Cancrinite, muscovite, and small amounts of zeolite occur as alteration products of nepheline. Some biotite is present as a replacement of hornblende. Alkali feldspar was the primary phase to crystallize followed by interstitial biotite and sodalite (cancrinite).

FeNS-10 Nepheline Syenite:

This is a holocrystalline, medium grained, allotriomorphic-porphyritic nepheline syenite with perthitic feldspar and nepheline phenocrysts. It contains 69.6% anhedral perthite (0.3 - 1.0 and 2.5 - 4.0 mm), 10.9% subhedral plagioclase (albite - oligoclase) (0.1 - 1.5 mm), 8.0% anhedral nepheline (0.4 - 1.0 and 2.5 - 4.5 mm), 4.0% anhedral cancrinite (0.1 - 0.3 mm), and 3.0% anhedral biotite (2.0 mm). Present in minor amounts are 2.3% subhedral opaques (3.0 mm) and 2.1% anhedral sodalite (0.08 mm). Traces of sphene and muscovite are also present. Perthite has undergone extensive alteration to kaolinite and nepheline is highly altered to cancrinite, muscovite, and sodalite. Alkali feldspar and nepheline were the first formed phases followed by biotite and plagioclase.

NK-23 Nepheline Syenite dike:

This is a holocrystalline, coarse grained, hypidiomorphic-porphyritic poikilitic nepheline syenite with perthitic feldspar and nepheline phenocrysts. It contains 86% subhedral perthite (0.3 - 1.0 and 4.0 - 7.0 mm)



and 10.7% subhedral to anhedral nepheline (0.4 - 1.0 and 2.0 - 3.0 mm). Present in minor amounts are 1.5% anhedral muscovite (0.05 mm) and 1.6% subhedral opaques (0.15 - 1.5 mm). Biotite and cancrinite are also present. Some larger grains of alkali feldspar contain small amounts of nepheline. Extensive alteration of the alkali feldspar to kaolinite is present. Nepheline has undergone moderate alteration to muscovite, cancrinite, and zeolite. Alkali feldspar and nepheline were the first phases to crystallize followed by the accessory minerals.

#### NK-3 Biotite Syenite:

This is a holocrystalline, medium to coarse grained, hypidiomorphic-granular biotite syenite. It contains 86% subhedral perthite (4.0 - 8.0 mm), 10.2% anhedral biotite (0.4 - 0.8 mm), and 2.9% anhedral muscovite (0.1 - 0.3 mm). Anhedral hornblende (0.7 - 1.3 mm) is present as a minor phase. Other minerals occurring in limited amounts are plagioclase, sphene, apatite, and opaques. Perthite is moderately altered to kaolinite. Hornblende occurs as a replacement of biotite. Muscovite may have formed as a deuteric alteration product of nepheline. Alkali feldspar was the first major phase to crystallize followed by biotite and hornblende.

#### NK-31 Biotite Syenite:

This is a holocrystalline, medium grained, xenomorphic-granular biotite syenite. It contains 90.2% subhedral-anhedral blocky perthite (1.5 - 3.5 mm) and 6.8% anhedral biotite (0.5 - 1.5 mm). Present in minor amounts are 1.3% subhedral-euhedral apatite (0.2 mm), 1.0% anhedral opaques (0.1 mm), and 1.0% interstitial anhedral plagioclase (0.05 - 0.15 mm). Small amounts of hornblende and sphene are also present. The perthite shows small amounts of alteration to kaolinite. Some biotite and magnetite appear to be late stage or secondary. Alkali feldspar was the first formed major phase and was followed by biotite crystallization in the interstitial areas.

NK-100 Biotite Syenite:

This is a holocrystalline, coarse grained, xenomorphic to hypidiomorphic-granular biotite syenite displaying a moderately well-developed trachyoidal texture. It contains 89.6% subhedral-euhedral perthite (0.1 - 0.3 to 3.5 - 8.0 mm) and 7.0% interstitial anhedral biotite (0.3 - 0.7 mm). Minor amounts of (1.3%) interstitial anhedral plagioclase (0.5 - 2.5 mm) and 0.9% anhedral opaques (0.1 mm) are also present. Also occurring are traces of apatite, sphene, muscovite, and hornblende. Perthite has undergone small amounts of alteration to kaolinite. Alkali feldspar was the first formed major phase followed by biotite crystallization in the interstitial areas.

NK-18 Malignite:

This is a holocrystalline, medium grained hypidiomorphic-granular hornblende malignite. It contains 38.0% subhedral hornblende (0.7 - 2.0 mm), 29.5% subhedral alkali feldspar (0.1 - 3.5 mm), 16.4% anhedral biotite (0.5 - 1.5 mm), and 12.2% anhedral nepheline (1.0 - 2.5 mm). Present in minor amounts are 7.5% euhedral sphene (1.3 mm) and 1.0% anhedral opaques (0.2 mm). Carbonate, apatite, and monoclinic pyroxene occur as accessory minerals. Alkali feldspar is moderately altered to kaolinite, and nepheline is slightly altered to cancrinite and zeolite. Alkali feldspar and hornblende were the first primary phases to form followed by biotite and finally nepheline.

NK-22 Malignite:

This is a holocrystalline, medium grained, xenomorphic-porphyritic hornblende malignite with phenocrysts composed of optically continuous clusters of alkali feldspar and carbonate crystals. It contains 42.0% subhedral biotite (0.5 - 2.0 mm), 38.2% anhedral hornblende (0.5 - 2.5 mm), 10.8% anhedral to subhedral alkali feldspar (0.4 - 1.2 mm), and 4.5%

anhedral nepheline (0.2 - 1.0 mm). Present in minor amounts are 2.6% anhedral carbonate (0.5 - 1.0 mm) and 1.4% subhedral sphene (1.0 mm). Monoclinic pyroxene, sodalite, muscovite, and opaques are also present. Alkali feldspar is moderately altered to kaolinite and nepheline is altered to sodalite, cancrinite, muscovite, and zeolite. Some hornblende is replaced by biotite. The crystallization history is not readily discernible, but probably is represented by alkali feldspar, hornblende, and biotite crystallizing initially followed by nepheline and finally carbonate as a late stage or deuteritic phase.

#### NK-24 Malignite:

This is a holocrystalline, medium grained, xenomorphic-porphyritic hornblende malignite containing phenocrysts composed of optically continuous clusters of alkali feldspar and biotite. It contains 46.3% anhedral hornblende (0.5 - 2.0 mm), 24.6% anhedral biotite (0.3 - 2.5 mm), 18.4% anhedral alkali feldspar (0.4 - 1.0 mm), 7.6% anhedral nepheline (1.0 - 2.0 mm), 1.8% subhedral sphene (0.1 - 1.0 mm), and 1.0% anhedral carbonate (1.0 mm). Minor amounts of monoclinic pyroxene (augite), apatite, and opaques are also present. Alkali feldspar is slightly altered to kaolinite. No definite crystallization sequence of the major minerals could be determined, but presumably it was similar to the other malignites.

#### NK-27 Malignite:

This is a holocrystalline, medium-grained, xenomorphic to hypidiomorphic-porphyritic hornblende malignite. It contains 39.8% subhedral to anhedral hornblende as phenocrysts (5.0 - 8.0 mm) and in the groundmass (0.8 - 1.5 mm), 29.1% anhedral alkali feldspar (0.5 - 2.0 mm), 20.5% subhedral to anhedral biotite (0.5 - 1.0 mm), and 8.0% anhedral nepheline (0.5 - 1.5 mm). Present in minor amounts are 1.1% subhedral sphene (3.0 mm) and 1.0% subhedral augite (1.0 mm). Accessory minerals include carbonate,

apatite, and opaques. Perthite is extensively weathered to kaolinite. Some biotite occurs as a replacement of hornblende and augite is rimmed by hornblende. The first major phase to crystallize appears to have been hornblende, followed by alkali feldspar and biotite, and ending with nepheline.

#### FeG-1 Olivine Gabbro:

This is a holocrystalline, medium-grained, hypidiomorphic-granular olivine gabbro. It contains 52.8% subhedral plagioclase (andesine to sodic labradorite (1.0 - 3.5 mm), 27.9% anhedral to subhedral augite (0.5 - 2.0 mm) with abundant schiller structure, 12.3% anhedral olivine (0.5 - 1.2 mm), 3.5% anhedral magnetite (0.35 mm), and 2.6% kaersutite (0.3 mm). Spinel occurs as an accessory mineral. A poikilitic texture is evidenced by augite containing smaller crystals of olivine and plagioclase. Olivine is altered to secondary serpentine and magnetite. Plagioclase is slightly altered to sericite. Deuteric kaersutite mantles most other phases. Plagioclase was the first major mineral to crystallize followed by olivine, augite, and magnetite.

#### FeG-6 Olivine Gabbro:

This is a holocrystalline, medium grained xenomorphic-granular olivine gabbro. It contains 66.3% subhedral plagioclase (calcic andesine to labrodorite) (0.3 - 2.5 mm), 17.8% anhedral olivine (2.7 - 3.0 mm), 7.5% anhedral augite (0.7 - 3.0 mm), and 6.0% subhedral magnetite (0.3 - 1.5 mm). Also present as a minor phase is 2.3% kaersutite (0.4 mm). Spinel is a common accessory mineral. Olivine is highly altered to serpentine and magnetite. Plagioclase is slightly altered to sericite. Augite and magnetite display deuteric kaersutite coronas. The crystallization sequence is similar to that which formed olivine gabbro FeG-1.

FeP-3 Gabbro:

This is a holocrystalline, medium grained, hypidiomorphic-granular pyroxenite. It contains 51% euhedral to subhedral zoned plagioclase (calcic andesine to sodic labradorite) (0.35 - 3.0 mm), 38.6% anhedral to subhedral augite (0.7 - 3.0 mm), and 5.5% anhedral olivine (0.4 - 2.0 mm). Also present are 2.1% anhedral kaersutite (0.2 - 1.0 mm), 1.5% anhedral magnetite (0.7 mm), and biotite. Augite poikilitically encloses plagioclase. Olivine is extensively altered to serpentine, magnetite, and iddingsite. Plagioclase shows minor alteration to sericite. Kaersutite occurs as a deuteric phase mantling pyroxene, olivine, and magnetite. Olivine and magnetite are interstitial minerals which crystallized in between the presumed plagioclase and augite cumulates.

FeP-1 Pyroxenite:

This is a holocrystalline, medium grained, hypidiomorphic-granular pyroxenite. It contains 81.0% euhedral to subhedral augite (0.7 - 1.7 mm), and 17.4% interstitial subhedral plagioclase (labradorite) (0.6 - 1.5 mm). Magnetite, biotite, kaersutite, olivine, and spinel are also present. Serpentine and magnetite are alteration products of olivine. Augite and plagioclase show minor alteration to chlorite and sericite respectively. Kaersutite is present as a deuteric alteration of augite and magnetite. Augite was the first mineral to crystallize, and formed a cumulate in the interstitial spaces of which crystallized plagioclase.

NK-33 Pyroxenite:

This is a holocrystalline, medium grained, xenomorphic granular pyroxenite. It contains 91.8% euhedral to subhedral augite (1.0 - 3.5 mm), and 3.3% anhedral plagioclase (0.35 mm). Minor amounts of (1.3%) anhedral olivine (0.7 - 1.5 mm) and (1.8%) anhedral kaersutite (1.0 mm) are also



present. Magnetite, carbonate, and biotite occur in small amounts. Olivine is altered to serpentine, magnetite, and carbonate. Augite is partially replaced by kaersutite and is strongly altered to chlorite and serpentine. Augite was the first formed mineral followed by interstitial plagioclase and olivine.

#### NK-29 Pyroxenite:

This is a holocrystalline, medium grained, hypidiomorphic-granular pyroxenite. It contains 83.0% euhedral to subhedral augite (1.0 - 3.5 mm) and 16.5% interstitial anhedral plagioclase (0.7 - 2.0 mm). A minor amount (0.6%) of anhedral magnetite (0.5 - 3.5 mm) is also present. Augite in some cases encloses small plagioclase crystals and is moderately altered to chlorite and serpentine. Plagioclase is extensively altered to sericite. Kaersutite occurs as a deuteric alteration phase of augite. Although augite is the dominant mineral, the poikilitic texture indicates that plagioclase crystallization may have preceded that of augite.

#### NK-1 Magnetite ore:

This is a holocrystalline, medium grained, hypidiomorphic-granular magnetite ore. It contains 81.2% euhedral to subhedral magnetite (1.5 - 3.5 mm), 5.3% anhedral plagioclase (0.35 - 1.7 mm), 7.3% euhedral to subhedral green spinel (0.1 - 1.0 mm), and 4.3% anhedral to subhedral kaersutite (0.01 - 1.0 mm). Occurring in minor amounts are 1.2% anhedral olivine (0.3 - 2.0 mm) and 0.8% anhedral augite (0.35 - 2.0 mm). Plagioclase is extensively altered to sericite. Augite is altered to chlorite and serpentine, whereas olivine is altered to serpentine. Kaersutite occurs as deuteric rims on most of the major phases. The rock formed as a result of magnetite accumulation from a crystallizing liquid and the subsequent interstitial precipitation of olivine and plagioclase.



NK-28 Anorthosite:

This is a holocrystalline, medium grained, hypidiomorphic-granular anorthosite. It contains 85.8% euhedral to subhedral plagioclase (labradorite) (1.0 - 2.5 mm), 9.4% anhedral pyroxene (0.5 - 2.1 mm), and 2.3% subhedral magnetite (0.2 - 0.9 mm). Apatite and spinel occur as accessory minerals. Biotite and kaersutite are deuteritic phases associated with pyroxene and magnetite. Plagioclase has been slightly altered to sercite. Plagioclase was the first mineral to crystallize followed by interstitial pyroxene and magnetite crystallization.

NK-32 Carbonatite:

This is a holocrystalline, medium grained, xenomorphic-granular sovite carbonatite. It contains 86.8% anhedral calcite (0.5 - 4.0 mm) and 12.4% anhedral opaques (0.5 - 1.5 mm). Pyrochlore, quartz, and green spinel are also present.

NK-34 Gabbro:

This is a holocrystalline, bimodal, hypidiomorphic-granular pyroxene rich gabbro. It contains 36.9% subhedral augite (0.05 - 0.5 mm and 0.35 - 1.5 mm) and 55.1% anhedral plagioclase (0.08 - 0.5 and 0.4 - 2.0 mm). Present in minor amounts are 3.9% subhedral magnetite (0.1 - 0.35 mm and 1.0 - 1.5 mm), 3.1% euhedral to subhedral apatite (0.01 - 0.2 mm), and 2% euhedral sphene (1.0 - 1.5 mm). Lesser quantities of carbonate, muscovite, sercite, and iron oxides are also present. Plagioclase is extremely altered to sercite, particularly in the finer grained zones. Plagioclase was the first major phase to crystallize, followed by augite and magnetite. The finer grained material presumably represents rapidly cooled residual liquid.

Table A-1. Modal analyses of McClure Mountain Rocks in percent by volume (1000 points).

	NK-4		NK-9		NK-10		NK-19		FeNS-4		FeNS-10		NK-23	
	Sodalite Syenite dike		Nepheline Cancrinite Syenite		Hornblende (Nepheline) Syenite		Feldspathoidal Syenite		Biotite Syenite		Nepheline Syenite		Nepheline Syenite dike	
Alkali														
Feldspar	68.9		67.1		70.7		80.0		87.0		69.6		86.0	
Hornblende	7.5		12.1		18.0		12.4		1.6		---		---	
Biotite	0.7		4.6		6.2		1.0		7.0		3.0		tr	
Nepheline	---		7.8		2.6		4.0		---		8.0		10.7	
Plagioclase	0.5		---		3.0		---		tr		10.9		---	
Sphene	0.8		0.7		tr		1.0		tr		tr		---	
Sodalite	21.4		---		---		1.0		---		2.1		---	
Cancrinite	tr		7.5		---		tr		2.9		4.0		tr	
Apatite	tr		tr		tr		tr		tr		---		---	
Opakes (Magnetite)	1.0		tr		tr		tr		tr		2.3		1.6	
Muscovite	---		---		tr		tr		tr		tr		1.5	
Carbonate	---		---		---		tr		---		---		---	
Augite														

Table A-1. Modal analyses of McClure Mountain rocks in percent by volume (1000 points) (Cont.)

	FeG-1		FeG-6		FeP-1 Pyroxenite	NK-33 Pyroxenite	NK-29 Pyroxenite	NK-1		NK-28 Anorthosite	NK-32 Carbonate	NK-34 Fenitized Gabbro
	Olivine Gabbro	Olivine Gabbro	FeP-3 Gabbro	Olivine Gabbro				Magnetite Ore				
Alkali												
Feldspar	---	---	---	---	---	---	---	---	---	---	---	---
Biotite	---	---	tr	tr	tr	---	---	---	tr	---	---	---
Plagioclase	52.8	66.3	51.0	17.4	3.3	16.5	5.3	85.8	---	---	---	55.1
Apatite	---	---	---	---	---	---	---	tr	---	---	---	3.1
Opakes (Magnetite)	3.5	6.0	1.5	tr	tr	0.6	81.2	2.3	---	12.4	---	3.9
Muscovite	---	---	---	---	---	---	---	---	---	---	---	tr
Carbonate	---	---	---	---	tr	---	---	---	---	86.8	---	tr
Augite	27.9	7.5	38.6	81.0	91.8	83.0	0.8	9.4	---	---	---	36.9
Olivine	12.3	17.8	5.5	tr	1.3	---	1.2	---	---	---	---	---
Kaersutite	2.6	2.3	2.1	tr	1.8	tr	4.3	tr	---	---	---	---
Spinel	tr	tr	---	tr	---	---	7.3	tr	---	tr	---	---
Pyrochlore	---	---	---	---	---	---	---	---	---	tr	---	---
Quartz	---	---	---	---	---	---	---	---	---	tr	---	---
Sphene	---	---	---	---	---	---	---	---	---	---	---	2.0

Table A-1. Modal analyses of McClure Mountain rocks in percent by volume (1000 points) (Cont.)

	NK-3			NK-31			NK-100			NK-18			NK-22			NK-24			NK-27		
	Biotite	Syenite		Biotite	Syenite		Biotite	Syenite		Biotite	Syenite	Malignite	Biotite	Syenite	Malignite	Biotite	Syenite	Malignite	Biotite	Syenite	Malignite
Alkali																					
Feldspar	86.0			90.2			89.6			29.5			10.8			18.4			29.1		
Hornblende	tr			tr			tr			38.0			38.2			46.3			39.8		
Biotite	10.2			6.8			7.0			16.4			42.0			24.6			20.5		
Nepheline	---			---			---			12.2			4.5			7.6			8.0		
Plagioclase	tr			1.0			1.3			---			---			---			---		
Sphene	tr			tr			tr			2.5			1.4			1.8			1.1		
Sodalite	---			---			---			---			tr			---			---		
Cancrinite	---			---			---			---			---			---			---		
Apatite	tr			1.3			tr			tr			---			tr			---		
Opaques (Magnetite)	tr			1.0			0.9			1.0			---			tr			tr		
Muscovite	2.9			---			tr			---			tr			---			---		
Carbonate	---			---			---			tr			2.6			1.0			tr		
Augite	---			---			---			tr			tr			tr			1.0		

## B. Sample Collection and Preparation

Samples of the major rock units of the McClure Mountain complex and many of its associated dikes and stocks analyzed in this study were collected in the summer, 1977. Samples were chosen such that maximum geographic range of the rock types was represented. Weathered surfaces were chipped away leaving only the freshest parts of the samples. Upon return to the lab, the samples were further trimmed using a diamond cutting saw.

Representative portions of the rock samples were sent to Rudolf von Huene labs, 1555 East Walnut Street, Pasadena, California, where covered thin sections were prepared.

Portions of the samples were reduced in size using a hammer and chisel. Samples to be analyzed using A.A. (Atomic Absorption Spectrophotometry) or INAA (Instrumental Neutron Activation Analyses) were further crushed using a Sturtevant Laboratory Roll Jaw Crusher (Model 1C1) and a BICO circular pulverizer (type UA). Samples for isotopic analyses were ground in a steel mortar and pestle instead of using the above method to minimize potentially serious contamination. Portions of both groups of samples were then transferred to a tungsten carbide-lined mixer mill (Spex Industries Catalogue number 8000) and ground for about 30 minutes after which time the samples were placed in clean glass bottles and stored for analyses.

### C. Atomic Absorption and Emission Spectrophotometry

Major and select minor elements were analyzed using atomic absorption and emission spectrophotometry. The method was adopted, with slight modification, from a procedure by Buckley and Cranston (1971).

#### Sample Dissolution

Approximately 0.10 g of each sample was weighed precisely ( $\pm 0.0002$  g) into a Parr decomposition vessel. Six ml ( $\pm 0.1$  ml) of HF acid and 1 ml ( $\pm 0.01$  ml) of aqua regia were added to the decomposition vessels which were then sealed and placed in a drying oven at  $110^{\circ}\text{C}$  for one hour. Vessels containing the samples were removed from the oven and cooled slowly to room temperature. Sample solutions were then transferred quantitatively to teflon beakers containing 4 g ( $\pm 0.1$  g) of  $\text{H}_3\text{BO}_3$  in approximately 20 ml of water. The resulting solutions were diluted to 200 ml in volumetric flasks and then transferred to polyethylene bottles.

A blank solution, which was used in the preparation of the standard solution, was prepared in a similar fashion as the sample solutions except that six times the amount of the blank was prepared each time. Thus, the blank was prepared in a one liter volume by weighing 20.0 g of  $\text{H}_3\text{BO}_3$  into 30 ( $\pm 0.1$  ml) ml of HF acid and 5 ( $\pm 0.05$  ml) ml of aqua regia.

#### Primary Standard Preparation

A number of liquid standards were prepared corresponding to the variety of rock types to be analyzed. Primary standard solutions were prepared in 200 ml volumes using appropriate amounts of standard stock solutions diluted with the pre-made blank solution. The standards were prepared such that the resulting concentrations matched the concentration of the associated samples diluted to 200 ml. In this way both the samples and corresponding



standards could be simultaneously diluted in the same proportions down to the concentration range necessary for analyses. Similar sample-standard concentrations alleviated any problems which might have developed from different sample-standard matrices.

The Si, Fe, K, Mg, and Na used for the primary standard solutions were obtained from 1000 ug/ml Fisher Scientific stock solutions of these elements. Analytical grade stock solutions of Al and Ca were prepared by dissolving appropriate amounts of reagent grade Al wire and  $\text{CaCO}_3$  in dilute acid and bringing the concentration to 1000 ug/ml with distilled deionized water. Table C-1 lists the concentrations of the elements in the primary standard solutions and the rock types which were analyzed with these solutions.

#### Sample and Standard Dilutions

Samples and standards often had to be diluted down from the above standard and sample solutions to the linear concentration range of the desired element. As the amount of dilution depended on the concentration of the element in the original sample, the dilution scheme for each rock type was unique. Blank solutions were diluted in the same manner as samples and standards so that a correction could be made for any impurities incorporated during the dissolution and dilution processes. To suppress the tendency of many of the elements to ionize during sample analyses, 1000 - 2000 ug/ml of an alkali salt was added to many of the samples, standards, and blanks during dilution. The type of salt used depended on which elements were to be analyzed from the diluted fractions. Table C-2 summarizes dilutions of samples, standards, and blanks.

Table C-1. Primary standard solution concentrations (ug/ml).

Elements	Standard 1 (Carbonatite)	Standard 2 (Syenite)	Standard 3 (Malignite)	Standard 4 (Pyroxenite, Gabbro)
Si	27.5	135	110	100
Al	10	45	60	27.5
Fe	25	17.5	17.5	35
Mg	17.5	10	7.5	40
Ca	125	7.5	60	65
Na	1.5	25	25	3
K	5.5	20	7.5	0.5

Table C-2 Dilution schemes for Atomic Absorption and Emission Spectrophotometry.

Rock Types	Ionization Suppressant	Final Dilution for Sample and Matched Standard	Elements Determined
Feldspathoidal Syenite	1500 ug/ml K*	6X	Al, Ca, Si
Biotite Hornblende	1000 ug/ml K	30X	Mg, Fe
Syenite	1000 ug/ml Rb*	30X	K
	1000 ug/ml K	60X	Na
	1000 ug/ml K	1.11X	Sr
	-	1X	Rb
Malignite,	1200 ug/ml K	6X	Al, Si
	1000 ug/ml K	12.5X	Fe, Ca
Anorthosite	1000 ug/ml Rb	12.5X	K
	1000 ug/ml K	50X	Mg, Na
	1000 ug/ml K	1.11X	Sr
	-	1X	Rb
Gabbro,	1000 ug/ml K	5X	Si, Al
Pyroxenite	1000 ug/ml Rb	5X	K
	1000 ug/ml K	20X	Fe, Mg, Ca, Na
	1000 ug/ml K	1.11X	Sr
	-	1X	Rb
Carbonatite	1000 ug/ml K	10X	Fe, Na
	1000 ug/ml Rb	12.5X	K
	1000 ug/ml K	50X	Mg, Ca
	1000 ug/ml K	1.11X	Si, Al, Sr
	-	1X	Rb

\*K was from reagent grade KCl, Baker Chemical Corporation.

Rb was from reagent grade RbCl, Baker Chemical Corporation.

### Sample Analyses

Samples were analyzed on a Perkin-Elmer model 305B spectrophotometer, and the optimum instrumental settings used in the analyses are summarized in Table C-3. The higher temperature Nitrous Oxide-Acetylene flame was used for Si, Al, Fe, Mg, Ca, and Sr to decrease chemical interferences.

### Sample Concentration Determinations

A minimum of two standard rocks were analyzed with each set of five unknown samples. The United States Geologic Survey (U.S.G.S.) standards were most commonly used, as extensive chemical analyses of these rocks are available (Flanagan, 1969, 1976). Two rocks of unusual composition not available from the U.S.G.S. were also used for this purpose (Cullers and Medaris, 1977). The standard rocks served as secondary standards for the determinations of Si, Na, Rb, and Sr in the unknowns. The Si concentrations in the standard rocks as determined by the primary (liquid) standards were consistently low. This disparity is presumably due to chemical complexing, believed to originate during or shortly after sample dissolution, and, therefore, should affect both sample and standard rocks alike. The liquid standards were improperly prepared for Na and, thus, proved ineffective in determining its concentration. Rb and Sr were determined using the standard rocks because secondary standards indicated that the liquid standards were contaminated with small but significant quantities of these elements.

The primary-secondary standard combination proved highly effective in sample analyses. The procedure proved particularly useful in analyzing both major and trace elements from a single sample decomposition and in providing a continuous check on the quality of analyses. In an attempt to delineate the quality of the analyses, U.S.G.S. standard rock W-1 was

analyzed as an unknown sample. Good agreement exists between the reported values (Flanagan, 1976) and the values for W-1 in this study. (Table C-4).

Table C-3. Instrument settings for atomic absorption spectrophotometer.

Element	Function	Wavelength Setting	Wavelength Range	Burner Height	Burner Size	C <sub>2</sub> H <sub>2</sub>	Gas Flow Rate	
							air	N <sub>2</sub> O
Si	Absorption	251.8	Ultraviolet	6.0	2 inch	5.25	-	4.75
Al	Absorption	309.2	Ultraviolet	7.0	2 inch	5.0	-	5.0
Fe	Absorption	248.5	Ultraviolet	7.0	2 inch	4.75	-	4.5
Mg	Absorption	285.3	Ultraviolet	5.25	2 inch	4.75	-	5.0
Ca	Absorption	211.4	Visible	6.2	2 inch	4.5	-	4.8
Na	Absorption	294.4	Visible	6.0	2 inch	5.0	5.0	-
K*	Emission	382.9	Visible	5	2 inch	4.75	5.25	-
Rb*	Emission	389.2	Visible	5.0	4 inch	9.0	10.0	-
Sr	Emission	230.2	Visible	7.0	2 inch	4.75	-	5.25

\*With red filter



Table C-4. Comparison of standard rock W-1 elemental analyses.

Element	This Study	Flanagan (1976)
$\text{SiO}_2$	53.4%	52.6%
$\text{Al}_2\text{O}_3$	15.1%	15.0%
$\text{MgO}$	6.44%	6.62%
$\text{Fe}_2\text{O}_3$	11.5%	11.1%
$\text{CaO}$	11.0%	11.0%
$\text{K}_2\text{O}$	0.63%	0.64%
$\text{Na}_2\text{O}$	2.20%	2.15%
Rb	28 ppm	21 ppm
Sr	218 ppm	190 ppm

#### D. Mass Spectrometry

Mass spectrographic analysis was used to determine the Rb and Sr isotopic concentrations of the samples. Absolute Rb and Sr concentrations were determined using isotope dilution techniques in which known quantities of  $^{87}\text{Rb}$  and  $^{84}\text{Sr}$  enriched "spike" solutions were added to the samples.

#### Sample Preparation

The freshest portions of the samples to be analyzed were ground in a steel mortar and pestle, transferred to a tungsten carbide-lined mixer mill (Spex Industries), and ground to 100 mesh.

X-ray emission was used to approximate Rb and Sr concentrations of the samples (Appendix E). Table E-1 lists the results of the X-ray emission analysis. These data were used to calculate the volume of spike solution to be added to sample solutions for isotope dilution, and in determining the  $^{87}\text{Rb}/^{86}\text{Sr}$  ratios of samples having low Rb/Sr ratios.

#### Sample Dissolution

The samples were dissolved using procedures similar to Chaudhuri (1966), Chaudhuri and Brookins (1969), and Methot (1973), so only deviations from their methods are reported below. Sample weights for isotope dilution were determined as follows: a) For spiked runs, sufficient sample was taken such that no less than 0.5 ml of spike needed to be added, b) No more than 2.5 g of sample was used to avoid using excess amounts of reagents, c) A minimum of 15 micrograms of Rb or Sr was estimated to give sufficient Rb or Sr for repeat analyses, and d) Excess Sr in the separatory column was discouraged as it may have led to future contamination problems. The samples were weighed into clean

100 ml teflon dishes, exact weights ( $\pm 0.0002$  g) being recorded only for the samples to be spiked. Samples were digested using about 20 ml hydrofluoric acid and 2 ml perchloric acid per gram of sample. The samples were heated several hours on a hot plate until evaporation produced a perchlorate mush. Samples to be analyzed for rubidium were cooled and stored for separation, whereas samples to be analyzed for strontium were redissolved in 20 ml 1N hydrochloric acid. The samples were evaporated to  $3/4$  of the original volume, cooled, purified by filtering out any residue, and stored for separation.

#### Sample Separation

Cation exchange was used for separating Rb and Sr from sample solutions. A cross-linked resin in bead form (Dowex 50W - X8) was used for Sr separation, whereas granular zirconium phosphate was used for Rb separation.

Exchange columns used for Sr separation were rinsed with 300 ml of 6N hydrochloric acid followed by 650 ml of 2N hydrochloric acid. Sample solutions were then poured into the columns and allowed to pass into the resins. The position of the Sr in the columns was determined by use of a separate "monitoring" column to which radioactive  $^{89}\text{Sr}$  had been added. The columns were rinsed with 2N hydrochloric acid, and when the monitoring column indicated that the Sr would soon be expelled, five to six 20 ml aliquots of solution were collected in teflon beakers from all columns. The beakers were placed on a hot plate until the solutions were evaporated. Beakers containing the aliquots of maximum Sr were identified by their relation to the radioactive aliquots collected from the monitoring column and by the color of the precipitate resulting from evaporation. The Sr salts are brown, whereas the ion salts preceding the Sr salts are cream, and those following are black. Two to three of the Sr-rich aliquots of each sample were redissolved with 10 ml of 2N hydrochloric acid and combined

together. The combined volumes were evaporated to dryness, and redissolved in 3 to 4 ml of 3N nitric acid. The nitric acid solutions were evaporated to a volume of 1 ml, transferred to 2 ml Vycor glass beakers, and evaporated to dryness. The resulting nitrates were heated over a burner to oxidize organic residues and stored for analysis.

The exchange columns of granular zirconium phosphate, which were to be used for Rb separation, were rinsed with 350 ml of 6N nitric acid followed by 100 ml of 0.5N nitric acid. The perchlorate residues obtained during sample dissolution were washed and centrifuged five times with methanol. The remaining precipitates were dissolved in 10 ml water, transferred to a teflon crucible, and evaporated to dryness. The samples were redissolved in 5 ml of 0.5N nitric acid and poured into the separatory columns. After the solutions had passed through the zirconium phosphate, the columns were washed with 50 ml of 0.5N nitric acid. The Rb was removed from the column by washing with 25 ml of 6N nitric acid. The Rb-bearing solutions were evaporated to a volume of 1 ml, transferred to 2 ml Vycor glass beakers, evaporated to dryness, and were stored for analysis.

### Sample Analysis

Rb and Sr isotopic concentrations were determined on a 6-inch radius,  $60^\circ$  sector, Nier-type mass spectrometer (Nuclide Corporation Model 6-60-S). Nitrates of Rb and Sr were evaporated onto a tantalum filament which, when heated by a current, served as a source of the elements during isotopic analysis.

Rb and Sr concentrations were determined using isotope dilution techniques (Chaudhuri, 1966; Faure, 1977; Methot, 1973). Known quantities of  $^{87}\text{Rb}$  and  $^{84}\text{Sr}$  enriched spikes were added to the samples. The spiking method used allowed the determination of the Rb and Sr concentrations of the samples as well as the  $^{87}\text{Sr}/^{86}\text{Sr}$  ratios of the strontium samples. Van Schmus'

(1966) method was used in calculating these values. The  $^{87}\text{Sr}/^{86}\text{Sr}$  ratios of a number of samples were obtained from separate unspiked runs. These direct determinations are more accurate than  $^{87}\text{Sr}/^{86}\text{Sr}$  ratios determined by isotope dilution, and are necessary for samples with low Rb/Sr ratios.

### E. X-Ray Fluorescence Spectrography

X-ray fluorescence was used to approximate the concentrations of Rb and Sr in samples to be analyzed by Mass Spectrometry. Detailed discussions of X-ray fluorescence theory and methods are provided by Methot (1973) and Smith (1967), but a brief summary of the technique is given below. A Phillips Vacuum Spectrograph equipped with a four position rotary sample holder, scintillation counter, lithium fluoride analyzing crystal, and Mo target, was used to make the determinations. The analyses were performed under atmospheric pressure because Rb and Sr K $\alpha$  radiations are only slightly absorbed in air.

Powdered samples (<200 mesh) and U.S.G.S. standard rock G-1 were packed with a clean glass slide into sample holders and placed in the rotary sample rack in groups consisting of three samples and a standard. The standard rock was analyzed after each sample to minimize systematic errors. X-ray intensities were recorded by means of a strip chart recorder, and sample/standard peak height ratios were calculated for Rb and Sr. The Rb and Sr concentrations of the samples were determined by multiplying the sample/standard ratios by the concentrations of these elements in the standard. The results of the X-ray Spectrography are summarized in Table E-1.



Table E-1. Rb and Sr values determined by X-ray emission.

Sample	Rb (ppm)	Sr (ppm)	Rb/Sr
P-1	25	243	---
NK-10	73	1468	0.050
NK-4	165	39	4.231
NK-33	5	64	0.078
NK-18	80	796	0.100
NK-100	132	79	1.671
NK-28	5	1229	---
NK-32	5	1597	---
NK-10 Biotite	261	52	5.019
NK-18 Biotite	253	94	2.691

## F. Instrumental Neutron Activation Analysis

Certain major, minor, and trace elements were determined by INAA (Instrumental neutron activation analysis). The method employed was adopted, with modification, from Gordon et al. (1968) and Jacobs et al. (1977). Koch (1978) presents a brief summary of the procedure.

### Sample Preparation

Two different procedures for INAA were used for analyses. Short irradiations followed by immediate sample radioassay was used to determine the Na and Mn concentrations. Longer periods of irradiation followed by repeated sample radioassay during a 40 day interval were used in determining the REE (La, Ce, Sm, Eu, Tb, Yb, Lu), Rb, Ba, Th, Hf, Ta, Co, Sc, Fe, and Na concentrations.

For Na and Mn determinations approximately 0.15 g ( $\pm 0.0002$  g) of the powdered samples and standards were weighed into clean polyethylene vials measuring 15 mm in length and 7 mm in diameter. The tops of the vials were sealed with a soldering gun. Usually 7 samples and one U.S.G.S. standard rock were symmetrically placed in a single plane of the rotary specimen rack located in the central thimble of the Kansas State University Triga Mark II reactor. This orientation minimized differences in neutron flux within the reactor core. The samples and standard were irradiated at full power (approximately  $1 \times 10^{13}$  neutrons/cm<sup>2</sup>/sec) for about 10 minutes, cooled for approximately 90 minutes, and quantitatively transferred to larger polyethylene vials (24 mm in length and 11 mm in diameter) for radioassay.

For the determination of the REE, Rb, Ba, Th, Hf, Ta, Co, Sc, Fe, and Na content, 0.2 - 0.3 g ( $\pm 0.0002$  g) of five powdered samples and a U.S.G.S. standard rock were weighed into clean polyethylene vials measuring 24 mm in length and 11 mm in diameter. The polyethylene vials were

heat-sealed with a warm soldering gun. Approximately 50 mg ( $\pm 0.0002$ ) of iron wire was wrapped spirally around the portion of the vial containing the samples to monitor variations in the neutron flux between samples and standard.

Samples and standard were irradiated for 4 hours at full power. After the irradiation, the samples and standard were allowed to cool until their activity was less than 1 Roentgen/hr. (about 2 days) at contact. Samples and standards were transferred to plastic bags measuring about 1.5 cm across and mounted with the same geometry, onto 8 X 8.5 cm cards for radioassay. The iron wires were removed from the vials rolled into a circle, mounted flat on similar cards as the samples, and stored for radioassay.

#### Sample Radioassay

The Gamma-ray spectra of the samples and standard were recorded using a 25 cm<sup>3</sup> Ge(Li) detector coupled with a Northern Scientific Corporation 4096-channel analyzer and associated electronics. A resolution of 4.0 KeV for the 1331 KeV peak of Co<sup>60</sup> is obtained using this detector-analyzer combination (Cullers et al., 1974).

For Na and Mn determination, the samples and standards were radioassayed for about 15 minutes, 2 to 3 hours after irradiation. For analyses of the REE, Rb, Th, Hf, Ta, Co, Sc, Fe, and Na, two different counting procedures were followed. In the first procedure samples and standards were radioassayed at approximately 4, 10, and 40 days after irradiation, whereas in the second, samples were radioassayed 7 and 40 days after irradiation. The 4 and 10 day count sets were often used in place of the 7 day sets because the samples could be placed closer to the detector on the 10 day set than on the 7 day set. This resulted in increased counting statistics for those elements determined using the 10 day count sets. The two short half-life nuclides <sup>153</sup>Sm and <sup>24</sup>Na were determined on the associated 4 day count sets.

Counting times for the 4 day counts were about one hour while the 7, 10, and 40 day sets were counted for approximately four hours. Iron wires were radioassayed for about 15 - 30 minutes approximately two weeks after irradiation.

Repeated sample radioassay with time allowed for the determination of elements with short half-lives on the earlier count sets, permitted the decay of interfering peaks from the gamma-ray spectra obtained during the later count sets, and allowed a much lower background radiation, and hence, improved peak to background ratios on the later count sets.

Table F-1 summarizes the elements analyzed using INAA and other information pertinent to sample analyses. Much of the information included was adapted from Gordon et al. (1968) and Jacobs et al. (1977).

#### Abundance Determinations

Elemental concentrations were calculated from the ratio of the peak areas of the samples to the standards. Corrections were applied for differences in sample weights, for changes in sample versus standard activity with time, and for neutron flux differences within the reactor.

Sample/standard peak area ratios were calculated directly using a computer program developed by Dana Clark (Kansas State University Computer Science Department) which he adapted from Jacobs et al. (1977). The gamma-ray spectra of the samples and standard were recorded onto magnetic tape which, along with the energies and channel numbers of the calibration peaks and the on-off times of the samples and standards, were fed into a computer in which the program is stored on a permanent disc. The computer program identifies the desired radionuclide using the channel versus energy calibration. Next, the program estimates the background on each side of the identified peak by determining the lowest pairs of 3-channel averages for adjacent channels in a specified energy range. The energy range is dependent

Table F-1. Summary of Nuclide Properties used in INAA. (adapted from Gordon et al. (1968) and Jacobs et al. (1977))

Element (Nuclide)	Energy (KeV)	Half-life	Radioassay time (Days after irradiation)	Significant Interferences*		
				Isotope	Energy (KeV)	Half-life
<sup>24</sup> Na	1368.4 1732	15.0 hr	2 hr, 4 d or 7d 2 hr			
<sup>46</sup> Sc	889.3 1120.5	83.9 d	7 d + 40 d or 10 d + 40 d			
<sup>56</sup> Mn	847 1811	2.58 hr	2 hr			
<sup>59</sup> Fe	1099.3 1291.5	45.6d	7 d + 40 d or 10 d + 40 d			
<sup>60</sup> Co	1173.2 1332.5	5.26 yr	7 d + 40 d or 10 d + 40 d			
<sup>140</sup> La	328.8 487.0	40.2 hr	10 d or 7 d			
<sup>141</sup> Ce	145.5	32.5 d	40 d	<sup>59</sup> Fe	142.5	46 d
<sup>153</sup> Sm	103.2		4 d or 7 d			
<sup>152</sup> Eu	121.8 244.7	12.7 yr	40 d	<sup>131</sup> Ba	124.2	12 d
<sup>130</sup> Tb	298.6	72.1 d	7 d + 40 d or 10 d + 40 d	<sup>233</sup> Pa	300.1	27 d

\*Interferences which were of significant size in comparison to peak of interest and which could not be corrected by counting samples during optimum time.

Table F-1. Summary of Nuclide Properties used in INAA (Cont.) (adapted from Gordon et al. (1968) and Jacobs et al. (1977)).

Element (Nuclide)	Energy (KeV)	Half-life	Radioassay time (Days after irradiation)	Significant Interferences*		
				Isotope	Energy (KeV)	Half-life
$^{175}\text{Yb}$	282.6 396.1	4.21 d	7 d or 10 d	$^{233}\text{Pa}$	398.5	27 d
$^{169}\text{Yb}$	177.2	32 d	40 d	$^{182}\text{Ta}$	179.4	115.1 d
$^{177}\text{Lu}$	208.3 133.0	6.74 d	7 d or 10 d			
$^{181}\text{Hf}$	482.2	42.5 d	40 d			
$^{182}\text{Ta}$	1221.3	115 d	40 d			
$^{86}\text{Rb}$	1077.2	18.7 d	7 d or 10 d			
$^{131}\text{Ba}$	496.3	12 d	7 d or 10 d			
$^{233}\text{Pa}$ ( $^{232}\text{Th}$ )	311.9	27.0 d	7 d + 40 d or 10 d + 40 d			

\*Interferences which were of significant size in comparison to peak of interest and which could not be corrected by counting samples during optimum time.



upon the particular element of interest and is chosen to minimize the potential error of accidentally including contributions from small interfering peaks. Each radionuclide has a separate computer card containing these energy ranges which is fed into the computer with the rest of the program. A line is then drawn between these three channel averages on each side of the peak to define the peak's average background energy, as shown in Figure F-1. The peak area is determined by summing the channels on both sides of the peak maximum, and then subtracting off the background. A channel ( $C_1$ , Fig. F-1) is included as part of the peak if the number of counts in the channel is greater than the calculated baseline for that channel and also if the channel is greater than the adjacent channel ( $C_2$ ) opposite the peak maximum ( $C$ ) by an amount representing the uncertainty in the baseline (equal to the square root of the baseline). The calculated baseline is summed over the same channels as the summed peak, and the baseline is subtracted from the total peak area to determine the net peak. The net peak of the samples and standard is divided by the total number of seconds that each was counted to determine the number of counts per second that each received.

The program also corrects for changes in activity due to the time difference between standard and sample radioassay. The counts per second of the sample ( $N_0$ ), the desired elements decay constant ( $\lambda$ ), and the difference between the standard and sample medium time ( $t$ ), are substituted into the equation:  $N_0 = N e^{\lambda t}$ .  $N$  represents the counts per second of the sample at the time the standard was radioassayed. Sample/standard ratios are then determined by dividing the counts per second of the samples by the counts per second of the standard.

The computer generated sample/standard ratios were good in most instances, but in some cases the peak areas and the sample/standard ratios

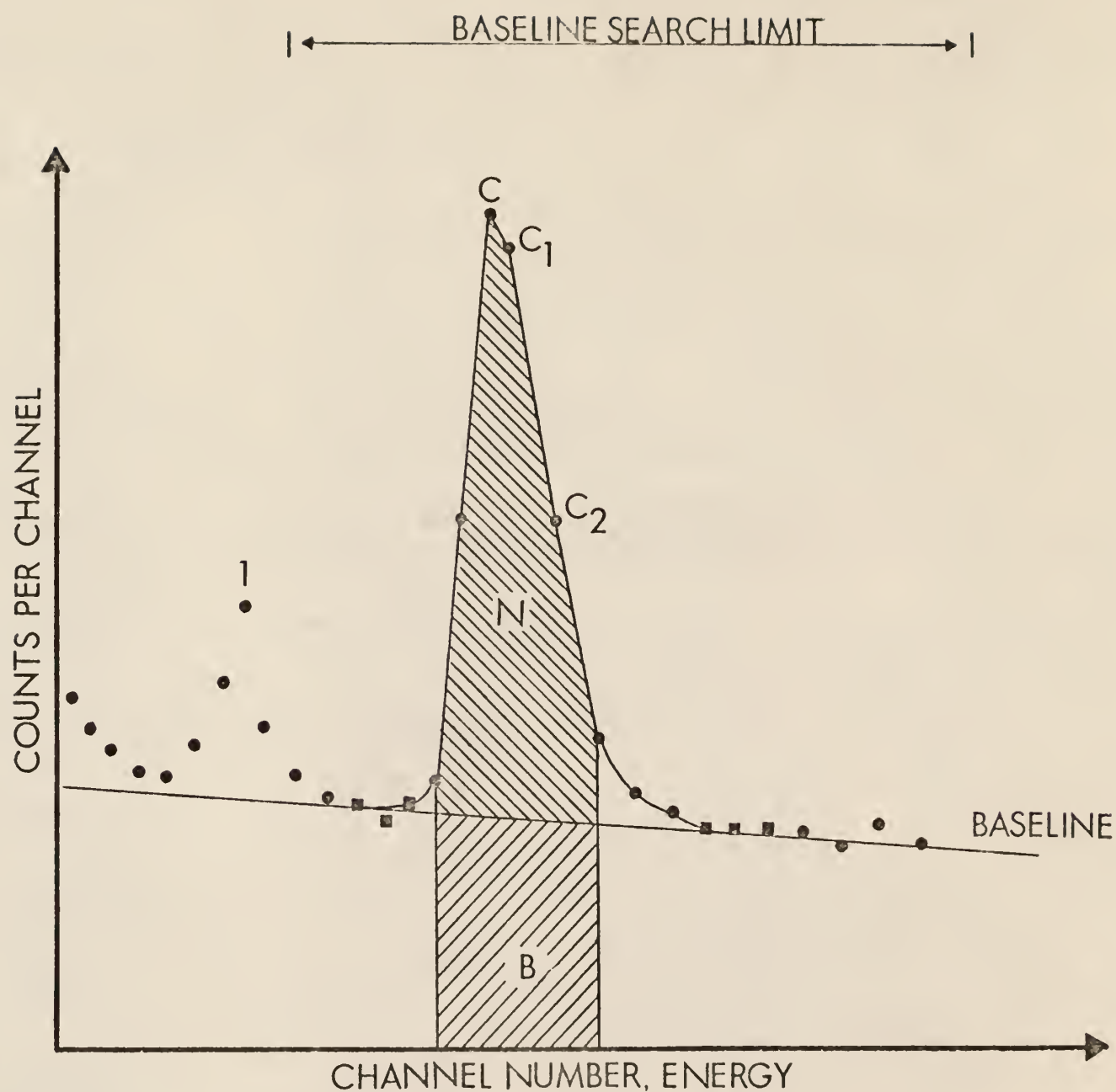


Figure F-1. Typical photopeak showing background (B), net peak area (N), and adjacent peak (1). Adjacent channels used to obtain lowest 3-channel averages for initial placement of background are placed in squares. (From Jacobs et al., 1977).

needed to be recalculated by hand. Hand calculations, with the exception of peak area determinations, were performed in a similar manner as those of the computer program. Consequently, only peak area determinations are discussed below.

The primary reason for recalculating peak areas was that a portion of a peak had not been included due to a channel not meeting the prescribed requirements outlined above. Peak areas were excluded when a) peaks were irregular in shape due to electronic gain shifts, b) interfering gamma-rays caused the peak to assume a non-symmetric form, or c) a low peak to background ratio had not defined a symmetrical peak. In determining a peak's area by hand, the peak was graphed with the background extended at least 15 channels on either side of the central channel. A baseline was determined by drawing a best fit "eyeballed" straight line through the graph of the background energy, being particularly careful to minimize differences in sample and standard baseline position. The number of channels used for peak determinations was the same for both samples and standards. For most peaks, the sum of the 5 or 6 central-most channels were used to calculate the peak areas. The number of summed channels was adjusted slightly for peaks which were significantly larger or smaller than average. In cases where interfering peaks could not be removed by simple corrections (Ce for example), the interfering peak was not included in the channels used to calculate peak area (Fig. F-2). This sometimes resulted in selecting channels which were assymmetrically placed about the central channel. The background correction was obtained by multiplying the baseline value of the central channel by the total number of channels summed. Net peak areas and sample/standard ratios were then determined as outlined above.

It is often necessary to remove contributions from species emitting gamma-radiation of a similar energy from the spectra of some elements. In

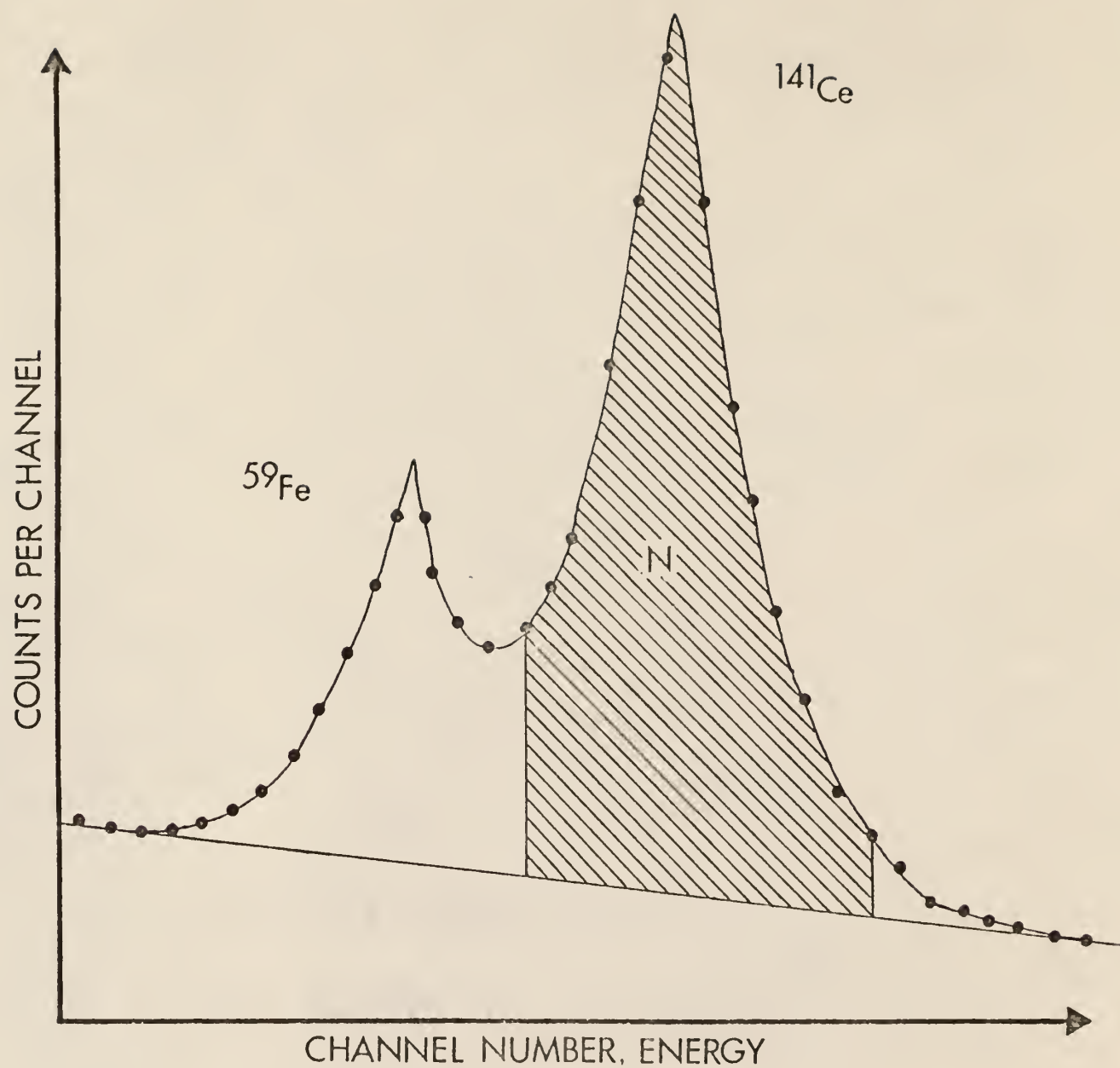


Figure F-2. Spectra illustrating the interference of  $^{59}\text{Fe}$  with  $^{141}\text{Ce}$ . (N) represents hand calculated net peak area (From Jacobs et al., 1977).

most cases, it was possible to remove the contributions from interfering nuclides which have other gamma-rays whose photopeak areas could be determined. The ratio of the area of the interfering peak to the area of the known peak was determined using published gamma-ray spectra of the elements (Gordon et al., 1968) and was multiplied by the number of counts per second of the known peak. For example, the 300.1 KeV peak of  $^{233}\text{Pa}$ , which interferes with the 298.6 KeV peak of  $^{130}\text{Tb}$  has an absolute intensity (number of photons per 100 disintegrations) of 6.3%, whereas the easily detectable 311.9 KeV peak of  $^{233}\text{Pa}$  has a relative intensity of 34%. The 300.1 KeV peak therefore has an intensity of  $6.3/34$  or 0.1853 times the intensity of the 298.6 KeV peak. This correction was subtracted off of the number of counts per second of the  $^{130}\text{Tb} + ^{237}\text{Pa}$  peak to obtain the corrected number of counts per second of the  $^{130}\text{Tb}$  peak. The correction was applied to both standard and "decay corrected" samples. The corrected activities of sample/standard ratios were then calculated. This method proved effective in correcting for the following interferences:

the 124.2 KeV peak of  $^{131}\text{Ba}$  in the 121.8 KeV peak of  $^{152}\text{Eu}$   
 the 300.1 KeV peak of  $^{233}\text{Pa}$  in the 298.6 KeV peak of  $^{130}\text{Tb}$   
 the 398.5 KeV peak of  $^{233}\text{Pa}$  in the 396.1 KeV peak of  $^{175}\text{Yb}$   
 the 179.4 KeV peak of  $^{182}\text{Ta}$  in the 177.2 KeV peak of  $^{169}\text{Yb}$

In cases where the interfering peaks were exceptionally large neither numerical nor graphical methods were effective in correcting for the interferences. Ce could not be determined in samples of the magnetite ore because of its high Fe content. Also, the 177 KeV peak of Yb was rendered useless in samples containing large quantities of Ta.

A correction for differences in neutron flux within the reactor core must be made for samples which were wrapped with iron wire. The specific activities (counts/second/mg wire) of 3 of the gamma-ray energies of  $^{59}\text{Fe}$



were calculated and the average of the ratio of the standard Fe specific activity to the sample Fe specific activity was determined.

In determining final sample concentrations, the sample/standard ratios for elements with more than one gamma-ray energy or determined on different count sets were averaged. When the net peak area of one gamma-ray energy, or when the net peak for one count set was significantly greater than another, weighted averages were used. The final concentrations of each element were calculated using the following equation:

$$C_{sa} = C_{st} \times \frac{S_a}{S_t} \times \frac{StWt}{SaWt} \times \frac{StFe}{SaFe}$$

Where,

$C_{sa}$  = Concentration of the element in the sample

$C_{st}$  = Concentration of the element in the standard

$\frac{S_a}{S_t}$  = Sample/standard peak area ratio

$\frac{StWt}{SaWt}$  = Standard/sample weight ratio

$\frac{StFe}{SaFe}$  = Standard/sample Fe specific activity

Analytical Accuracy.--One U.S. Geological Survey standard rock, G-2, and reference soil S0-1 (bottle 487) of the Canada Certified Reference Materials Project have been analyzed at Kansas State University using INAA procedures similar to those outlined above. Table F-2 shows the results of the analysis of Soil S0-1 compared to one other analyst. The results of G-2, analyzed by Koch (1978) at Kansas State University, are listed in Table F-3. Good agreement was obtained for all elements reported. The Fe, Na, and Rb concentrations of many of the analyzed samples were also determined using atomic absorption and emission spectrophotometry. Generally good agreement between the two techniques was obtained.

To check the reproducibility of the analyses and to improve elemental determinations, many of the samples were re-analyzed. Repeat analyses from



some of the major rock types, representing a large range of elemental concentrations, are in Table F-4. Included in the table are the results of the multiple analyses of sample NK-1 (magnetite ore) which, because of its low trace element content represents the lower limit of precision for this study. The range of precision listed for each element is a measure of the statistical error in the peak calculation and is determined using the following equations:

$$ERR = \sqrt{\frac{(\#Chan \times \sqrt{Tot\ BI / \#Chan})^2 + Total\ PK}{Net\ PK \times 100}}$$

Where,

ERR = Statistical error in a single peak calculation

Chan = Number of channels

Total BI = Total baseline

Total PK = Total peak

and

$$ERROR = \sqrt{(ERR_{std})^2 + (ERR_{sam})^2}$$

Where,

ERROR = Statistical error in sample/standard ratio of sample sam and standard std.

Jacobs et al. (1977) have estimated that there is an additional 1.5 percent precision loss due to uncertainties in sample weights, counting geometries, and standard homogeneity. Multiple sample analyses therefore indicate that the reproducibility of most element determinations is well within experimental error.

Table F-2. Analytical results of instrumental activation analysis for Reference Soil S0-1 (bottle 487) of the Canada Certified Reference Materials Project. (ppm unless otherwise noted)

	Soil S0-1 (bottle 487) Kansas State University (Avg. of 5)	Soil S0-1 (bottles 501 and 164) Phil Helmke University of Wisc. Soil Sci. Dept. (Avg. of 10)
La	53.2	52.5
Ce	97.2	101
Nd	45	43.5
Sm	7.9	7.85
Eu	1.57	1.50
Tb	0.88	0.84
Yb	2.31	2.21
Lu	0.32	0.329
Rb	150	144
Ba	$8.3 \times 10^2$	778
Th	11.8	13.4
Hf	2.8	2.48
Ta	0.57	---
Co	27.7	26.9
Sc	16.9	16.9
Fe(%)	5.87	5.57
Cr	$1.9 \times 10^2$	181
Mn	$8.8 \times 10^2$	875
Na <sub>2</sub> O(%)	2.71	2.66

Table F-3. Analytical results of instrumental activation analysis for U.S.G.S. Standard G-2. (ppm unless otherwise noted)

Reference	La	Ce	Sm	Eu	Tb	Yb	Lu	Fe <sub>2</sub> O <sub>3</sub> *	Na <sub>2</sub> O*	MnO*	Ba	Rb
Koch (1978) Kansas State University, INAA	84.6	163.	6.94	1.51	0.41	0.66	0.12	2.71	4.2	.034	1700	140
Flanagan (1969), Various methods	112.	166.	8.3	1.5	0.52	1.0	0.18	2.77	4.16	.037	1950	168
Jacobs et al., (1977), INAA	87.9	163.	7.17	1.64	0.44	0.74	0.111	2.65	4.12	---	---	---
Gordon et al., (1968), INAA	81.	144.	8.7	1.37	0.52	0.8	0.18	2.46	3.98	.030	1800	130

\*weight percent oxide

Table F-4 Multiple analyses of McClure Mountain major rock types (ppm unless otherwise noted).

	NK-19			NK-100			NK-24			FeG-1	
	Feldspathoidal Syenite			Biotite Syenite			Malignite			Gabbro	
La	76.2 ± 1.5	76.6 ± 1.5		60.5 ± 1.8	58.2 ± 2.4		63.1 ± 2.5	64.7 ± 2.9	5.7 ± 1.4	5.3 ± .36	
Ce	133 ± 3.3	133 ± 4.6		116 ± 2.9	118 ± 3.5		120 ± 4.3	127 ± 4.6	10.1 ± 1.0	14.9 ± 1.2	
Sm	6.5 ± .04	6.6 ± .04		5.0 ± .03	5.5 ± .45		8.1 ± .05	8.0 ± .46	1.8 ± .11	2.1 ± .02	
Eu	4.4 ± .1	3.5 ± .05		1.7 ± .04	1.7 ± .03		2.9 ± .08	2.9 ± .07	0.93 ± .04	0.87 ± .03	
Tb	0.85 ± .07	0.89 ± .07		0.70 ± .06	0.83 ± .06		1.1 ± .12	1.0 ± .08	0.40 ± .10	0.45 ± .09	
Yb	2.5 ± .17	2.5 ± .17		1.9 ± .19	1.9 ± .15		2.1 ± .23	2.0 ± .24	0.57 ± .23	0.81 ± .14	
Lu	0.38 ± .02	0.36 ± .02		0.23 ± .01	0.24 ± .01		0.31 ± .02	0.32 ± .02	0.16 ± .02	0.13 ± .02	
Rb	1.1 X 10 <sup>2</sup> ± .14	1.1 X 10 <sup>2</sup> ± .14		1.0 X 10 <sup>2</sup> ± .13	1.3 X 10 <sup>2</sup> ± .13		1.3 X 10 <sup>2</sup> ± .16	1.2 X 10 <sup>2</sup> ± .12		11 ± 2.7	
Ba	5.7 X 10 <sup>3</sup> ± .4	4.6 X 10 <sup>3</sup> ± .34		2.8 X 10 <sup>2</sup> ± .28	3.0 X 10 <sup>2</sup> ± .27		3.2 X 10 <sup>3</sup> ± .25	3.2 X 10 <sup>3</sup> ± .22		1.24 X 10 <sup>2</sup> ± .27	
Th	5.4 ± .25	5.8 ± .35		4.5 ± .21	4.1 ± .17		4.6 ± .28	4.1 ± .21		0.59 ± .18	
Hf	7.9 ± .5	8.1 ± .57		2.8 ± .22	2.6 ± .19		4.7 ± .42	4.4 ± .35	0.74 ± .21	0.56 ± .13	
Ta	7.0 ± .7	6.8 ± .9		10.0 ± 1.5	10.0 ± 1.3		10.0 ± 1.6	9.8 ± 1.3	5.0 ± .85		
Co	32.2 ± .5	37.1 ± .4		23.0 ± .4	19.0 ± .25		41.8 ± .63	42.5 ± .68	51.8 ± .60	56.3 ± 1.52	
Sc	4.4 ± .03	4.6 ± .03		3.2 ± .03	3.4 ± .04		23.9 ± .10	22.9 ± .09	23.2 ± .09	24.9 ± 1.24	
Fe <sub>2</sub> O <sub>3</sub> (%)	5.8 ± .05	6.0 ± .06		3.2 ± .04	3.1 ± .03		11.7 ± .10	11.8 ± .09	10.2 ± .08	10.7 ± .11	
Na <sub>2</sub> O(%)	6.3 ± .15			6.5 ± .14	6.0 ± .04		4.4 ± .11	4.1 ± .23	1.9 ± .01	2.0 ± .01	

Table F-4. Multiple analyses of McClure Mountain major rock types (Cont.). (ppm unless otherwise indicated)

	NK-33 Pyroxenite				NK-1 Magnetite ore			
La	5.2 ± 1.1	6.1 ± .73	4.3 ± .86	4.5 ± .63	1.3 ± .51	2.7 ± .81	1.9 ± .16	1.1 ± .42
Ce	15.5 ± 3.7		19.4 ± 4.6	14.9 ± 2.5				
Sm	3.3 ± .05	3.0 ± .10	3.6 ± .14	2.8 ± .03	0.38 ± .08	0.51 ± .04	0.39 ± .02	0.33 ± .12
Eu	0.95 ± .06	1.01 ± .05	0.98 ± .06	0.83 ± .03	0.14 ± .02	0.20 ± .03	0.25 ± .04	0.18 ± .02
Tb	0.67 ± .28	0.68 ± .19	0.62 ± .19	0.64 ± .19				
Yb	0.8 ± .22	1.1 ± .34	1.7 ± .53	1.2 ± .3				
Lu	0.46 ± .03	0.34 ± .03	0.47 ± .03	0.39 ± .02	0.19 ± .02	0.28 ± .03	0.18 ± .02	
Rb								
Ba								
Tb				1.4 ± .38		0.5 ± .14	0.4 ± .13	
Hf	1.6 ± .34	2.1 ± .50	1.7 ± .36	2.0 ± .32		2.7 ± .35		
Ta	0.8 ± .22			0.46 ± .07		0.27 ± .08		
Co	48.1 ± .85	48.3 ± .77	49.6 ± .90	43.5 ± .70	233.4 ± 2.85	239.6 ± 3.35	243.0 ± 3.4	233.1 ± 2.3
Sc	85.0 ± .29	85.0 ± .26	86.7 ± .35	73.4 ± .25	14.4 ± .12	14.6 ± .12	14.8 ± .47	14.6 ± .09
Fe <sub>2</sub> O <sub>3</sub> (%)	7.7 ± .09	7.5 ± .09	7.6 ± .11	6.6 ± .07	72.4 ± .36	72.6 ± .51	73.3 ± .48	67.6 ± .40
Na <sub>2</sub> O(%)	0.36 ± .05	0.60 ± .02	0.60 ± .01	0.43 ± .01	0.25 ± .01	0.26 ± .01	0.20 ± .05	0.17 ± .05

### G. Gravimetric Determinations

Adsorbed water and the total volatile concentration of the samples were determined using a combination of heating and loss on ignition. Platinum crucibles were placed in a muffle furnace at  $1000^{\circ}\text{C}$  for 30 minutes, removed, and placed in a desiccator. The cooled crucibles were then carefully weighed. Approximately 0.5 g ( $\pm 0.0002$  g) of sample was added to the crucibles. The crucibles with the samples were placed in a drying oven at  $110^{\circ}\text{C}$  for one hour, reweighed, and then placed in a muffle furnace at  $1000^{\circ}\text{C}$  for one hour. The change in sample weight at  $110^{\circ}\text{C}$  for one hour was recorded as adsorbed water (+ water). The ignited samples were cooled in a desiccator and then reweighed. The weight lost between  $110^{\circ}\text{C}$  and  $1000^{\circ}\text{C}$  was recorded as loss on ignition.

The quality of the analysis was determined by analyzing standard carbonate 400. The value 47.37%  $\text{CO}_2$  (ignition loss) obtained in this study is in excellent agreement with a value of 47.36%  $\text{CO}_2$  reported by Ingamells and Suhr (1967).



H. Distribution Coefficients

Mineral	Olivine	Clinopyroxene		Orthopyroxene		Garnet	Plagioclase	Hornblende	
Use**	A	B	A	B	A	A	B	B	C
La	0.004	0.007*	0.060*	0.15*	0.014*	0.101*	0.16*	0.15*	0.07*
Ce	0.004	0.007	0.077	0.19	0.016	0.118	0.12	0.24	0.12
Sm	0.004	0.009	0.260	0.54	0.026	0.96	0.07	0.58	0.34
Eu	0.004	0.007	0.273	0.52	0.030*	0.60	0.35	0.67	0.36
Tb	0.005	0.010*	0.33*	0.53*	0.045*	6.9*	0.07*	0.65	0.49
Yb	0.007	0.014	0.294	0.61	0.132	16.1	0.05	0.50	0.46
Lu	0.009	0.018*	0.28*	0.71	0.176*	14.17	0.04*	0.40	0.44
Co		3.0		1.5			0.03	5.6	5.6
Sc		0.3		3.0			0.10	10	12
Sr		0.014		0.12			1.83	0.46	0.46
Ba		0.009		0.02			0.30	0.42	0.42
Rb		0.009		0.022			0.07	0.29	0.29

References \*\*\*  
REE

Other Trace Elements	(1,2,3,4,6,10,17,21)	(8,13,14,22)	(8,13,14,20)	(13,22)	(13,22)	(8,13,14)	(8,14)
	(1,2,3,4,6,10,17,21)	(1,2,3,5,7,8,13,14,17,20)	(1,2,8,11,12,13,14,20,21)	(2,8,9,14,15,17,19,20)			

\*Values by interpolation

\*\*\* (A) Partial Melting (B) Mafic Fractional Crystallization (Gabbros, Pyroxenites, Anorthositic, Malinite)  
(C) Felsic Fractional Crystallization (Feldspathoidal Syenites, Biotite Syenites) (D) Liquid Immiscibility  
\*\*\* (1) Paster et al., 1974 (2) Philpotts and Schnetzler, 1970a (3) Frey et al., 1974 (4) Gunn, 1971 (5) Onuma et al., 1968 (6) Watson, 1977 (7) Duke, 1976 (8) Higuchi and Nagasawa, 1969 (9) Nagasawa and Schnetzler, 1971 (10) Leeman and Scheidegger, 1977 (11) Sun et al., 1974 (12) Dudas et al., 1971 (13) Schnetzler and Philpotts, 1970 (14) Schnetzler and Philpotts, 1968 (15) Ewart and Taylor, 1969 (16) Berlin and Henderson, 1969 (17) Griffin and Murthy, 1969 (18) Cullers and Medaris, 1977 (19) Weinrich-Verbeek, 1975 (20) Sun and Hanson, 1976 (21) Barker et al., 1977 (22) Philpotts et al., 1972

## H. Distribution Coefficients (Cont.)

Min- eral	Biotite		Magnetite		Kaersutite		Orthoclase (Perthite)		Feldspathoids		Sphene		Apatite		Carbonate	
	Use**	B C	B	C	B	C	B	C	B C	C	B C	B C	B C	B C	B D	D
La	0.06	0.22	0.42	0.88*	0.05*	0.05*	0.12	10.8	8.6*	2.50						
Ce	0.09*	0.30	0.61	1.24	0.04	0.04	0.14	16.2	11.2	2.65						
Sm	0.12	0.62	0.09	2.46	0.02	0.02	0.22	30.3	14.6	2.15						
Eu	0.10	0.58	1.14	1.90	0.75	0.75	0.26	31.9	9.6	1.80						
Tb	0.21	0.45*	0.87*	2.30	0.01*	0.01*	0.33	27.4	15.4	2.10						
Yb	0.58	0.26	0.51	1.4	0.01	0.01	0.33	10	8.1	2.75						
Lu	0.60*	0.32	0.75	1.29	0.01*	0.01*	0.34	10	6.0	3.60						
Co	28	5	7		0.01	0.01			0.2							
Sc	11	1.3	2		0.01	0.05			0.35							
Sr	0.3	0.06	0.06		2.0	1.83			3.0							
Ba	8	0.04	0.04		4.0	6.0										
Rb	2.2				0.30	0.30										
References	(8)	(1,18)	(20)	(13)	(18)	(18)	(18)	(18)	(1,20)	(18)						

REE

Other Trace

Elements (2,8) (1,18,19,21)

(2,13,16,20,21)

(1,20,21)

\*Values by interpolation

\*\* (A) Partial Melting (B) Mafic Fractional Crystallization (Gabbros, Pyroxenites, Anorthosites, Malig-  
nites) (C) Felsic Fractional Crystallization (Feldspathoidal Syenites, Biotite Syenites) (D) Liquid  
Immiscibility.

\*\*\* (1) Paster et al., 1974 (2) Philpotts and Schnetzler, 1970a (3) Frey et al., 1974 (4) Gunn, 1971

(5) Onuma et al., 1968 (6) Watson, 1977 (7) Duke, 1976 (8) Higuchi and Nagasawa, 1969 (9) Nagasawa and  
Schnetzler, 1971 (10) Leeman and Scheidegger, 1977 (11) Sun et al., 1974 (12) Dudas et al., 1971

(13) Schnetzler and Philpotts, 1970 (14) Schnetzler and Philpotts, 1968 (15) Ewart and Taylor, 1969

(16) Berlin and Henderson, 1969 (17) Griffin and Murthy, 1969 (18) Cullers and Medaris, 1977

(19) Weinrich-Verbeek, 1975 (20) Sun and Hanson, 1976 (21) Baker et al., 1977 (22) Philpotts et al.,  
1972.

## BIBLIOGRAPHY

- Alexander, D.H.: Petrography and origin of an orbicular lamprophyre dike, Fremont County, Colorado. M.S. Thesis, The University of Michigan, 106 p. (1974).
- Alexander, D.H., Heinrich, E.Wm.: Geology and Petrogenesis of the McClure Mountain mafic-alkalic-carbonatitic complex, Fremont County, Colorado. Geol. Soc. of Am. Abstracts 10, p. 245 (1978).
- Bailey, D.K.: Feldspar-liquid equilibria in peralkaline liquids -- The orthoclase effect. Am. J. Sci. 262, 1198-1206 (1964).
- Bailey, D.K.: Application of experiments to alkaline rocks. In: The Evolution of the Crystalline Rocks, Bailey, D.K., MacDonald, R., Eds., New York: Academic Press, 419-484 (1976).
- Bailey, D.K., Schairer, J.F.: The system  $\text{Na}_2\text{O}-\text{Al}_2\text{O}_3-\text{Fe}_2\text{O}_3-\text{SiO}_2$  at 1 atmosphere and the petrogenesis of alkaline rocks. Jour. Pet. 7, 114-170 (1966).
- Barker, B.H., Goles, G.G., Leeman, W.P., Lindstrom, M.M.: Geochemistry and petrogenesis of a basalt-benmoreite-trachyt suit from the southern part of the Gregory Rift, Kenya. Contrib. Mineral. Petrol. 64, 303-332 (1977).
- Barth, T.F.W.: Studies of the igneous rock complex of the Oslo segia: Systematic petrography of the plutonic rocks. Norske Vid-Akad. Shrift No. 1, Mat.-Neturv., Kl., 9, 104 p. (1945).
- Barth, T.F., Ramberg, I.B.: The Fen circular complex. In: Carbonatites, Tuttle, O.F., and Gittins, J., Eds., New York: John Wiley and Sons, 225-257 (1966).
- Becker, R.M., Shannon, S.S., Jr., Rose, C.K.: Iron Mountain titaniferous magnetite deposits, Fremont County, Colorado. U.S. Bur. Mines Rept. Inv. 5864, 18 p. (1961).
- Bell, K., Powell, J.L.: Strontium isotopic studies of alkaline rocks: the alkaline complexes of eastern Uganda. Bull. Geol. Soc. Amer. 81, 3481-3490 (1970).
- Berlin, R., Henderson, C.M.B.: The distribution of Sr and Ba between the alkali feldspar, plagioclase, and groundmass phases of porphyritic trachytes and phonolites. Geochim. Cosmochim. Acta 33, 247-255 (1969).

- Buckley, D.E., Cranston, R.E.: Atomic absorption analyses of 18 elements from a single decomposition of aluminosilicates. *Chem. Geol.* 7, 273-284 (1971).
- Chaudhuri, S.: The geochronology of the Keeweenawan rocks of Michigan and the origin of the copper deposits. PhD. Thesis, Ohio State University, 200 p. (1966).
- Chaudhuri, S.: Strontium isotopic composition of several oilfield brines from Kansas and Colorado. *Geochim. Cosmochim. Acta* 42, 329-331 (1978).
- Chaudhuri, S., Brookins, D.G.: The isotopic age of the Flathead Sandstone, Montana, *Jour. Sed. Pet.* 39, 364-368 (1969).
- Chauvenet, R.: Preliminary notes on the iron resources of Colorado, Colorado School Mines Ann. Rept., Fieldwork, p. 5-16 (1886).
- Chauvenet, R.: The iron resources of Colorado. *Am. Inst. Mining Engineers Trans.*, 18, p. 266-273 (1890).
- Christman, R.A., Brock, M.R., Pearson, R.C., Singwald, Q.D.: Geology and thorium deposits of the Wet Mountains, Colorado, a progress report. *U.S. Geol. Survey Bull.* 1072-H, 491-535 (1959).
- Christman, R.A., Heyman, A.M., Dellwig, L.F., Gott, G.B.: Thorium investigations 1950-52, Wet Mountains, Colorado. *U.S. Geol. Survey Circ.* 290 (1953).
- Coombs, D.S., Wilkinson, J.F.G.: Lineages and fractionation trends in undersaturated volcanic rocks from the East Otago volcanic province (New Zealand) and related rocks. *J. Petrol.* 10, 440-501 (1969).
- Cullers, R.L., Medaris, L.G.: Rare Earth Elements in Carbonatite and Cogenetic Alkaline Rocks: Examples from Seabrook Lake and Calender Bay, Ontario. *Contrib. Min. Petrol.* 65, 143-153 (1977).
- Cullers, R.L., Yeh, L.T., Chaudhuri, S., Guidotte, C.V.: Rare earth elements in Silurian pelitic schists from N.W. Main. *Geochim. Cosmochim. Acta* 38, 389-400 (1974).
- Dahlem, D.H.: Geology of the Lookout Mountain area, Fremont County, Colorado. PhD. Thesis, The University of Michigan, 188 p. (1965).
- Dasch, E.J.: Strontium isotopes in weathering profiles, deep-sea sediments, and sedimentary rock. *Geochim. Cosmochim. Acta* 33, 1521-1552 (1969).
- Drake, M.J., Weill, D.F.: Partition of Sr, Ba, Ca, Y,  $\text{Eu}^{2+}$ ,  $\text{Eu}^{3+}$ , and other REE between plagioclase feldspar and magmatic liquid: an experimental study. *Geochim. Cosmochim. Acta* 39, 689-712 (1975).
- Dudas, M.J., Schmitt, R.A., Howard, M.E.: Trace element partitioning between volcanic plagioclase and dacitic pyroclastic matrix. *Earth Planet. Sci. Lett.* 11, 440-446 (1971).



- Duke, J.M.: Distribution of the period four transition elements among olivine, calcic clinopyroxene, and mafic silicate liquid. Experimental results. *J. Petrology* 17, 499-521 (1976).
- Eby, G.N.: Abundance and distribution of the rare-earth elements and Yttrium in the rocks and minerals of the Oka carbonatite complex, Quebec. *Geochim. Cosmochim. Acta* 39, 597-620 (1975).
- Edgar, A.D.: Experimental studies. In: *The Alkaline Rocks*, Sorenson, H., Ed. New York: John Wiley and Sons, 355-389 (1974), 127-146 (1969).
- Ewart, A., Taylor, S.R.: Trace element geochemistry of the rhyolitic volcanic rocks, Central North Islands, New Zealand, Phenocrypt Data. *Contrib. Mineral. Petrol.* 22, 127-146 (1969).
- Faure, G.: *Principles of Isotope Geology*. New York: John Wiley and Sons, 464 p. (1977).
- Faure, G., Hurley, P.M.: The isotopic composition of strontium in oceanic and continental basalts: Application to the origin of igneous rocks. *Jour. Petr.* 4, 31-50 (1963).
- Faure, G., Powell, J.L.: *Strontium Isotope Geology*: New York, Springer-Verlag, 188 p. (1972).
- Fenton, M.D., Faure, G.: Rb-Sr whole-rock age determinations of the Iron Hill and McClure Mountain carbonatite-alkalic complexes, Colorado. *The Mountain Geologist* 7, 268-275 (1970).
- Flanagan, F.J.: U.S. Geological Survey standards -- II. First compilation of data from the new U.S.G.S. rocks. *Geochim. Cosmochim. Acta* 33, 81-120 (1969).
- Flanagan, F.J.: 1972 Compilation of Data on U.S.G.S. Standards in Flanagan, F.J.: *Description and Analyses of Eight New U.S.G.S. Rock Standards*. Geological Survey Professional Paper 840 (1976).
- Floor, P.: Alkaline gneisses. In: *The Alkaline Rocks*, Sorensen, H., Ed., New York: John Wiley and Sons, 124-142 (1974).
- French, R.B., Alexander, D.H., VanDerVoo, R.: Paleomagnetism of upper Precambrian to lower Paleozoic intrusive rocks from Colorado. *Geol. America Bull.*, 88, p. 1785-1792 (1977).
- Frey, F.A., Bryan, W.B., Thompson, G.: Atlantic Ocean floor: Geochemistry and petrology of basalts from legs 2 and 3 of the Deep-Sea drilling project. *J. Geophys. Res.* 79, 5507-5527 (1974).
- Garson, M.S.: Carbonatites in Malawi. In: *Carbonatites*, Tuttle, O.F., and Gittins, J., Eds., New York: John Wiley and Sons, 33-72 (1966).
- Gast, P.W.: Trace element fractionation and the origin of tholeiitic and alkaline magma types. *Geochim. Cosmochim. Acta* 32, 1057-1086 (1968).

- Gerasimarsky, V.I.: Trace elements in selected groups of alkaline rocks. In: *The Alkaline Rocks*, Sorensen, H., Ed., New York: John Wiley and Sons, 402-412 (1974).
- Gold, D.: Average chemical composition of carbonatites. *Econ. Geol.* 58, 988-991 (1963).
- Gordon, G.E., Randle, K., Goles, G.G., Corliss, J.B., Beeson, M.H., Oxley, S.S.: Instrumental Activation analysis of standard rocks with high-resolution  $\gamma$ -ray detectors. *Geochim. Cosmochim. Acta* 32, 369-396 (1968).
- Green, D.H., Ringwood, A.E.: The genesis of basaltic magmas. *Contrib. Mineral. Petrol.* 15, 103-190 (1967).
- Griffin, W.L., Murthy, V.R.: Distribution of K, Rb, Sr, and Ba in some minerals relevant to basalt genesis. *Geochim. Cosmochim. Acta* 33, 1389-1414 (1969).
- Gunn, B.M.: Trace element partitioning during olivine fractionation of Hawaiian basalts. *Chem. Geol.* 8, 1-13 (1971).
- Haskin, L.A., Allen, R.O., Helmke, P.A., Paster, T.P., Anderson, M.R., Korotev, R.S., Zweifel, K.A.: Rare earths and other trace elements in Apollo 11 lunar samples. *Proc. Apollo 11 Lunar Sci. Conf.*, *Geochim. Cosmochim. Acta*, Suppl. 1, 2, 1213-1231 (1970).
- Haskin, L.A., Frey, F.A., Wildeman, T.R.: Relative and absolute terrestrial abundances of the rare earths. In: *Origin and Distribution of the Elements*, Ahrens, L.H., Ed., *Intern. Ser. Monography Earth Sc.* 30, 889-912 (1968).
- Hayden, F.V.: United States geological survey of the Territories. 7th annual report for 1873; Washington, 718 p.
- Heinrich, E.Wm.: The geology of carbonatites. Chicago: Rand McNally, 555 p. (1966).
- Heinrich, E.Wm.: Aluminofluoride Minerals of the Goldic Carbonatite Fremont County, Colorado. *The Mountain Geologist* 14, 33-46 (1977).
- Heinrich, E.Wm., Alexander, D.H.: Exotic and prosaic lamprophyres, McClure Mountain province, Colorado. *Geol. Soc. of Am. Abstracts* 7, p. 777-778 (1975).
- Heinrich, E.Wm., Anderson, R.J.: Carbonatites and alkalic rocks of the Arkansas River area, Fremont County, Colorado. 2. Fetid gas from carbonatite and related rocks. *Am. Mineralogist* 50, 1914-1920 (1965).
- Heinrich, E.Wm., Dahlem, D.H.: Carbonatites and alkalic rocks of the Arkansas River area, Fremont County, Colorado. *Inter. Mineral. Assoc. Papers and Proc. 4th Gen. Meeting*, p. 37-44 (1966).



- Heinrich, E.Wm., Dahlem, D.H.: Carbonatites and alkalic rocks of the Arkansas River area, Fremont County, Colorado. 4. The Pinon Peak breccia pipes. *Am. Mineralogist* 52, 817-831 (1967).
- Heinrich, E.Wm., Dahlem, D.H.: Dikes of the McClure Mountain-Iron Mountain alkalic complex, Fremont County, Colorado, U.S.A. *Bull. Volcanology* 33, 960-976 (1969).
- Heinrich, E.Wm., Moore, D.G., Jr.: Metasomatic potash feldspar rocks associated with igneous alkalic complexes. *Canadian Mineralogist* 10, 571-584 (1970).
- Heinrich, E.Wm., Salotti, C.A.: A colloform carbonatite, McCoy Gulch, Fremont County, Colorado. *Mtn. Geologist* 12, 103-111 (1975).
- Heinrich, E.Wm., Shappirio, J.R.: Alkalic rocks and carbonatites of the Arkansas River Canyon. 3. The Amethyst carbonatites. *Am. Mineralogist* 51, 1088-1106 (1966).
- Helmke, P.A., Cullers, R.L., Medaris, L.G.: The evolution of high pressure peridotites in southwestern Oregon, U.S.A.: Trace element evidence. In preparation (1978).
- Higuchi, H., Nagasawa, H.: Partition of trace elements between rock-forming minerals and the host volcanic rocks. *Earth Planet Sci. Lett.* 7, 281-287 (1969).
- Hyndman, D.W.: Petrology of igneous and metamorphic rocks. New York: McGraw-Hill, 533 p. (1972).
- Ingamells, C.O., Suhr, H.G.: Chemical and spectrochemical analysis of standard carbonate rocks. *Geochim. Cosmochim. Acta* 31, 1347-1350 (1967).
- Jacobs, J.W., Korstev, R.L., Blanchard, D.P., Haskin, L.A.: A well-tested procedure for instrumental neutron activation analyses of silicate rocks and minerals. *J. Radioanal. Chem.* 40, 93-114 (1977).
- Jaffe, H.W., Gottfried, D., Waring, C.L., Worthing, H.W.: Lead-alpha age determinations of accessory minerals of igneous rocks (1953-1957). *U.S. Geol. Survey Bull.* 1097-B, B65-B148 (1959).
- Kay, R.W., Gast, P.W.: The rare earth content and origin of alkali-rich basalts. *Jour. Geol.* 81, 653-682 (1973).
- Kemp, J.F.: A brief review of the titaniferous magnetites. *Colorado School Mines Quart.* 20, 323-356 (1899).
- Khalfin, S.L.: Petrology of the Kogtakch differentiated massif. *Geol. Geofiz.* 7 (1961).
- King, B.C., Sutherland, D.S.: Alkaline rocks of east and south Africa, Parts I, II, and III. *Sci. Prog.* 48, 298-321, 504-524, 709-720 (1960).

- King, B.C., Sutherland, D.S.: The Carbonatite complexes of eastern Uganda, In: Carbonatites, Tuttle, O.F., and Gittins, J., Eds., New York: John Wiley and Sons (1966).
- Koch, R.J.: Petrogenesis of the Precambrian Bevos and Musco Groups, St. Francois Mountains Igneous Complex, Missouri. M.S. Thesis, Kansas State University, 105 p. (1978).
- Koster van Groos, A.F., Wyllie, P.J.: Liquid Immiscibility in the system  $\text{Na}_2\text{O}-\text{Al}_2\text{O}_3-\text{SiO}_2-\text{CO}_2$  at pressures to 1 Kb. Amer. Jour. Sci. 264, 234-255 (1966).
- Koster van Groos, A.F., Wyllie, P.J.: Liquid immiscibility in the group  $\text{NaAlSi}_3\text{O}_8-\text{Na}_2\text{CO}_3-\text{H}_2\text{O}$  and its bearing on the genesis of carbonatites. Amer. Jour. Sci. 266, 932 (1968).
- Koster van Groos, A.F., Wyllie, P.J.: Liquid immiscibility in the join  $\text{NaAlSi}_3\text{O}_8-\text{CaAlSi}_2\text{O}_8-\text{Na}_2\text{CO}_3-\text{H}_2\text{O}$ . Amer. Jour. Sci. 273, 465 (1973).
- Larson, E.E., Mutschler, F.E.: Anomalous paleomagnetic pole from isotopically dated Cambro-Ordovician intrusives in Colorado. Geol. Soc. America Bull. 82, 1657-1666 (1971).
- Leeman, W.P., Scheidegger, K.F.: Olivine/liquid distribution coefficients and a test for crystal-liquid equilibrium. Earth Planet. Sci. Lett. 35, 247-257 (1977).
- Lo, H.H., Goles, G.G.: Composition of Formosan basalts and aspects of their petrogeneses. Lithos 9, 149-159 (1976).
- Logan, J.M.: Structure and petrology of the eastern margin of the Wet Mountains, Colorado. Ph.D. Thesis, The University of Oklahoma, 237 p. (1966).
- Loubet, M., Bernat, M., Javory, M., Allegre, C.J.: REE contents in carbonatites. Earth Planet. Sci. Lett. 24, 226-232 (1972).
- Mathias, M., Siebert, J.C., Rickwood, P.C.: Some aspects of the mineralogy and petrology of ultramafic xenoliths in kimberlite. Contrib. Mineral. Petrol. 26, 75-123 (1970).
- Methot, R.: Internal geochronologic study of two large pegmatites, Conn. Ph.D. Thesis, Kansas State University, 123 p. (1973).
- Mitchell, R.H., Brunfelt, A.O.: REE geochemistry of the Fen alkaline complex, Norway. Contrib. Min. Petrol. 52, 247-259 (1976).
- Moore, D.G., Jr.: Geology, mineralogy, and origin of feldspar rocks associated with alkalic carbonatite complexes, Northern Wet Mountains, Colorado. Ph.D. Thesis, The University of Michigan, 182 p. (1969).

- Nagasawa, H., Schnetzler, C.C.: Partitioning of rare earth, alkalic, and alkaline earth elements between phenocrysts and acidic igneous magma. *Geochim. Cosmochim. Acta* 35, 953-968 (1971).
- O'Hara, M.J., Yoder, H.S.: Formation and fractionation of basic magmas at high pressures. *Scott. J. Geol.* 3, 67-117 (1967).
- Olson, J.C., Marvin, R.F., Parker, R.L., Mehnert, H.H.: Age and tectonic setting of lower Paleozoic alkalic and mafic rocks, carbonatites, and thorium veins in south central Colorado. *U.S. Geol. Survey Jour. Research* 5, 673-687 (1977).
- Onuma, N., Higuchi, H., Wakita, H., Nagasawa, H.: Trace element partition between two pyroxenes and the host volcanic rocks. *Earth Planet. Sci. Lett.* 5, 47-51 (1968).
- Parker, R.L., Hildebrand, F.A.: Preliminary report on alkalic intrusive rocks in northern Wet Mountains, Colorado. *U.S. Geol. Survey Prof. Paper* 450-E art. 181, E8-E10 (1963).
- Parker, R.L., Sharp, W.N.: Mafic-ultramafic igneous rocks and associated carbonatites of the Gem Park Complex, Custer and Fremont counties, Colorado. *U.S. Geol. Survey Prof. Paper* 649, 1-24 (1970).
- Paster, T.P., Schauwicker, D.S., Haskin, L.A.: The behavior of some trace elements during solidification of the Skaergaard layered series. *Geochim. Cosmochim. Acta* 38, 1549-1577 (1974).
- Peacock, M.A.: Classification of igneous rock series. *J. Geol.* 39, 54-67 (1931).
- Philpotts, J.A., Schnetzler, C.C.: Phenocryst-matrix partition coefficients for K, Rb, Sr, and Ba, with applications to anorthosite and basalt genesis. *Geochim. Cosmochim. Acta* 34, 307-322 (1970a).
- Philpotts, J.A., Schnetzler, C.C.: Speculations on the genesis of alkaline and sub-alkaline basalts following exodus of the continental crust. *Can. Mineralogist* 10, 374-379 (1970b).
- Philpotts, J., Schnetzler, C., Thomas, H.H.: Petrogenetic implications of some new geochemical data on eclogite and ultrabasic inclusions. *Geochim. Cosmochim. Acta* 36, 1131-1166 (1972).
- Powell, J.L., Hurley, P.M., Fairbairn, H.W.: Strontium isotopic composition and origin of carbonatites. In: *Carbonatites*, Tuttle, O.F., and Gittins, J., Eds., New York: John Wiley and Sons, 365-378 (1966).
- Putnam, B.T.: Notes on the samples of iron ore collected west of the 100th meridian: *U.S. 10th Census* 15, 469-505 (1886).
- Reid, J.B., Frey, F.A.: Rare earth distributions in lherzolite and garnet pyroxenite xenoliths and the constitution of the upper mantle. *J. Geophys. Res.* 76, 1184-1196 (1971).

- Reuss, R.L.: Mineralogy and Petrology of the Gem Park carbonatites, Custer and Fremont counties, Colorado. M.S. Thesis, The University of Michigan, 33 p. (1967).
- Ringwood, A.E.: Composition and petrology of the earth's mantle, New York: McGraw-Hill, 618 p. (1975).
- Roden, M.K.: Rare earth elements distributions and strontium isotopic data from the Gem Park igneous complex, Colorado. M.S. Thesis, Kansas State University, 103 p. (1977).
- Roden, M.K., Cullers, R.L.: Rare earth element contents and strontium isotope data from the Gem Park igneous complex, Colorado. Geol. Soc. of Am. Abstracts 8, 622-623.
- Schairer, J.F.: The alkali-feldspar join in the system  $\text{NaAlSi}_3\text{O}_8$ - $\text{KAlSi}_3\text{O}_8$ - $\text{SiO}_2$ . J. Geol. 58, 512-517 (1950).
- Schnetzler, C.C., Philpotts, J.A.: Partition coefficients of rare-earth elements and barium between igneous matrix material and rock-forming-mineral phenocrysts -- I. In: Origin and Distribution of the Elements, Ahrens, L.H., Ed. Pergamon Press, 929-938 (1968).
- Schnetzler, C.C., Philpotts, J.A.: Partition coefficients of some rare-earth elements between igneous matrix material and rock-forming-mineral phenocrysts -- II. Geochim. Cosmochim. Acta 34, 331-340 (1970).
- Shaw, D.M.: Trace element fractionation during anatexis. Geochim. Cosmochim. Acta 34, 237-243 (1970).
- Shawe, D.L., Parker, R.L.: Mafic-ultramafic layered intrusion at Iron Mountain, Fremont County, Colorado. U.S. Geol. Survey Bull. 1251-A, A1-A28 (1968).
- Singwald, J.T., Jr.: The titaniferous iron ores in the United States. U.S. Bur. Mines Bull. 64, 145 p. (1913).
- Smith, J.P.: Petrography of Brite Ignimbrite, Trans Pecos, Texas. M.S. Thesis, Kansas State University, 88 p. (1967).
- Sood, M.K., Platt, R.G., Edgar, A.D.: Phases relations in portions of the system diopside-nepheline-kalsitite-silica and their importance in the genesis of alkaline rocks. Can. Mineralogist 10, 380-394 (1970).
- Sorenson, H.: Internal structures and geological setting of the three agpaite intrusions -- Khibina and Lovozero of the Kola Peninsula and Illemaussog, South Greenland. Can. Mineralogist 10, 299-334 (1970).
- Sorensen, H., (Ed.): The Alkaline Rocks. New York: John Wiley and Sons, 622 p. (1974).



- Sorensen, H.: Origin of the alkaline rocks -- a summary and retrospect. In: The Alkaline Rocks, Sorensen, H., Ed., New York: John Wiley and Sons, 535-542 (1974).
- Spencer, B.C., Heinrich, E.Wm., Alexander, D.H.: Geochemistry and mineralogy of stratiform magnetite-ilmenite ores of the McClure Mountain mafic-alkalic complex, Fremont County, Colorado. Geol. Soc. of Am. Abstracts 10, p. 332 (1978).
- Staatz, M.H., Conklin, N.M.: Rare-earth thorium carbonatite veins of the Road Gulch area, northern Wet Mountains, Colorado. U.S. Geol. Survey Prof. Paper 550-B, B130-B133 (1966).
- Sun, S., Hanson, G.N.: Rare earth element evidence for differentiation of McMurdo volcanics, Ross Island, Antarctica. Contrib. Mineral. Petrol. 54, 139-155 (1976).
- Sun, C., Williams, R.J., Sun, S.: Distribution coefficients of Eu and Sr for plagioclase-liquid and clinopyroxene-liquid equilibria in oceanic ridge basalts: an experimental study. Geochim. Cosmochim. Acta 38, 1415-1433 (1974).
- Tilley, C.E., Yoder, H.S.: The pyroxenite facies conversion of volcanic and subvolcanic, melilite-bearing and other alkali ultramafic assemblages. Carnegie Inst. Wash. Year Book 66, 457-460 (1968).
- Turner, F.J., Verhoogen, J.: Igneous and Metamorphic Petrology, McGraw-Hill Book Co., New York, 694 p. (1960).
- Tuttle, O.F., Gittins, J. (Eds.): Carbonatites. New York: John Wiley and Sons, 591 p. (1966).
- U.S. Geological Survey: McClure Mountain intrusive complex. U.S. Geol. Survey Prof. Paper 750-A, A42-A43 (1971).
- Watkinson, D.H.: Experimental studies bearing on origin of alkalic rock-carbonatite complex and Nb mineralization at Oka, Quebec. Can. Mineral. 10, 350-361 (1970).
- Watkinson, D.H., Wyllie, P.J.: Experimental study of the composition join  $\text{NaAlSi}_3\text{O}_8\text{-CaCO}_3\text{-H}_2\text{O}$  and the genesis of alkalic rocks-carbonatite complexes. Jour. Pet. 12, 357-378 (1971).
- Watson, E.B.: Partitioning of Mn between forsterite and silicate liquid. Geochim. Cosmochim. Acta 41, 1363-1374 (1977).
- Weinrich-Verbeek, K.J.: Trace and major element chemistry and the petrogenesis of Lavas from the upper portion of San Francisco Mountain, Arizona. Ph.D. Thesis, Pennsylvania State Univ., 209 p. (1975).
- Wyllie, P.J., Haas, J.L.: Melting relationships with excess vapor at 1Kb pressure. Geochim. Cosmochim. Acta 29, 871-892 (1965).

- Wyllie, P.J., Haas, J.L.: The system  $\text{CaO-SiO}_2\text{-CO}_2\text{-H}_2\text{O}$  II. The petrogenetic model. *Geochim. Cosmochim. Acta* 30, 525-543 (1966).
- Wyllie, P.J., Huang, W.L.: Peridotite, kimberlite, and carbonatite explained in the system  $\text{CaO-MgO-SiO}_2\text{-CO}_2$ . *Geology* 31, 621-624 (1975).
- Wyllie, P.J., Huang, W.: Carbonation and melting reactions in the system  $\text{CaO-MgO-SiO}_2\text{-CO}_2$  at mantle pressures with geophysical and petrological applications. *Contrib. Min. Petrol.* 54, 79-107 (1976).
- York, D.: Least squares fitting of a straight line with correlated errors. *Earth Planet. Sci. Lett.* 5, 320-324 (1969).



PETROGENESIS OF THE MCCLURE MOUNTAIN MAFIC-ULTRAMAFIC AND ALKALIC COMPLEX,  
FREMONT COUNTY, COLORADO

by

NEIL ANTHONY KILBANE

B. S. Cleveland State University, 1976

---

AN ABSTRACT OF A MASTER'S THESIS

submitted as partial fulfillment of the

requirements of the degree

MASTER OF SCIENCE

Department of Geology

KANSAS STATE UNIVERSITY  
Manhattan, Kansas

1978

## ABSTRACT

Samples of the malignite, biotite syenite, feldspathoidal syenite, mafic rocks of the layered series and associated dikes, representing the major rock types of the McClure Mountain mafic-ultramafic and alkalic igneous complex, Fremont County, Colorado, have been analyzed for major elements, for Rb, Ba, Sr, Th, Hf, Ta, Co, Sc, for REE (rare earth elements), and for Rb-Sr isotopic contents. These data suggest that the major rock units in the complex are comagmatic and were formed approximately 520 million years ago. In addition, initial Sr isotopic ratios indicate that the rocks of the complex were derived from the upper mantle.

An alkali basaltic parent magma could have formed initially by about 0.5 percent melting of upper mantle peridotite. Data obtained for the mafic-ultramafic rocks of the layered series suggest that they were derived as melts or cumulates by fractional crystallization from portions of the parental magma which rose to shallow depths (pressure  $< 8$  Kb).

A hypothetical "ijolitic" magma was formed when part of the alkali basaltic parent magma underwent extensive (approximately 70 percent) high pressure (15 - 23 Kb) fractional crystallization of clinopyroxene. Some "ijolitic" magma then could have risen to levels similar to the layered series and produced the malignite, feldspathoidal syenite, and biotite syenite as cumulates by progressive fractional crystallization of the "ijolitic" magma at high water pressure. The malignites could have formed as a cumulate by a combination of 30 percent crystallization of the "ijolitic" magma along with the incorporation of 30 percent of the residual liquid. Fifty percent fractional crystallization of the remaining liquid along with the incorporation of 20 percent of the residual liquid produced the feldspathoidal

syenite. The biotite syenites were formed as cumulates from 35 percent fractionation of the liquid remaining after the formation of the feldspathoidal syenite. The nepheline syenite dikes and stocks of the complex may have formed from portions of the residual liquids produced during the formation of the malignite and feldspathoidal syenite.

The carbonatite dikes in the McClure Mountain complex may have formed as an immiscible liquid from the "ijolitic" magma or the residual liquid accumulating during the crystallization of the malignite.

The data obtained in this study together with existing data available for the nearby Gem Park Complex (Roden, 1977) suggest that a genetic relationship may exist between the two complexes.

